EUROPEAN ORGANISATION FOR NUCLEAR RESEARCH (CERN)

Submitted to: EPJ C

CERN-EP-2025-243
20th November 2025

Measurements of $ZZ \to \ell\ell\nu\nu$ and $ZZjj \to \ell\ell\nu\nu jj$ productions in pp collisions at $\sqrt{s} = 13$ TeV with the ATLAS detector

The ATLAS Collaboration

This article presents measurements of Z boson pair production cross-sections at a center-of-mass energy of $\sqrt{s} = 13$ TeV, using 140 fb^{-1} of proton–proton data collected with the ATLAS detector at the Large Hadron Collider. The analysis includes both inclusive ZZ production and ZZ production in association with two jets ($ZZjj$), where one Z boson decays into a pair of charged leptons $\ell^+\ell^-$ ($\ell = e, \mu$), and the other decays into a neutrino pair. The measured fiducial cross-section of the inclusive ZZ production is 21.0 ± 1.0 fb, while for the $ZZjj$ production it is $0.96^{+0.18}_{-0.16}$ fb. Extrapolation of the ZZ cross-section to the full phase space, for Z bosons within the mass range $66 - 116$ GeV, yields $\sigma(pp \to ZZ) = 15.38 \pm 0.81$ pb. Differential cross-sections are presented for an extended set of kinematic observables. The results are found to be in good agreement with Standard Model predictions. Constraints on anomalous gauge boson self-interactions are derived using both the vertex function formalism and the effective field theory framework.

Contents

1 Introduction

Precise measurements of total and differential cross-sections for diboson production at the Large Hadron Collider (LHC) [1] are essential to test the predictions of the Standard Model (SM) and probe for potential physics beyond it.

This article presents measurements of integrated and differential cross-sections for Z boson pair (ZZ) production at $\sqrt{s}$ = 13 TeV using ATLAS proton–proton (pp) collision data recorded in 2015–2018, corresponding to an integrated luminosity of 140 fb^{-1}. The measurements include inclusive ZZ production and ZZ production with two associated jets ($ZZjj$), where one Z boson decays into a pair of charged leptons $\ell^+\ell^-$ ($\ell = e, \mu$) and the other decays into neutrinos. Decays of Z bosons via τ-leptons, where the τ later decays leptonically, are included in the signal definition, but their contribution is negligible after event selection. The measurement targets final states with two on-shell Z bosons.

In the SM, Z boson pairs are produced at the LHC primarily through quark–antiquark ($q\bar{q}$) annihilation, as illustrated in Figure 1(a), which shows a leading-order (LO) Feynman diagram. An additional contribution arises from gluon–gluon (gg) fusion via a quark loop, depicted in Figure 1(b), which accounts for approximately 10% of the total ZZ production cross-section for $\sqrt{(s)}$ = 13 TeV pp collisions. Production via the s-channel, shown in Figure 1(c), is forbidden at LO in the SM, as it would involve an anomalous triple gauge coupling (aTGC) through a ZZZ or $ZZ\gamma$ vertex. Consequently, ZZ production serves as a sensitive probe of neutral anomalous triple gauge couplings (aTGCs) predicted by physics theories beyond the SM (BSM) [2].

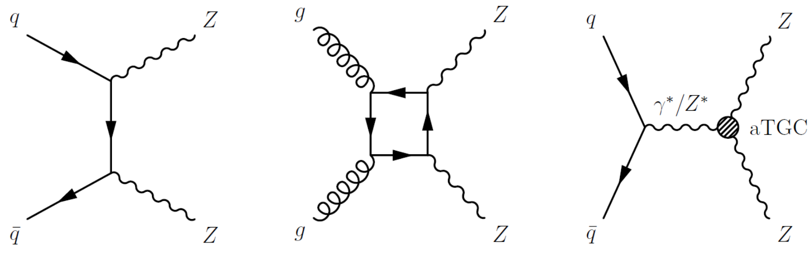

(a) (b) (c)

Figure 1: Example of Feynman diagrams for the production of a pair of Z bosons from the (a) $q\bar{q}$ and (b) gg initial states at the LHC. The s-channel diagram (c) is not allowed at LO in the SM; it represents an anomalous triple gauge coupling (aTGC) of a ZZZ or $ZZ\gamma$ vertex.

Various measurements of ZZ production at the LHC were carried out by the ATLAS Collaboration [3–7] and the CMS Collaboration [8–11] using data taken at $\sqrt{s}$ = 7, 8, and 13 TeV. Two complementary final states originating from the decays of the Z boson pairs are used in those measurements, one with four charged leptons (4ℓ) and the other with two charged leptons and two neutrinos ($\ell\ell\nu\nu$). At 13 TeV, the ATLAS Collaboration measured the inclusive fiducial cross-section in the $\ell\ell\nu\nu$ channel with uncertainty of 7% [6].

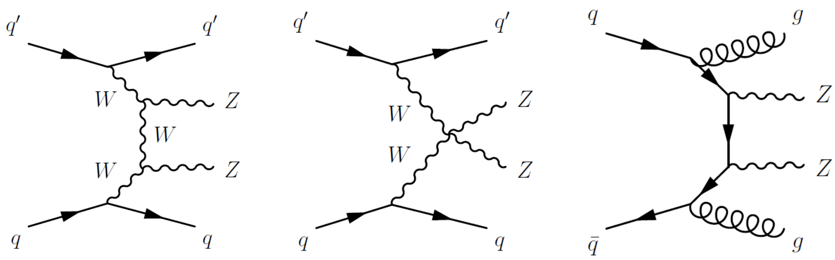

(a) (b) (c)

Figure 2: Typical diagrams for the production of $ZZjj$ events. The electroweak production, containing triple and quartic interaction vertices, is shown in (a) and (b), while (c) shows the QCD production with gluons in the final state.

The analysis also targets inclusive $ZZjj$ production, with contributions from both QCD- and electroweak-induced processes. The electroweak component is dominated by the vector boson scattering (VBS) topology. Representative Feynman diagrams for these processes are shown in Figure 2. The EW production of $ZZjj$ events is particularly sensitive to the WWZ and $WWZZ$ weak-boson self-interactions, which arise from the non-Abelian structure of the electroweak interactions. These are depicted in Figure 2(a) and Figure 2(b), respectively.

As a result, $ZZjj$ production serves as a powerful channel for investigating if these triple and quartic gauge couplings are in agreement with the SM predictions and for setting constraints on aTGCs and anomalous quartic gauge couplings (aQGCs).

The EW $ZZjj$ production was observed using a combination of the $ZZjj \to 4\ell jj$ and $ZZjj \to \ell\ell\nu\nu jj$ channels [12]. The ATLAS Collaboration has also measured the differential cross-section for $ZZjj \to 4\ell jj$

production [13], from which limits on aQGCs were derived at the 95% confidence level (CL). In the present analysis, the $ZZjj \to \ell\ell\nu\nu jj$ final state is studied, providing greater sensitivity to aQGCs as the branching ratio is approximately six times larger than that of the $4\ell jj$ channel.

Using nearly four times the integrated luminosity of the previous statistically limited measurement [6], this article presents cross-section measurements of $\ell\ell\nu\nu$ and $\ell\ell\nu\nu jj$ production in fiducial phase spaces. The cross-sections are extracted by fitting signal and background models to data in dedicated regions. The total $pp \to ZZ$ production cross-section is obtained by extrapolating the fiducial measurement to the full phase space, defined in terms of the invariant masses of the Z bosons as reconstructed from their decay leptons. Differential cross-sections are measured by correcting for detector effects (unfolding) in terms of eight and seven kinematic variables for the inclusive ZZ and $ZZjj$ production processes, respectively.

The inclusive ZZ measurement is used to search for aTGCs by fitting the transverse momentum (p_{T}) distribution of the dilepton system from the Z boson decay. The $ZZjj$ measurement is used to probe aQGCs by fitting the transverse mass (m_{T}) distribution of the ZZ system, defined in Section 8. Limits on aTGCs and aQGCs are derived using a simplified model within the SM Effective Field Theory (SMEFT) framework [14–16]. For comparison with previous results, the anomalous Lagrangian vertex function (VF) formalism [17] is also employed to set limits on aTGC parameters.

The structure of this article is as follows. Section 2 provides an overview of the ATLAS detector subsystems. Section 3 describes the data samples and Monte Carlo (MC) simulations used for both signal and background processes. The event selection criteria are detailed in Section 4, while the definition of the experimental fiducial phase space is presented in Sections 5. Section 6 discusses the estimate of systematic uncertainties in the measurements. The SM cross-section predictions are presented in Section 7. The results of the integrated and differential cross-section measurements are reported in Section 8. The interpretation of the results, including the study of anomalous gauge boson self-interactions and the constraints on aTGC and aQGC parameters, is presented in Section 9. Finally, Section 10 summarises the key results.

2 The ATLAS detector

The ATLAS experiment [18] at the LHC is a multipurpose particle detector with a forward–backward symmetric cylindrical geometry and a near 4π coverage in solid angle.[1]

The detector consists of an inner tracking detector (ID) surrounded by a thin superconducting solenoid providing a 2 T axial magnetic field, electromagnetic and hadronic calorimeters, and a muon spectrometer (MS). The inner tracking detector covers the pseudorapidity range $|\eta| < 2.5$. It consists of silicon pixel, silicon microstrip, and transition radiation tracking detectors. Lead/liquid-argon (LAr) sampling calorimeters provide electromagnetic (EM) energy measurements with high granularity within the region $|\eta| < 3.2$. A steel/scintillator-tile hadronic calorimeter covers the central pseudorapidity range ($|\eta| < 1.7$). The endcap and forward regions are instrumented with LAr calorimeters for EM and hadronic energy measurements up to $|\eta| = 4.9$. The muon spectrometer surrounds the calorimeters and is based on three large superconducting air-core toroidal magnets with eight coils each. The field integral of the toroids ranges between 2.0 and 6.0 T m across most of the detector. The muon spectrometer includes a system

[1] ATLAS employs a right-handed coordinate system with its origin at the nominal interaction point (IP) at the detector's centre. The z-axis aligns with the beam direction, while the x-axis points from the IP to the LHC ring's centre, and the y-axis points upwards. The transverse plane (x, y) is described using cylindrical coordinates (r, ϕ), where ϕ denotes the azimuthal angle around the beam direction. The pseudorapidity η is defined by the polar angle θ as $\eta = -\ln\tan(\theta/2)$.

of precision tracking chambers up to $|\eta| = 2.7$ and fast detectors for triggering up to $|\eta| = 2.4$. The luminosity is measured by the LUCID–2 [19] detector, which is located close to the beampipe. A two-level trigger system is used to select events [20]. The first-level trigger is implemented in hardware and uses a subset of the detector information to accept events at a rate close to 100 kHz. This is followed by a software-based trigger that reduces the accepted rate of complete events to 1.25 kHz on average depending on the data-taking conditions. A software suite [21] is used for simulation, reconstruction, and analysis of real data and simulated events, and for detector operations, trigger and data acquisition.

3 Data and Monte Carlo simulations

The data used for this analysis were recorded using single-lepton (e, μ) and multi-lepton triggers, corresponding to an integrated luminosity of 140 fb^{-1} [22] after the application of data quality requirements [23]. For the single-lepton trigger, the transverse momentum thresholds vary from 20 to 26 GeV, while for the multi-lepton triggers, they vary from 10 to 14 GeV, depending on the data-taking periods [24, 25]. The overall trigger efficiency for the $ZZ \to \ell\ell\nu\nu$ events selected in this analysis is higher than 99%.

Simulated events for the signal and background processes are produced using MC event generators that model the underlying physics processes in pp collisions. After the initial event generation, the final-state particles are passed through a detector simulation [26] based on the Geant4 framework [27]. The simulated events are processed using the same reconstruction algorithms and trigger requirements as those used in the data. The event samples also include simulations of additional pp interactions from the same and neighbouring bunch crossings, commonly referred to as pile-up, which are simulated using Pythia 8.1 [28] with the A3 tune [29]. The simulated events are reweighted to reproduce the pile-up conditions observed in the data.

Scale factors, derived from data control samples (such as $Z \to \ell^+\ell^-$ and $J/\psi \to \ell^+\ell^-$ decays), are applied to simulated events to correct for discrepancies between data and MC simulations. These corrections account for differences in the trigger efficiencies, reconstruction, identification, isolation, and interaction vertex reconstruction for electrons and muons. The electron and jet energies and the muon momenta in the simulated events are smeared to account for the differences in resolution between data and MC simulations.

The signal processes $pp \to ZZ \to \ell\ell\nu\nu$ and $pp \to ZZjj \to \ell\ell\nu\nu jj$ can occur via either QCD or EW production mechanisms. For QCD production, both quark-initiated ($q\bar{q} \to ZZ$) and gluon-initiated ($gg \to ZZ$) processes were modelled using Sherpa 2.2.2 [30], including off-shell effects and Higgs boson (H) contributions, where appropriate. For the quark-initiated process, the events were simulated using matrix elements at NLO accuracy in QCD for up to one additional parton and at LO accuracy for up to three additional parton emissions. Samples for the loop-induced processes $gg \to ZZ$ were simulated using LO-accurate matrix elements in QCD for up to one additional parton emission. A k-factor of 1.7 was applied to normalise the gg-induced cross-section to NLO accuracy [31]. The NLO EW corrections [32, 33] were also included in the $q\bar{q} \to \ell\ell\nu\nu$ process with a $p_{\text{T}}(Z)$ dependent k-factor, where $p_{\text{T}}(Z)$ is the transverse momentum of the Z boson decaying into neutrinos.

The matrix element calculations were matched and merged with the Sherpa parton shower based on Catani–Seymour dipole factorisation [34, 35] using the MEPS@NLO prescription [36–39]. The virtual QCD corrections were provided by the OpenLoops library [40–42]. The NNPDF3.0nnlo set of PDFs was used [43], along with the dedicated set of tuned parton-shower parameters developed by the Sherpa authors.

An alternative sample for the quark-initiated QCD production of the $pp \to ZZ \to \ell\ell\nu\nu$ process was produced with Powheg Box v2 [44–46] at NLO accuracy in QCD. Events were interfaced to Pythia 8.210 [47] for the modelling of the parton shower, hadronisation, and underlying event, with parameters set according to the AZNLO tune [48]. The CT10 PDF set [49] was used for the hard-scattering processes, whereas the CTEQ6L1 PDF set [50] was used for the parton shower.

MadGraph5 [51] in combination with the NNPDF2.3lo PDF set [52] was used to simulate the electroweak contributions to both the ZZ and $ZZjj$ fiducial cross-sections. The calculation is accurate to LO in perturbative QCD and uses the NNPDF2.3lo PDF set [53]. The events were interfaced with Pythia 8.2 to provide parton showering, hadronisation, and underlying-event activity using the A14 set of tuned parameters [54].

An alternative sample for the electroweak production of $ZZjj \to \ell\ell\nu\nu jj$ events was produced using Sherpa 2.2.2 at LO accuracy. The NNPDF3.0nlo PDF set [43] was used. Events were produced with the default Sherpa parton shower, hadronisation, and underlying-event modelling. Matrix-element calculations included all relevant tree-level electroweak diagrams and were merged with the Sherpa parton shower using the MEPS@LO prescription [36–39].

The main backgrounds for the inclusive $ZZ \to \ell\ell\nu\nu$ and the $ZZjj \to \ell\ell\nu\nu jj$ signals originate from both resonant and non-resonant $\ell^+\ell^-$ production along with a significant missing transverse momentum component, either from neutrinos or from mismeasured jets accompanying the charged leptons. In both the $\ell\ell\nu\nu$ and the $\ell\ell\nu\nu jj$ final states, the dominant contribution comes from the WZ production process, particularly in the decay channels $WZ \to \ell\nu\ell\ell$ (where the third lepton evades detection) and $WZ \to q\bar{q}\ell\ell$. This process is considered a resonant background, as it results in an $\ell^+\ell^-$ pair originating from an on-shell Z boson. Another important background is the Z+jets production process, i.e., the production of single Z bosons in association with jets, where the Z boson decays into $\ell^+\ell^-$. Non-resonant backgrounds arise mainly from processes such as $WW \to \ell\nu\ell\nu$ and top (t) pair production, $t\bar{t} \to WWbb \to \ell\nu\ell\nu bb$. Other backgrounds arise from processes producing top quarks in association with W or Z bosons (tW, $t\bar{t}V$ with $V = W, Z$), ZZ without neutrinos in the decay, i.e., $ZZ(\to 4\ell, 2\ell 2q)$, tribosons VVV, W bosons in association with jets (Wj), single Z bosons decaying into $\tau\tau$, and WH events.

The diboson background samples were simulated using Sherpa or Powheg as follows. The $WZ \to \ell\nu\ell\ell$ and $ZZ \to 4\ell$ samples were simulated using Sherpa 2.2.2. The WZ and ZZ samples with "semileptonic" final states, where one boson decays leptonically and the other hadronically, and the gluon-initiated WW sample, were generated with Sherpa 2.2.1. The quark-initiated WW samples were generated with Powheg Box v2. Interference effects between WW and ZZ for same-flavour charged leptons and neutrinos were not considered.

The production of $t\bar{t}$ events was modelled using the Powheg Box v2 [45] generator at NLO in QCD, with the NNPDF3.0nlo PDF set. The h_{damp} parameter, which regulates the matching between Powheg matrix elements and the parton shower, was set to be 1.5 times the top quark mass [55]. The events were interfaced with Pythia 8.230 for modelling the parton shower, hadronisation, and underlying event, using the A14 tune and the NNPDF2.3lo PDF set [43].

For associated production of top quarks with W bosons (tW), the Powheg Box v2 generator was again used at NLO in QCD, employing the five-flavour scheme and the NNPDF3.0nlo set of PDFs. To avoid double counting with the $t\bar{t}$ production, the diagram-removal scheme [56] was applied. As with $t\bar{t}$

production, events were interfaced to Pythia 8.230 using the A14 tune and the NNPDF2.3lo PDF set. The production of $t\bar{t}V$ events was modelled using the MadGraph5_aMC@NLO 2.3.3 [52] generator at NLO with the NNPDF3.0nlo PDF set. The events were interfaced to Pythia 8.210 using the A14 tune and the NNPDF2.3lo PDF set.

The production of V+jets ($V = W, Z$), with all three lepton flavours, was simulated with the Sherpa 2.2.1 generator, using NLO matrix elements for up to two partons and LO matrix elements for up to four partons. These events were matched with the Sherpa parton shower using the MEPS@NLO prescription, with the set of tuned parameters developed by the Sherpa authors. The NNPDF3.0nnlo set of PDFs was used, and the samples were normalised to an NNLO prediction [57].

The triboson backgrounds ZZZ, WZZ, and WWZ with fully leptonic decays with at least four prompt charged leptons were modelled using Sherpa2.2.2 at LO accuracy in QCD and the CT10 PDF set [49]. The $Z \to \tau\tau$ events were simulated using Sherpa 2.2.1, with up to two partons at NLO and up to four partons in total, merged using the ME+PS@NLO scheme. The WH samples were simulated using Powheg Box v2 at NLO accuracy in QCD, interfaced to Pythia 8.186 [28] for the modelling of parton showering and hadronisation.

For all simulated samples, except those generated with Sherpa, the decays of b- and c-hadrons are handled by EvtGen [58].

The MC samples used in the interpretation of the analysis in terms of aTGCs and aQGCs are discussed in Section 9.

4 Event selection

The event selection in both the ZZ and $ZZjj$ signal regions (SRs) and the background control regions (CRs) relies on multiple reconstructed objects, including electrons, muons, jets, and the missing transverse momentum $E_{\mathrm{T}}^{\mathrm{miss}}$.

Events are first required to have a collision vertex associated with at least two tracks, each with p_{T} greater than 0.5 GeV. The vertex with the highest sum of p_{T}^2 of the associated tracks is identified as the primary vertex.

Electrons are reconstructed from energy clusters in the EM calorimeter that match to tracks in the ID. They are identified using a likelihood function based on EM shower shapes, track properties and track-to-cluster matching. Electrons must meet a “medium” likelihood requirement, achieving an overall identification efficiency of approximately 90% [59]. The electron momentum is calculated from the cluster energy and track direction. The cluster’s pseudorapidity must be within $|\eta| < 2.47$, excluding the transition region between the barrel and endcap calorimeter regions $1.37 < |\eta| < 1.52$. The leading (subleading) electron is required to have a transverse momentum (p_{T}) greater than 30 GeV (20 GeV).

Muons are identified by tracks reconstructed in the MS, which are then matched to tracks reconstructed in the ID. A “medium” identification selection is applied, based on requirements for the number of hits in both the ID and the MS [60]. The muon pseudorapidity must satisfy $|\eta| < 2.5$. The muon momentum is determined by combining the MS measurement, corrected for energy deposited in the calorimeters, with the ID measurement. The leading (subleading) muon is required to have $p_{\mathrm{T}} > 30$ GeV (20 GeV).

Electron and muon candidates are required to originate from the primary vertex. They are required to satisfy $|d_0/\sigma_{d_0}| < 3(5)$ for muons (electrons), where d_0 is the transverse impact parameter calculated relative to the measured beam-line position and σ_{d_0} is its uncertainty. They must also have a longitudinal impact parameter, z_0 (the difference between the value of z of the point on the track at which d_0 is defined and the longitudinal position of the primary vertex), which satisfies $|z_0 \cdot \sin(\theta)| < 0.5$ mm.

To suppress hadronic and non-prompt lepton background, electrons and muons are required to be isolated from other particles by satisfying the particle-flow isolation criteria [60, 61], which are based on clusters of energy deposits in the calorimeter and inner detector track information.

Jets are reconstructed using the anti-k_t algorithm [62] with a radius parameter of $R = 0.4$, applied to particle-flow objects that combine information from the inner detector and calorimeter [63]. The jet-energy scale is derived from simulation and further refined using in situ techniques based on dijet, γ+jet and Z+jet events [64]. A jet-vertex tagger [65] is applied to jets with $p_T < 60$ GeV and $|\eta| < 2.4$ to suppress jets originating from pile-up. In addition, jets with $p_T > 20$ GeV and $|\eta| < 2.5$ containing b-hadrons are identified using the DL1r multivariate b-tagging algorithm [66, 67]. The 85% efficiency working point is used, which corresponds to rejection factors of 6.3 for c-jets and 33 for light-flavour jets. Jets are required to have transverse momentum $p_T > 30$ GeV and pseudorapidity $|\eta| < 4.5$.

Overlaps between reconstructed objects are accounted for with a removal procedure that is mainly based on the angular separation between the different final-state objects (electrons, muons, jets). The procedure is the same as the one described in Ref. [68].

The neutrinos in the $\ell\ell\nu\nu$ final state do not interact with the ATLAS detector and cannot be reconstructed. Their presence is identified using the E_T^{miss} variable, which is computed as the magnitude of the negative vector sum of transverse momenta of all leptons and jets and the tracks originating from the primary vertex but not associated with any of the leptons or jets [69]. Another quantity used in the event selection is the total transverse energy, H_T, which is the scalar sum of the transverse momenta of all selected leptons and jets.

4.1 Signal regions

The event selection criteria are designed to maximize the sensitivity to the ZZ and $ZZjj$ signal processes while effectively reducing background contributions. Two signal regions are defined: one targeting inclusive ZZ production and another targeting the $ZZjj$ topology. In both SRs events are required to contain exactly two oppositely charged electrons or muons, with an invariant mass between 80 and 100 GeV. The azimuthal angle between the missing transverse momentum and the Z boson decaying into a charged lepton pair must satisfy $\Delta\phi(E_T^{miss}, Z) > 2.2$. The angular separation between the two leptons, defined as $\Delta R_{\ell\ell} = \sqrt{(\Delta\eta)^2 + (\Delta\phi)^2}$, must satisfy $\Delta R_{\ell\ell} < 1.8$.

Events containing b-tagged jets, referred to as b-jets in the following, with $p_T > 30$ GeV and $|\eta| < 2.5$ are rejected. The ratio of the missing transverse momentum to the total transverse energy, E_T^{miss}/H_T, must be greater than 0.65 to ensure a p_T balance between the two Z bosons.

For the ZZ SR, events are required to have $E_T^{miss} > 110$ GeV. The $ZZjj$ SR has a stricter E_T^{miss} requirement of $E_T^{miss} > 150$ GeV to minimize the background contribution from Z+jets production.

4.2 Background control regions

For the $ZZ \rightarrow \ell\ell\nu\nu$ and $ZZjj \rightarrow \ell\ell\nu\nu jj$ processes, background sources are categorised into "resonant" and "non-resonant" types. Resonant backgrounds include WZ production, dominated by $W \rightarrow \ell\nu$ decays where the lepton is not reconstructed, and the Z+jets process, where two leptons form a Z candidate, with "fake" $E_{\mathrm{T}}^{\mathrm{miss}}$ arising from jet mis-measurement. Non-resonant backgrounds encompass WW and top-quark processes.

In all considered backgrounds, lepton candidates are either prompt or originate from τ-lepton decays following W or Z decays. The contribution from non-prompt or fake leptons, predominantly from W+jets production, is negligible in this analysis. It is therefore included in the “other” background category in the tables and estimated from simulation.

Background contributions are estimated using a simultaneous fit across multiple control regions designed to constrain dominant processes contributing to the selected final states. In the inclusive ZZ phase space, three dedicated CRs are defined with an enhanced contribution from the main background processes: WZ, WW, and $t\bar{t}$. Additionally, three CRs target the Z+jets background: Z+0jets, Z+1jet, and Z+≥2jets.

For the WZ control region, events are required to contain a third lepton with $p_{\mathrm{T}} > 20$ GeV that satisfies the medium identification criteria, along with a same-flavour opposite-charge (SFOS) lepton pair whose invariant mass is consistent with the Z boson mass in the region $80 < m_{\ell\ell} < 100$ GeV. If multiple such pairs are found, the one with the mass closest to the Z boson mass is selected. To suppress non-WZ contributions, several further selections are applied:$E_{\mathrm{T}}^{\mathrm{miss}} > 70$ GeV, $E_{\mathrm{T}}^{\mathrm{miss}}/H_{\mathrm{T}} > 0.3$, a b-jet veto, and $m_{\mathrm{T}}^{W} > 30$ GeV. The transverse mass of the W (m_{T}^{W}) is constructed from the third lepton's transverse momentum ($\vec{p}_{\mathrm{T}}^{\,\ell}$) and the $\vec{E}_{\mathrm{T}}^{\mathrm{miss}}$ vector representing the transverse momentum of the neutrino ($\vec{p}_{\mathrm{T}}^{\,\nu}$), using the formula

$$m_{\mathrm{T}}^{W} = \sqrt{2 \cdot p_{\mathrm{T}}^{\nu} \cdot p_{\mathrm{T}}^{\ell} \cdot [1 - \cos\Delta\phi(\ell, \nu)]}$$

where $\Delta\phi(\ell, \nu)$ is the angle between the lepton and the neutrino in the transverse plane.

The non-resonant background is estimated using two $e^{\pm}\mu^{\mp}$ CRs, where exactly one electron and one muon with opposite charges are selected, fulfilling a Z mass requirement of $80 < m_{\ell\ell} < 100$ GeV. Additional selections are applied:$E_{\mathrm{T}}^{\mathrm{miss}} > 70$ GeV and $E_{\mathrm{T}}^{\mathrm{miss}}/H_{\mathrm{T}} > 0.3$. These selections ensure a sample highly populated by WW and $t\bar{t}$ events, with minimal signal contamination. To suppress the $t\bar{t}$ contribution and enhance the WW purity in the WW CR, a veto on b-jets is imposed, whereas for the Top CR, at least one b-jet is required.

Three CRs for the Z+jets background are defined by requiring two SFOS leptons with $80 < m_{\ell\ell} < 100$ GeV and selecting events in the plane $\{E_{\mathrm{T}}^{\mathrm{miss}}, E_{\mathrm{T}}^{\mathrm{miss}}/H_{\mathrm{T}}\}$ chosen to be well separated from the signal region. Events must satisfy either $70 < E_{\mathrm{T}}^{\mathrm{miss}} < 80$ GeV and $E_{\mathrm{T}}^{\mathrm{miss}}/H_{\mathrm{T}} > 0.3$, or $E_{\mathrm{T}}^{\mathrm{miss}} > 80$ GeV and $0.3 < E_{\mathrm{T}}^{\mathrm{miss}}/H_{\mathrm{T}} < 0.45$. A b-jet veto is applied, and events are categorised into exactly 0-jet, exactly 1-jet, and at least 2-jet bins. Each of these jet-multiplicity regions is used as a single-bin control region in the fit, as no significant statistical gain is achieved by further binning.

For the $ZZjj \rightarrow \ell\ell\nu\nu jj$ process, two CRs are defined: one for the resonant $WZjj$ background and one for the non-resonant backgrounds ($WWjj$ and $t\bar{t}$). The non-resonant background is constrained using the $e^{\pm}\mu^{\mp}$ CR, with an additional requirement of at least two jets. The $WZjj$ background is estimated using the three-lepton CR described above, with the requirement of at least two jets present. The Z + jets background contribution is estimated from MC simulations and found to be negligible in the signal region.

The event yields for both data and MC simulations in the inclusive ZZ signal region and the six control regions are summarised in Table 1. Similarly, the event yields in the signal and control regions for the $ZZjj$ selection are detailed in Table 2. They include uncertainties from both MC statistical and systematic sources, which are described in Section 6.

Table 1: Pre-fit MC yields for the inclusive ZZ phase-space. The “Other” category includes events from the processes $ZZ(\rightarrow 4\ell, 2\ell 2q)$, VVV $(V = W, Z)$, Wj, $Z(\rightarrow \tau\tau)$, and WH. The selected number of data events in the SR and the CRs are also provided.

	SR	WZ CR	WW CR	Top CR	Z+0j CR	Z+1j CR	Z+≥2j CR
ZZ	1650 ± 36	2.6 ± 0.7	0.58 ± 0.11	0.005 ± 0.011	100 ± 12	150 ± 20	160 ± 34
WZ	740 ± 43	2100 ± 140	22 ± 2	0.9 ± 0.3	80 ± 12	250 ± 28	310 ± 60
Z+0j	80 ± 34	40 ± 17	0.6 ± 1.0	0	1700 ± 670	0	0
Z+1j	80 ± 40	40 ± 14	2.2 ± 0.7	0.12 ± 0.08	0	3800 ± 1460	0
Z+≥2j	13 ± 7	20 ± 12	0.4 ± 0.6	0.15 ± 0.16	0	0	4700 ± 1700
WW	36.2 ± 1.9	0.65 ± 0.12	672 ± 41	13.9 ± 1.6	48 ± 6	46 ± 5	18.5 ± 1.9
Top	114 ± 20	57 ± 8	1850 ± 290	5700 ± 710	92 ± 25	200 ± 39	250 ± 43
Other	48 ± 4	91 ± 7	46 ± 13	3.4 ± 1.3	12 ± 3	44 ± 10	48 ± 10
Total prediction	2760 ± 120	2340 ± 150	2590 ± 310	5720 ± 710	2050 ± 700	4510 ± 1500	5470 ± 1700
Data	2917	2409	2903	5736	2691	5733	5769

Table 2: Pre-fit MC yields for the $ZZjj$ phase-space. The “Other” category includes events from the processes of $ZZ(\rightarrow 4\ell, 2\ell 2q), VVV(V = W, Z), Wj, Z(\rightarrow \tau\tau)$, and WH. The selected number of data events in the SR and the CRs are also provided.

	SR	WZ CR	WW and Top CR
ZZ	108 ± 12	1.0 ± 0.3	0.006 ± 0.004
WZ	62 ± 12	280 ± 60	4.8 ± 1.0
Z+jets	2.4 ± 1.2	15 ± 8	0.4 ± 0.2
WW and Top	7.2 ± 1.5	8.2 ± 1.8	620 ± 90
Other	3.0 ± 0.7	12 ± 3	12 ± 14
Total prediction	183 ± 21	320 ± 60	640 ± 100
Data	184	317	678

5 Phase space definitions

The $ZZ \rightarrow \ell\ell\nu\nu$ and $ZZjj \rightarrow \ell\ell\nu\nu jj$ production cross-sections are measured within experimental fiducial phase spaces, which are defined by the kinematic acceptance at the stable-particle level in the MC simulation (particles with a proper lifetime $\tau > 10$ ps), as summarised in Table 3. The fiducial phase space is defined for final states with electrons or muons. The particle-level selections are defined to closely mimic the selection applied at detector level, and with a relaxed minimum $E_{\mathrm{T}}^{\mathrm{miss}}$ by 15 – 20 GeV, about one standard deviation from the value used at the reconstruction level and with a more relaxed dilepton mass window around the Z pole. Electrons and muons are required to be prompt, i.e. not originating from the decay of hadrons or τ-leptons. A dressed lepton is defined as the momentum four-vector sum of the lepton (electron or muon) and all prompt photons within a cone of $\Delta R_{\ell\gamma} < 0.1$. Dressed leptons are used to reconstruct the Z boson candidates, requiring SFOS lepton pairs. The $E_{\mathrm{T}}^{\mathrm{miss}}$ is calculated from the transverse momentum of the $\nu\bar{\nu}$ system, which results from the decay of the other Z boson in the event. Hadronic jets are labelled as "j" in the table. In addition to the fiducial phase space, Table 3 also includes the definition of the total phase space.

Table 3: Fiducial and total phase space definitions for inclusive ZZ and $ZZjj$ cross-section measurements and for the total ZZ cross-section.

Common fiducial phase space definition	**Kinematic cut**
A lepton is "dressed" with photons within an angular separation of	$\Delta R_{\ell\gamma} < 0.1$
Lepton pseudorapidity range	$\|\eta^{\ell}\| < 2.5$
Transverse momentum of leading (sub-leading) lepton	$p_{\mathrm{T}}^{\ell} > 30\ (20)$ GeV
Invariant mass of the dilepton system	$76 < m_{\ell\ell} < 106$ GeV
Missing transverse energy	$E_{\mathrm{T}}^{\mathrm{miss}} > 95$ GeV
Angular separation of the two leptons	$\Delta R_{\ell\ell} < 1.8$
Azimuthal angular separation of the dilepton system and $E_{\mathrm{T}}^{\mathrm{miss}}$	$\Delta\phi(E_{\mathrm{T}}^{\mathrm{miss}}, p_{\mathrm{T}}^{\ell\ell}) > 2.2$
$E_{\mathrm{T}}^{\mathrm{miss}}$ over H_{T}	$E_{\mathrm{T}}^{\mathrm{miss}}/H_{\mathrm{T}} > 0.65$
Additional requirements for $ZZjj$ phase space	
At least 2 hadronic jets with	$p_{\mathrm{T}}^{j} > 30$ GeV and $\|\eta^{j}\| < 4.5$
$E_{\mathrm{T}}^{\mathrm{miss}}$ requirement	$E_{\mathrm{T}}^{\mathrm{miss}} > 130$ GeV
Total phase space definition	
Invariant masses $m_{\ell\ell}$ and $m_{\nu\nu}$	$66 \leq m_{\ell\ell}, m_{\nu\nu} \leq 116$ GeV

6 Systematic uncertainties

Experimental systematic uncertainties are assessed to account for residual discrepancies between data and simulation in the modelling of trigger efficiencies, leptons, jets, $E_{\mathrm{T}}^{\mathrm{miss}}$, luminosity, and the average number of proton–proton interactions per bunch crossing.

The total integrated luminosity of the dataset is known to a precision of 0.83%, determined using a combination of van der Meer beam separation scans in dedicated data-taking sessions and calibrated luminosity-sensitive detectors during regular data-taking periods [22].

The number of proton–proton interactions per bunch crossing varies across the dataset and is modelled in simulation by reweighting events to match the distribution observed in data. An uncertainty arises from the limited precision in the ratio of predicted to measured inelastic cross-sections within the ATLAS acceptance region [70]. To account for this, a systematic variation is applied to the average number of interactions in the simulation.

Efficiencies for lepton reconstruction, identification, isolation, and trigger selections are corrected in simulation using scale factors derived from control samples in data, as discussed in Section 3. The uncertainties in these corrections are propagated by varying the scale factors within their uncertainties [24, 25, 60, 71]. Differences between data and simulation in the lepton momentum scale and resolution are evaluated by applying additional scaling and smearing variations [71, 72].

Jets are calibrated as discussed in Section 4. The jet energy scale (JES) is derived using test-beam data, LHC collision data, and simulation information. The JES calibration [64] includes corrections that account for detector effects, jet fragmentation, the impact of pile-up, and differences between data and MC simulation. The impact of the uncertainty in the jet energy resolution (JER) [64] is evaluated by applying additional smearing to the jet energy in the simulated samples to match the resolution observed in data. An additional uncertainty arises from the correction applied to simulated events associated with the jet-vertex-tagger selection. The uncertainty in the b-tagging efficiency, and the corresponding uncertainties in the c-jet and light-jet rejection scale factors, are also taken into account [73]. Uncertainties in $E_{\mathrm{T}}^{\mathrm{miss}}$ are evaluated by varying the soft term and propagating the lepton and jet energy scale and resolution uncertainties to the $E_{\mathrm{T}}^{\mathrm{miss}}$ calculation.

Theory systematic uncertainties associated with the modelling of ZZ production affect the measurement. Two main sources are considered: (i) QCD scale variations, arising from missing higher-order corrections in the simulation and evaluated by varying the factorisation and renormalisation scales, and (ii) uncertainties from parton distribution functions and the α_s value used in the PDF.

Uncertainties from missing higher orders are evaluated [74] using independent variations of the factorisation and renormalisation scales by multiplicative factors of 0.5, 1, and 2. This results in seven scale combinations, including the nominal pair of scales $(1, 1)$ and excluding the two extreme cases where one scale is halved and the other is doubled. The envelope of these variations defines the QCD scale uncertainty for each prediction. For $ZZjj$, the QCD- and EW-induced components are treated separately with uncorrelated scale uncertainties.

PDF uncertainties are evaluated following the PDF4LHC prescription [75], taking the RMS of the 100 replicas of the NNPDF set (excluding α_s variations). The effect of the strong coupling constant is assessed separately by varying α_s by ± 0.001.

The uncertainty due to generator modelling is assessed by replacing the nominal quark-initiated Sherpa ZZ sample with the alternative Powheg Box ZZ sample described in Section 3. The resulting difference in the extracted cross-section is taken as a systematic uncertainty. The uncertainty in the parton showering is calculated in Sherpa by varying the shower recoil scheme.

In the $ZZjj$ phase space, the Z + jets background is estimated using MC simulation. A conservative normalisation uncertainty of 50% is assigned to account for potential mismodelling in events with multiple jets. This value is motivated by the observation in the inclusive $Z+ \geq 2$ jets region, where a correction factor of $1.10^{+0.44}_{-0.31}$ was found (see Sec. 8).

Theoretical modelling uncertainties for the background samples are treated analogously to those for the signal, and are included as separate nuisance parameters in the fit.

The experimental and theory uncertainties are incorporated into the analysis through variations in relevant nuisance parameters in simultaneous fits to data performed separately for the $ZZ \to \ell\ell\nu\nu$ and $ZZjj \to \ell\ell\nu\nu jj$ channels. In each case, the signal and corresponding control regions are fitted simultaneously, and the uncertainties are constrained by the data.

The systematic uncertainties evaluated for the cross-sections for both fiducial phase spaces, ZZ and $ZZjj$, are categorised and summarised in Table 4.

7 Theory predictions

A precise test of the SM requires higher-order perturbative QCD calculations for detailed comparisons with experimental data. The Matrix [76] framework, a parton-level MC generator, is used with the NNPDF3.0nnlo PDF [43] to compute integrated total and fiducial cross-sections, and differential fiducial cross-sections up to NNLO and NLO accuracies in QCD and EW calculations, respectively. The fiducial phase space acceptance A_{ZZ}, i.e., the fraction of events inside the fiducial volume relative to the events in the total phase space, is used to extrapolate the ZZ production cross-section measured in the fiducial phase space to the total phase space. It is defined as $A_{ZZ} = \sigma_{\text{fid}}/\sigma_{\text{total}}$, where σ_{fid} and σ_{total} denote the fiducial and total inclusive cross-sections, respectively.

Table 4: The impact of systematic uncertainties on the measured fiducial cross-sections $\sigma_{ZZ\to\ell\ell\nu\nu}$ and $\sigma_{ZZjj\to\ell\ell\nu\nu jj}$, decomposed into their major categories. For each category, the contribution is obtained by summing in quadrature the impacts of its individual contributions. The total systematic uncertainty is calculated similarly by combining the impacts of individual contributions in quadrature. The statistical uncertainty is calculated as the square root of the difference of the squares of the total uncertainty and the total systematic uncertainty.

Systematic source	**Impact on $\sigma_{ZZ\to\ell\ell\nu\nu}$**	**Impact on $\sigma_{ZZjj\to\ell\ell\nu\nu jj}$**
Scale variation	0.99%	3.5%
PDF and α_s	0.15%	0.42%
Alternative signal generator	0.38%	0.93%
Z+jets modelling	–	0.43%
Jet energy scale and resolution	1.7%	8.7%
MC statistics	1.6%	2.9%
Pile-up reweighting	0.39%	4.1%
$E_{\mathrm{T}}^{\mathrm{miss}}$	1.4%	0.97%
Electrons	0.38%	0.24%
Muons	0.35%	0.42%
b-tagging	0.28%	1.2%
Luminosity	0.87%	0.82%
Total systematics	3.1%	11%
Statistics	3.6%	14%
Total	4.8%	18%

The inclusive $ZZ \to \ell\ell\nu\nu$ production cross-sections in the fiducial and total phase space, calculated using Matrix, are presented in Table 5. Like everywhere else in this article, $\ell\ell$ and $\nu\nu$ are the direct Z decay products, with $\ell = e, \mu$ as usual. The calculation includes NNLO QCD corrections for $q\bar{q} \to ZZ \to \ell\ell\nu\nu$ and NLO QCD corrections for $gg \to ZZ \to \ell\ell\nu\nu$, along with NLO EW corrections. Following the prescription given in Matrix, three different ways of combining QCD and EW corrections are presented. One additive prescription (NNLO QCD + EW) and two multiplicative prescriptions, where the factorisation of the EW corrections is complete (NNLO QCD × EW) or restricted to the $q\bar{q}$ channel. The differences between those prescriptions allow to assess the impact of QCD-EW mixed effects of $O(\alpha_s\alpha)$ and related theory uncertainties. As seen in Table 5, these differences are at the level of the MC statistical uncertainty. The result of the additive QCD+EW prescription lies between the results of the other two (multiplicative) configurations and is taken as the nominal Matrix prediction. The QCD scale uncertainty covers the variations of predictions from changing the QCD renormalisation and factorisation scales, as described in Section 6. While the QCD scale uncertainty (see Section 6) is considered, uncertainties associated to PDFs are not included in the Matrix prediction. The derived fiducial phase space acceptance A_{ZZ} is also listed in Table 5.

The fiducial cross-sections for the processes $ZZ \to \ell\ell\nu\nu$ and $ZZjj \to \ell\ell\nu\nu jj$ are calculated using a combination of Sherpa and MadGraph5 MC samples. The QCD-induced production is simulated with Sherpa and the electroweak production is simulated with MadGraph5, as detailed in Section 3. The predicted cross-sections, including theory uncertainties, are presented in Table 6 for both the ZZ and $ZZjj$ fiducial phase spaces.

For the inclusive ZZ production, the fiducial cross-section calculated with Matrix is about 3% to 6% higher than the one calculated with Sherpa, primarily due to the inclusion of higher-order QCD corrections. Despite this difference, the results from both MC generators are consistent within their respective uncertainties. The acceptance correction factor C_{ZZ}, defined as the ratio of generated signal events passing the selection criteria using reconstructed objects to the number passing the fiducial criteria using generator-level objects, is found to be $C_{ZZ} = 0.59$.

Table 5: Predicted $ZZ \to \ell\ell\nu\nu$ ($\ell = e, \mu$) production cross-sections at $\sqrt{s} = 13$ TeV from MATRIX, calculated in the fiducial and total phase spaces. The first uncertainty reflects the MC statistical uncertainty, while the second reflects the QCD scale variations. In the third column, the fiducial phase space acceptance, A_{ZZ}, is presented along its corresponding theory uncertainty.

Higher-order corrections	$\sigma^{\text{fid.}}_{ZZ\to\ell\ell\nu\nu}$ **[fb]**	$\sigma^{\text{total}}_{ZZ\to\ell\ell\nu\nu}$ **[fb]**	A_{ZZ} **[%]**
($q\bar{q}$ NNLO + gg NLO) QCD + NLO EW	$21.03 \pm 0.27\,^{+0.08}_{-0.13}$	$413.9 \pm 4.7\,^{+10}_{-9.5}$	5.08 ± 0.13
($q\bar{q}$ NNLO + gg NLO) QCD × NLO EW	$20.74 \pm 0.27\,^{+0.10}_{-0.10}$	$407.6 \pm 4.5\,^{+10}_{-9.0}$	5.09 ± 0.13
($q\bar{q}$ NNLO) QCD × NLO EW + gg NLO QCD	$21.28 \pm 0.27\,^{+0.08}_{-0.11}$	$409.7 \pm 4.5\,^{+10}_{-9.4}$	5.14 ± 0.13

Table 6: Fiducial cross-sections for $ZZ \to \ell\ell\nu\nu$ and $ZZjj \to \ell\ell\nu\nu jj$ productions at $\sqrt{s} = 13$ TeV. The ZZ and $ZZjj$ cross-sections are obtained with the QCD production simulated using SHERPA and the electroweak production simulated using MADGRAPH5 (NLO EW). Theory uncertainties from QCD scale variations, PDFs, and α_s are quoted.

Cross-section	**Calculated value [fb]**
$\sigma^{\text{fid}}_{ZZ\to\ell\ell\nu\nu}$	20.1 ± 1.0 (QCD scale) ± 0.3 (PDF) ± 0.2 (α_s)
$\sigma^{\text{fid}}_{ZZjj\to\ell\ell\nu\nu jj}$	0.94 ± 0.19 (QCD scale) ± 0.01 (PDF) ± 0.02 (α_s)

8 Cross-section measurements

The signal strengths in the ZZ and $ZZjj$ signal regions are extracted using a binned profile-likelihood fit to the $\Delta\phi(\ell\ell, \vec{E}_{\text{T}}^{\text{miss}})$ distribution, performed simultaneously across the SRs and the relevant CRs. The likelihood function is constructed using the HISTFACTORY framework [77] implemented in ROOSTATS [78]. Background normalisation factors are included as free parameters in the fit and are primarily determined by data in the CRs, while the systematic uncertainties described in Section 6 are included as Gaussian-constrained nuisance parameters. All nuisance parameters are taken as fully correlated across analysis regions, except for theory uncertainties: QCD scale and PDF uncertainties are correlated across regions and uncorrelated between processes, while the alternative generator uncertainties, which apply only to the signal, are treated as uncorrelated.

For each SR, a signal strength and a set of background normalisation factors are obtained from the fit. The signal strength parameters, denoted as $\mu_{\text{s}}^{\text{ZZ}}$ and $\mu_{\text{s}}^{\text{ZZjj}}$, are defined as the ratio of the observed to predicted number of signal events in the ZZ and $ZZjj$ SRs, respectively: $\mu_{\text{s}}^{\text{SR}} = \frac{N_{\text{data}}^{\text{SR}}}{N_{\text{MC}}^{\text{SR}}}$. The predicted number of events come from the signal simulations by SHERPA and MADGRAPH5 described in Section 3. For the inclusive ZZ case, the background scale factors are μ_{WZ}, μ_{top}, μ_{WW}, $\mu_{\text{Z+0jets}}$, $\mu_{\text{Z+1jet}}$ and $\mu_{\text{Z+}\geq 2\text{jets}}$. For the $ZZjj$ case, the WW and top backgrounds are grouped in the non-resonant category and the normalisation factors used are μ_{WZ} and $\mu_{\text{non-resonant}}$. The Z+jets background in the $ZZjj$ case and all other minor backgrounds are taken from their MC predictions.

The measured signal strength in each SR is later used to derive the cross-section in the corresponding fiducial phase space. Theory systematic uncertainties are propagated to the measured cross-section via the ratio of reconstructed to fiducial number of MC signal events, in order to avoid double counting, as the signal strength $\mu_{\text{s}}^{\text{SR}}$ is defined relative to the reconstructed prediction.

In the inclusive ZZ case, the fitted signal strength is $\mu_{\mathrm{s}}^{ZZ} = 1.05 \pm 0.05$. The background scale factors are found to be: $1.00^{+0.06}_{-0.05}$ for WZ, $0.98^{+0.13}_{-0.10}$ for top, $1.27^{+0.18}_{-0.17}$ for WW, $1.14^{+0.44}_{-0.30}$ for Z+0jets, $1.06^{+0.37}_{-0.28}$ for Z+1jet, and $1.10^{+0.44}_{-0.31}$ for $Z+\geq$ 2jets.

In the $ZZjj$ case, the fitted signal strength is $\mu_s^{ZZjj} = 1.02^{+0.19}_{-0.17}$. The background normalisation factors are found to be $0.97^{+0.24}_{-0.20}$ for WZ and $1.08^{+0.19}_{-0.15}$ for the non-resonant backgrounds.

The post-fit $\Delta\phi(\vec{E}_{\mathrm{T}}^{\mathrm{miss}}, Z)$ distributions in the ZZ and $ZZjj$ SRs and in the various CRs are shown in Figure 3. Representative post-fit kinematic distributions in the signal regions are shown in Figure 4, where the transverse mass of the ZZ system is defined as $m_{\mathrm{T}}^{ZZ} = \sqrt{\left[\sqrt{m_{\mathrm{Z}}^2 + (p_{\mathrm{T}}^{\ell\ell})^2} + \sqrt{m_{\mathrm{Z}}^2 + (E_{\mathrm{T}}^{\mathrm{miss}})^2}\right]^2 - |\vec{p}_{\mathrm{T}}^{\,\ell\ell} + \vec{E}_{\mathrm{T}}^{\mathrm{miss}}|^2}$.

8.1 Integrated cross-sections

The integrated cross-sections for the processes $ZZ \to \ell\ell\nu\nu$ and $ZZjj \to \ell\ell\nu\nu jj$ in their respective fiducial phase spaces are calculated by multiplying the measured signal strengths (μ_{s}^{ZZ} and $\mu_{\mathrm{s}}^{ZZ\mathrm{jj}}$) by the SM cross-section predictions (σ_{MC}^{ZZ} and σ_{MC}^{ZZjj}), calculated with the Sherpa MC simulations, as shown in Table 6.

The measured fiducial cross-section for the inclusive $ZZ \to \ell\ell\nu\nu$ production process is found to be

$$\sigma_{ZZ}^{\mathrm{fid}} = 21.03 \pm 0.73\,(\mathrm{stat}) \pm 0.57\,(\mathrm{exp}) \pm 0.18\,(\mathrm{theory}) \pm 0.18\,(\mathrm{lumi})\ \mathrm{fb}.$$

where the uncertainty is separated into the data statistical uncertainty (stat), the uncertainty from experimental systematic uncertainties (exp), the uncertainty from theory systematic uncertainties (theory) and the luminosity uncertainty (lumi). The measured cross-section is in agreement with the SM prediction of 20.1 ± 1.1 fb from Sherpa+MadGraph5 and 21.03 ± 0.30 fb from Matrix.

For the $ZZjj \to \ell\ell\nu\nu jj$ production process, the measured fiducial cross-section is

$$\sigma_{ZZjj}^{\mathrm{fid}} = 0.96^{+0.15}_{-0.11}\,(\mathrm{stat}) \pm 0.10\,(\mathrm{exp}) \pm 0.04\,(\mathrm{theory}) \pm 0.01\,(\mathrm{lumi})\ \mathrm{fb}.$$

This is compatible with the theory prediction of 0.94 ± 0.20 fb from Sherpa+MadGraph5.

The $ZZ \to \ell\ell\nu\nu$ fiducial production cross-section is extrapolated to the total phase space, using the fiducial acceptance reported in Table 5 and the branching ratio [79] of the ZZ decay mode $ZZ \to 2\ell 2\nu$. The total $pp \to ZZ$ production is found to be:

$$\sigma_{\mathrm{measured}}^{\mathrm{total}}(pp \to ZZ) = 15.38 \pm 0.81\ \mathrm{pb}.$$

This measurement is in agreement with the SM prediction calculated using Matrix:

$$\sigma_{\mathrm{SM}}^{\mathrm{total}}(pp \to ZZ) = 15.40 \pm 0.38\ \mathrm{pb}.$$

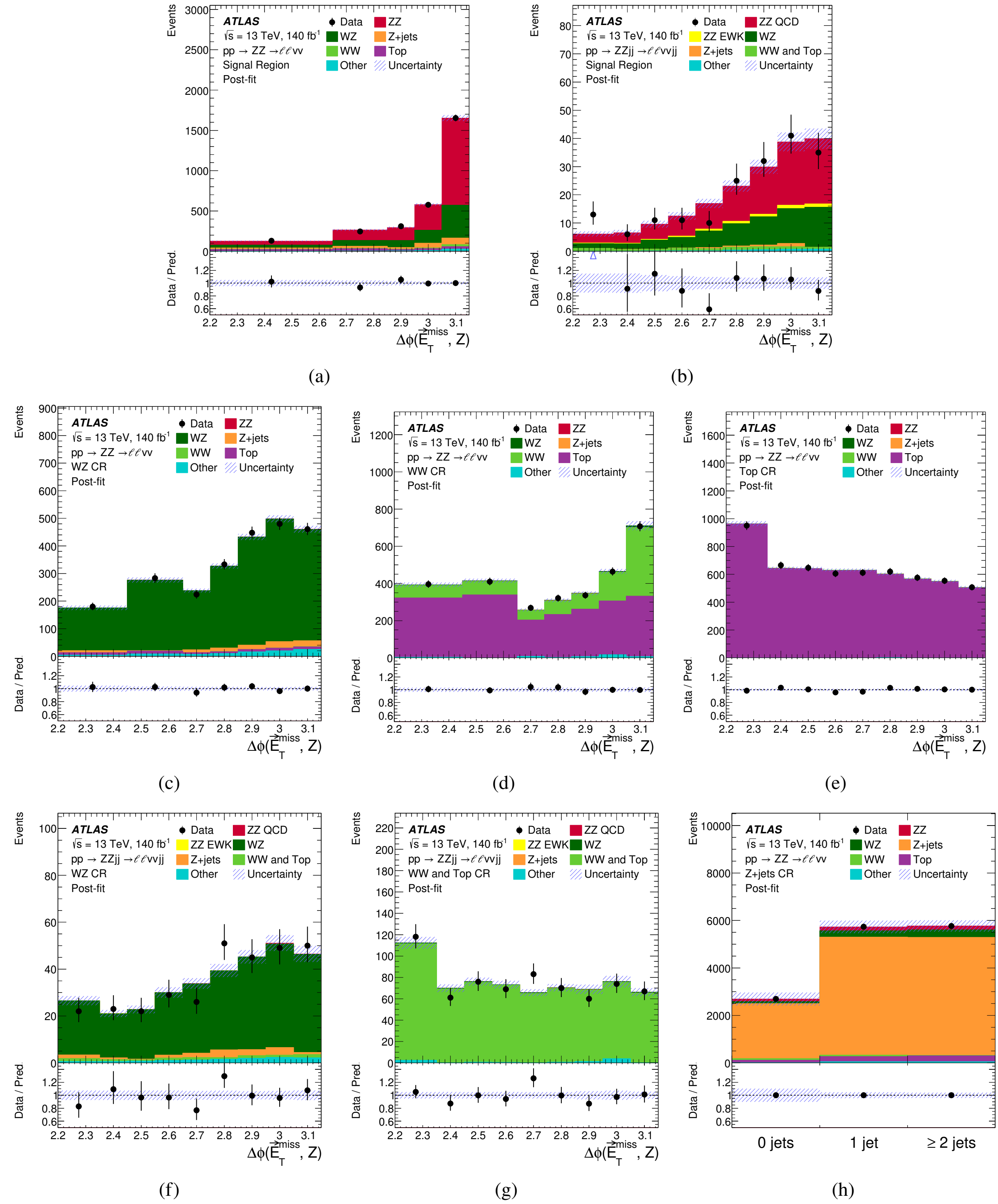

Figure 3: The post-fit distributions of $\Delta\phi(\vec{E}_{\mathrm{T}}^{\mathrm{miss}}, Z)$. Panels (a) and (b) show the signal regions for the inclusive ZZ and $ZZjj$ production, respectively. The "Other" category counts events from processes of $ZZ(\rightarrow 4\ell$, $2\ell 2q)$, $VVV(V = W, Z)$, Wj, $Z(\rightarrow \tau\tau)$, and WH. Panels (c), (d) and (e) illustrate the background CRs for inclusive ZZ production, while panels (f) and (g) display the $ZZjj$ CRs. Panel (h) presents the post-fit event yields for background events in the Z+jets CRs for the inclusive ZZ analysis. Data points are shown with statistical error bars, while the shaded band represents the total post-fit uncertainty in the prediction, combining statistical and systematic uncertainties. Open markers indicate data points lying outside the vertical range of the plot.

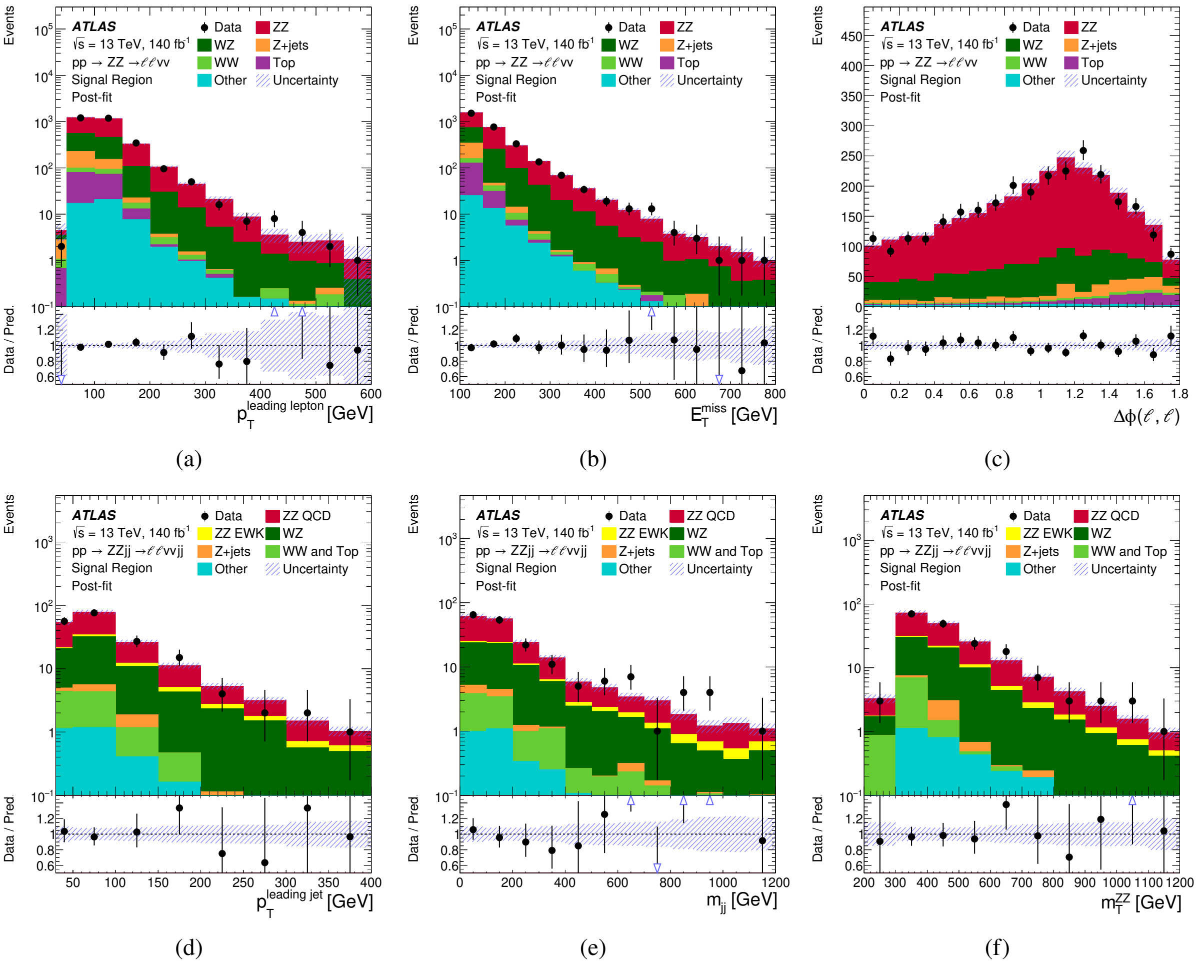

Figure 4: Post-fit kinematic distributions for the inclusive ZZ SR are shown in the top row: (a) the transverse momentum of the leading lepton $p_{\mathrm{T}}^{\text{leading lepton}}$, (b) $E_{\mathrm{T}}^{\text{miss}}$ and (c) the azimuthal angle separation between two charged leptons $\Delta\phi(\ell,\ell)$. For the $ZZjj$ SR, the bottom row shows: (d) the leading jet $p_{\mathrm{T}}^{\text{leading jet}}$, (e) the invariant mass of the dijet system m_{jj}, and (f) the transverse mass of the ZZ system m_{T}^{ZZ}. The data points are shown with statistical error bars, while the shaded band represents the total post-fit uncertainty in the prediction, combining statistical and systematic uncertainties. Open markers indicate data points lying outside the vertical range of the plot.

8.2 Differential cross-sections

Differential cross-sections are measured in the fiducial phase spaces by counting the data events in each bin of the relevant observables, subtracting the expected background contributions and correcting for detector effects. Detector-level distributions are unfolded to stable particle level using an iterative Bayesian method [80], which accounts for resolution effects, reconstruction inefficiencies and bin migrations. The response matrices are derived from simulated signal samples and encode the probability of an event generated in a given particle-level bin being reconstructed in a particular detector-level bin. The number of iterations, between two and five depending on the observable, is optimised to balance statistical uncertainty and unfolding stability. The binning is designed based on purity and efficiency criteria to ensure reliable unfolding and preserve the shape of the distributions. The last bin of each observable is open-ended and extends to the kinematic limit, so that it includes the full tail of the distribution; no separate overflow bin is used. Validation tests with the nominal and alternative samples are performed in the simulation and no significant bias is observed. The kinematic variables used for the differential cross-section measurements are summarised in Table 7.

A CP-sensitive angular variable, $\sin(\varphi)\cos(\theta)$, is constructed in the ZZ signal region following the prescription of Refs. [81–83]. The polar angle θ and the azimuthal angle φ are defined for the negatively charged lepton in the dilepton rest frame, using a special coordinate system in which the z-axis is aligned with the dilepton momentum in the ZZ rest frame. The x-axis lies in the reaction plane, sharing the same polar direction as the z-axis and the y-axis completes a right-handed system. Since neutrinos from $Z \to \nu\bar{\nu}$ decays are not directly detected, the dineutrino momentum is assumed to follow the relation $\vec{p}^{\,\nu\nu} = -\vec{p}^{\,\ell\ell}$, corresponding to the assumption of the ZZ system being at rest in the laboratory frame, and the same assumption is used at particle level to ensure a consistent definition. The differential cross-section as a function of this variable is unfolded to particle level in the fiducial phase space.

Figures 5 and 6 display the measured differential cross-sections. The uncertainties shown in the plots and tables include both statistical and systematic contributions, propagated through the unfolding procedure. Statistical uncertainties in the data dominate the measurement in most bins; however, systematic uncertainties are significant in specific kinematic regions.

Table 7: Kinematic variables for the differential cross-section measurements.

Observable description	**Observable**	**SR**
Azimuthal angular separation of the two leptons	$\Delta\phi(\ell,\ell)$	ZZ and $ZZjj$
Transverse momentum of the leading lepton	$p_{\mathrm{T}}^{\text{leading lepton}}$	ZZ only
Transverse momentum of the Z boson	p_{T}^{Z}	ZZ and $ZZjj$
Rapidity of the visible $Z \to \ell\ell$	$\lvert y^{Z}\rvert$	ZZ and $ZZjj$
Transverse momentum of the ZZ system	p_{T}^{ZZ}	ZZ and $ZZjj$
Transverse mass of the ZZ system	m_{T}^{ZZ}	ZZ and $ZZjj$
Number of jets	N_{jets}	ZZ only
CP-sensitive angular variable	$\sin(\varphi)\cos(\theta)$	ZZ only
Invariant mass of the dijet system	m_{jj}	$ZZjj$ only
Transverse momentum of the leading jet	$p_{\mathrm{T}}^{\text{leading jet}}$	$ZZjj$ only

The measured differential cross-sections in the ZZ fiducial phase space show good agreement with SM predictions from the nominal SHERPA+MADGRAPH5 MC simulation (denoted as SHERPA+MG5 in the plots) and from the MATRIX calculation. The MATRIX predictions exhibit slightly better agreement with the data, which can be attributed to the inclusion of NNLO QCD corrections.

In the $ZZjj$ phase space, the results are compared with SM predictions obtained using Sherpa for strong production and MadGraph5 for electroweak production. The total uncertainties in the $ZZjj$ measurements are larger than in the inclusive ZZ case, reflecting the higher statistical uncertainty and the larger jet-related systematic uncertainties. The Sherpa prediction describes well the data within uncertainties.

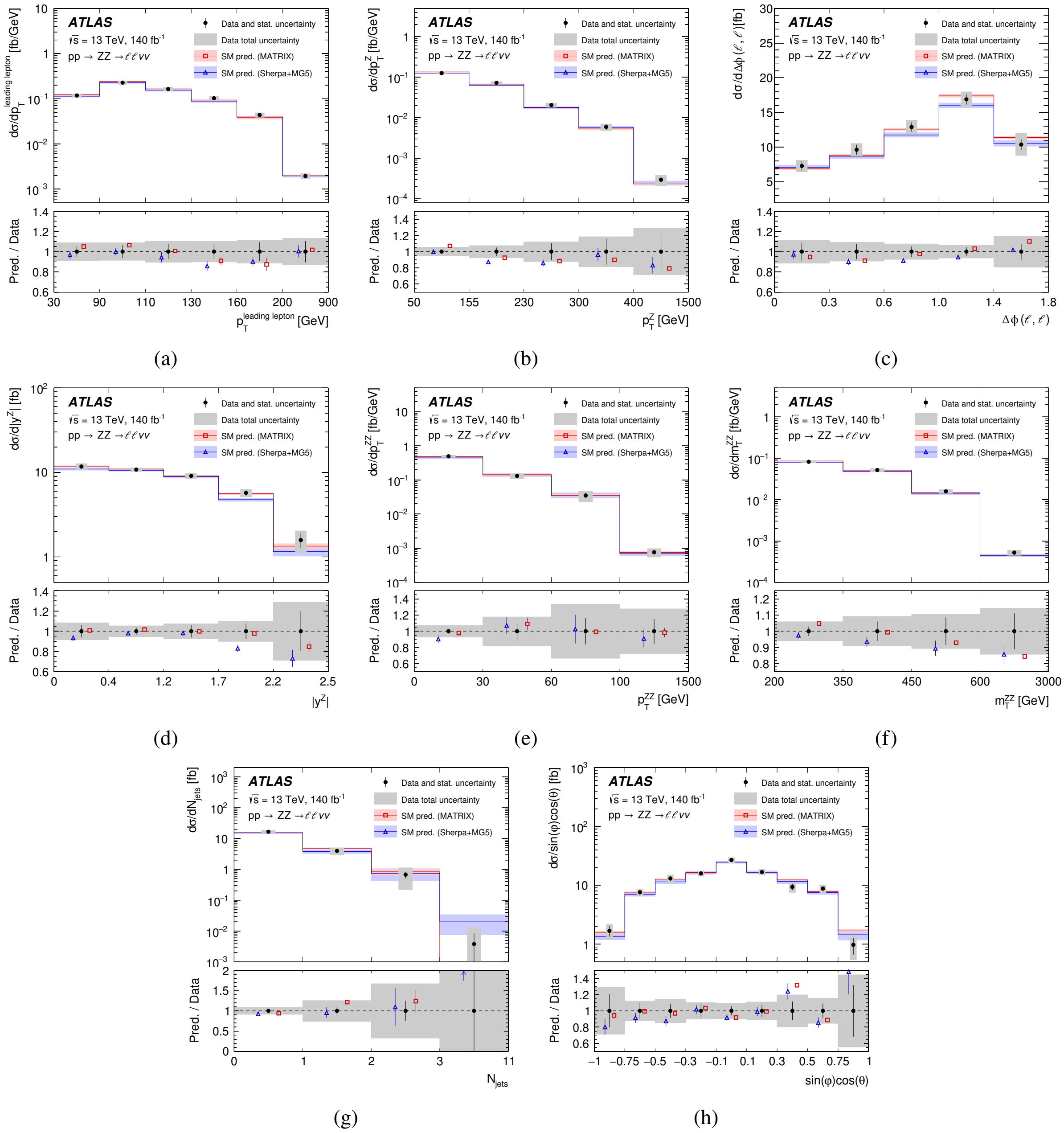

Figure 5: Differential cross-section measurements in the inclusive $ZZ \to \ell\ell\nu\nu$ fiducial phase space, compared with MC predictions calculated with the nominal Sherpa simulation and with Matrix for a set of kinematic variables: (a) $p_{\mathrm{T}}^{\text{leading lepton}}$, (b) p_{T}^{Z}, (c) $\Delta\phi(\ell,\ell)$, (d) $|y^Z|$, (e) p_{T}^{ZZ}, (f) m_{T}^{ZZ}, (g) N_{jets}, and (h) a CP-sensitive angular variable, $\sin(\varphi)\cos(\theta)$. The statistical and total uncertainties in the data points are displayed in both the differential cross-sections and the corresponding ratios. The total theory uncertainties in the Sherpa and Matrix predictions are represented as shaded bands in the cross-section panels and as error bars in the ratio panels.

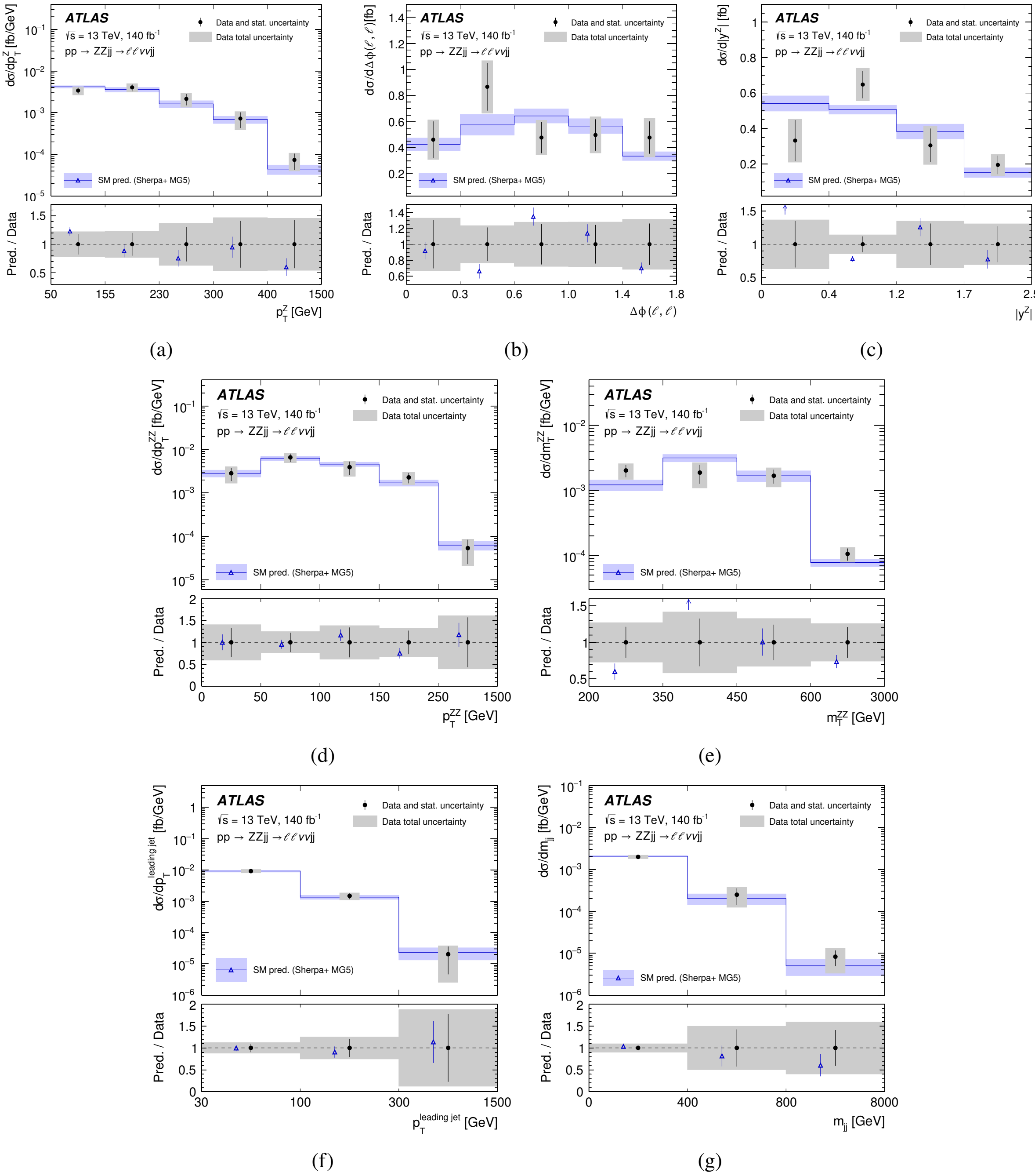

Figure 6: Differential cross-section measurements in the $ZZjj \to \ell\ell\nu\nu jj$ fiducial phase space, compared with SM predictions for a set of kinematic variables: (a) p_{T}^{Z}, (b) $\Delta\phi(\ell,\ell)$, (c) $|y^{Z}|$, (d) p_{T}^{ZZ}, (e) m_{T}^{ZZ}, (f) $p_{\mathrm{T}}^{\text{leading jet}}$, and (g) m_{jj}. The SM predictions are obtained using Sherpa for strong production and MadGraph5 for electroweak production. The statistical and total uncertainties in the data points are displayed in both the differential cross-sections and the corresponding ratios. The total theory uncertainties in the MC predictions are represented as shaded bands in the cross-section panels and as error bars in the ratio panels.

9 Probing anomalous gauge boson self-interaction couplings

The measured fiducial and total cross-sections are found to be in good agreement with the SM predictions within the quoted uncertainties. The inclusive ZZ and $ZZjj$ production processes in pp collisions are sensitive to deviations from SM predictions, particularly in the self-interactions between gauge bosons. Among all the contributing Feynman diagrams, shown in Figures 1 and 2, those involving aTGCs, specifically the ZZZ and $ZZ\gamma$ vertices and the triple gauge boson WWZ and the quartic gauge boson $WWZZ$ couplings, are of particular interest. These diagrams are directly connected to two fundamental aspects of the SM electroweak theory, namely the non-Abelian gauge group structure and spontaneous electroweak symmetry breaking. The ZZ production process serves as a key channel for probing aTGCs [84] while the $ZZjj$ production, which involves both triple and quartic gauge-boson self-interactions, enables searches for both aTGCs and aQGCs [85].

Since no unified framework simultaneously describing aTGC and aQGC is currently available, the inclusive ZZ measurement is used to constrain aTGC, while the $ZZjj$ process is used to search for aQGC.

Simulation samples for aTGC and aQGC are produced using the decomposition method, which expresses the matrix element for a process as:

$$|A_{\mathrm{SM}} + \sum_i c_i A_i|^2 = |A_{\mathrm{SM}}|^2 + \sum_i c_i\, 2\,\mathrm{Re}(A_{\mathrm{SM}} A_i^*) + \sum_i c_i^2 |A_i|^2 + \sum_{i\neq j} c_i c_j\, 2\,\mathrm{Re}(A_i A_j^*), \quad (1)$$

where A_{SM} is the SM amplitude, A_i the BSM (i.e., anomalous) contributions, and c_i the corresponding coupling coefficients. Apart from the pure SM contribution in the first term, the second term captures the interference between the SM amplitude and each BSM contribution, referred to as the linear term, the third term is the pure contribution from each BSM amplitude, referred to as the quadratic term, while the final term describes the interference between different BSM amplitudes. For both the aTGC and aQGC interpretations, all BSM contributions in Eq. (1) are taken into account, including the linear interference terms (c_i), the pure BSM quadratic terms (c_i^2), and the cross terms ($c_i c_j$).

The MC samples used for the interpretation of the aTGCs were generated at LO in QCD using MadGraph5 with the NNPDF3.0nnlo PDF set, employing Universal FeynRules Output (UFO) models [86], which provide the matrix-element implementation of the effective operators used for the signal generation. Parton showering, hadronisation, and modelling of the underlying event were performed using Pythia 8.2 with the A14 tune.

The MC predictions of the aQGCs in the final state $ZZjj \to \ell^+\ell^-\nu\bar{\nu}jj$ are generated using MadGraph5 with the NNPDF3.0 LO [43] PDF set. The events were interfaced with Pythia 8.2 with the A14 tune for modelling the parton shower, hadronisation, and underlying events.

Limits are derived under the linear+quadratic assumption, in which both the interference between the SM and dimension-eight SMEFT operators, and the quadratic contributions of those operators, are included in the cross-section. For both the aTGC and aQGC interpretations, detector-level distributions are used as inputs to the fit, as they allow optimised binning in the most sensitive regions while avoiding uncertainties associated with unfolding.

9.1 Constraints on anomalous neutral triple gauge couplings

As discussed in Section 1, aTGCs are absent at tree level in the SM. Consequently, any measurable deviation in the kinematic tails of ZZ production could be an evidence for aTGC. This subsection presents the corresponding limits, probing both CP-even and CP-odd couplings within two theoretical frameworks: a VF parameterisation [17, 87] and the SMEFT [15, 16].

The most general anomalous ZZV (where $V = Z, \gamma$) VF for on-shell Z bosons is given by [88]:

$$g_{ZZV}\Gamma^{\alpha\beta\mu}_{ZZV} = e\frac{P^2 - m_V^2}{m_Z^2}\left[if_4^V(P^\alpha g^{\mu\beta} + P^\beta g^{\mu\alpha}) + if_5^V\epsilon^{\mu\alpha\beta\rho}(q_1 - q_2)_\rho\right],$$

where g_{ZZV} represents the ZZV coupling, $\Gamma^{\alpha\beta\mu}_{ZZV}$ is the ZZV vertex function, e is the proton charge, P, q_1 and q_2 indicate the momenta of the V and two on-shell Z bosons, respectively. The anomalous triple gauge coupling parameters are f_4^V, which are CP-violating, and f_5^V, which are CP-conserving.

In this analysis, both anomalous triple and quartic gauge couplings are modelled via dimension-eight SMEFT operators; hence, the same extended Lagrangian is used for both cases. The SMEFT Lagrangian is extended as

$$\mathcal{L}_{\text{SMEFT}} = \mathcal{L}_{\text{SM}} + \sum_i \frac{C_i^{(8)}}{\Lambda^4}O_i^{(8)}, \tag{2}$$

where O_i are dimension-eight operators and C_i are their Wilson coefficients. In this analysis, the SMEFT formulation incorporates the dimension-eight operators $O_{G+}, O_{G-}, O_{\widetilde{B}W}, O_{BB}, O_{BW}$, and O_{WW}, each entering the Lagrangian with the corresponding Wilson coefficients C_{G+}/Λ^4, C_{G-}/Λ^4, $C_{\widetilde{B}W}/\Lambda^4$, C_{BB}/Λ^4, C_{BW}/Λ^4, and C_{WW}/Λ^4 [15, 16]. The energy scale Λ denotes the mass scale of heavy new physics that is integrated out and is set to $\Lambda = 1$ TeV throughout this analysis.

The sensitivity to both CP-even and CP-odd aTGCs arises from an enhancement in the high-energy tail of the ZZ production spectrum. Such a tail contains a low number of events and, therefore, the reconstructed variable distribution is more effective compared to the unfolded one. The distribution of the transverse momentum of the dilepton system, p_{T}^Z, is identified as the most sensitive observable and is used to extract limits on aTGCs. A binned likelihood fit is performed on the p_{T}^Z differential distribution shown in Figure 7, using the same phase space as defined for the ZZ cross-section measurement, to extract 95% confidence level intervals for the anomalous parameters. Systematic uncertainties are incorporated as nuisance parameters in the fit, and the results are shown in Table 8, where limits are derived on one coupling coefficient given all other anomalous couplings set to zero. Using the same distribution, limits on two parameters at a time are provided and presented in Figures 8 and 9.

Compared to other results, the limits shown in Table 8 on the VF parameters are better by about a factor of 1.7 with respect to those from the previous ATLAS $pp \to ZZ \to \ell\ell\nu\nu$ analysis based on a subset (36.1 fb^{-1}) of the dataset [6].

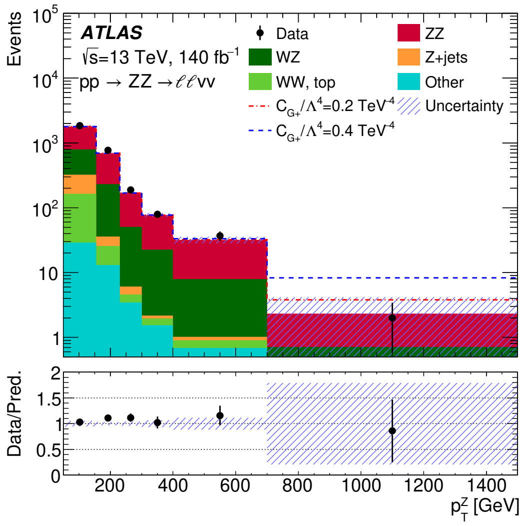

Figure 7: Distribution of the dilepton transverse momentum, p_{T}^{Z}, at detector level. The dashed band represents the total uncertainty in the pre-fit SM prediction, with no normalization factors applied from the signal extraction fit. The expected effects of an aTGC induced by the operator O_{G+}, for two different values of the Wilson coefficient, are also shown.

Table 8: Expected and observed 95% CL intervals on the parameters of the VF and the SMEFT formalisms in the inclusive ZZ channel, obtained without applying any unitarization procedure. The results are derived by setting all other aTGC parameters to zero.

Coefficient	Expected	Observed
f_4^{γ}	$[-7.7,\ 7.7] \times 10^{-4}$	$[-6.4,\ 6.4] \times 10^{-4}$
f_4^{Z}	$[-6.8,\ 6.8] \times 10^{-4}$	$[-5.7,\ 5.7] \times 10^{-4}$
f_5^{γ}	$[-7.8,\ 7.7] \times 10^{-4}$	$[-6.4,\ 6.5] \times 10^{-4}$
f_5^{Z}	$[-6.9,\ 6.9] \times 10^{-4}$	$[-5.8,\ 5.8] \times 10^{-4}$
C_{G+}/Λ^4 [TeV^{-4}]	$[-0.36,\ 0.36]$	$[-0.29,\ 0.30]$
C_{G-}/Λ^4 [TeV^{-4}]	$[-1.1,\ 1.2]$	$[-0.95,\ 0.95]$
$C_{\tilde{B}W}/\Lambda^4$ [TeV^{-4}]	$[-1.3,\ 1.3]$	$[-1.1,\ 1.1]$
C_{BB}/Λ^4 [TeV^{-4}]	$[-1.6,\ 1.6]$	$[-1.3,\ 1.3]$
C_{BW}/Λ^4 [TeV^{-4}]	$[-2.9,\ 2.9]$	$[-2.4,\ 2.4]$
C_{WW}/Λ^4 [TeV^{-4}]	$[-2.4,\ 2.4]$	$[-2.0,\ 2.0]$

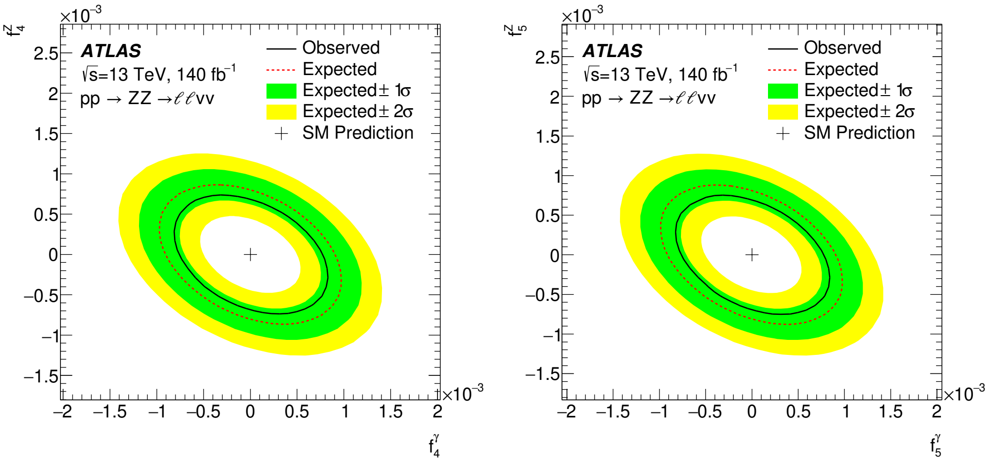

(a)

(b)

Figure 8: Two-dimensional 95% confidence level limit contours on the aTGC parameters, (a) f_4^γ vs. f_4^Z and (b) f_5^γ vs. f_5^Z of the vertex function formalism. The inner (outer) bands show the expected $\pm 1\sigma$ ($\pm 2\sigma$) regions around the expected limit contours, corresponding to the range of fluctuations from statistical and systematic uncertainties under the Standard Model hypothesis. The results were obtained without applying any unitarization procedure and by setting the other parameters to zero.

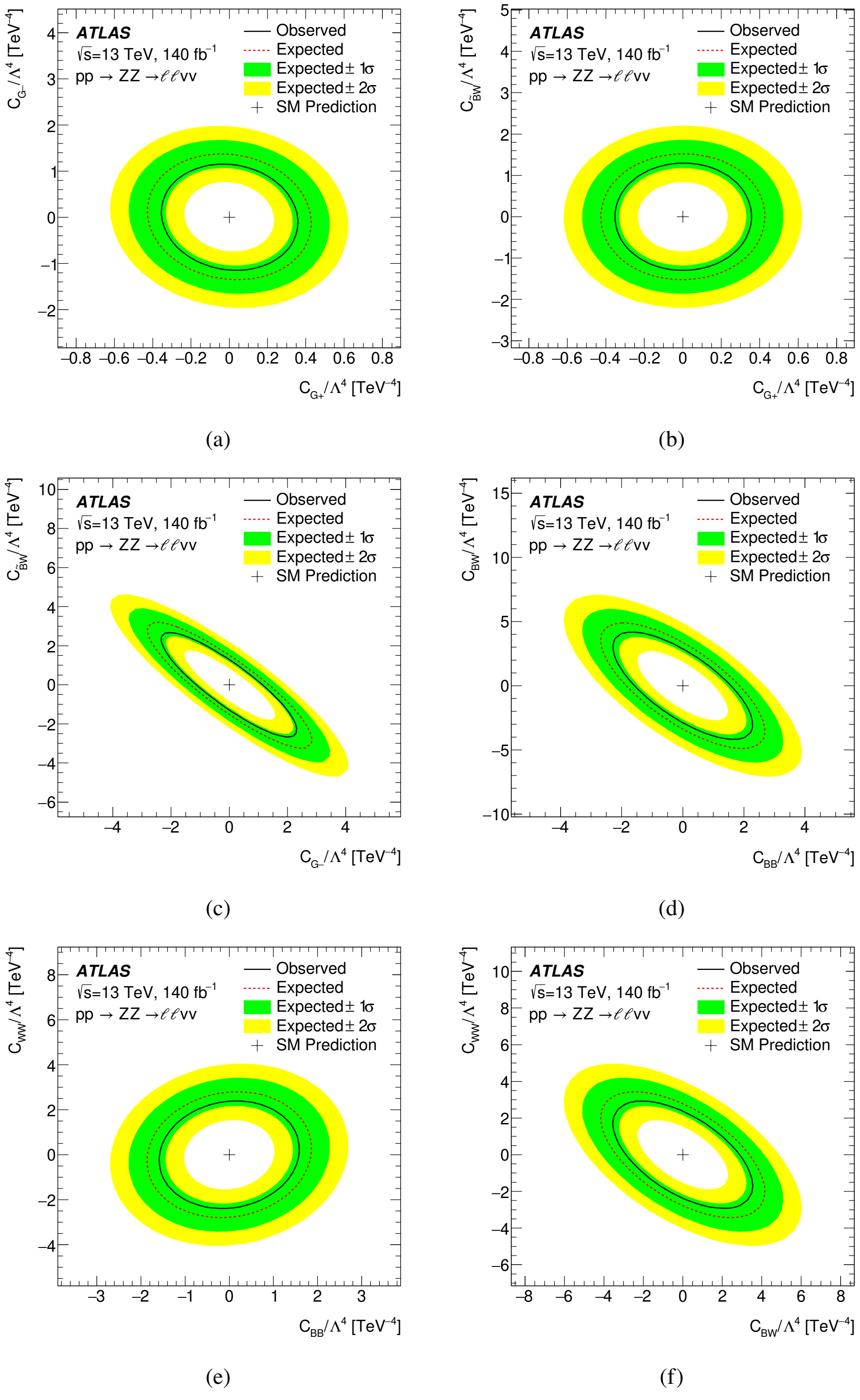

Figure 9: Two-dimensional 95% confidence level limit contours on aTGC Wilson coefficients with the EFT formalism. The inner (outer) bands show the expected $\pm 1\sigma$ ($\pm 2\sigma$) regions around the expected limit contours, corresponding to the range of fluctuations from statistical and systematic uncertainties under the Standard Model hypothesis. The results were obtained without applying any unitarization procedure and by setting the other Wilson coefficients to zero.

9.2 Constraints on anomalous quartic gauge couplings

The measurement of $ZZjj$ production is particularly sensitive to VBS processes, which offer a unique probe of quartic electroweak gauge boson interactions. In the context of the SMEFT framework, such effects are parameterised by extending the SM Lagrangian with higher-dimensional operators. Dimension-8 operators are considered here, as they directly contribute to quartic gauge couplings, which do not arise at lower dimensions [89].

As in Eq. (2), the SMEFT Lagrangian includes dimension-eight operators $O_{T,i}$, each associated to a Wilson coefficient $f_{\mathrm{T,i}}/\Lambda^4$, where $i = 0, 1, \ldots, 9$, to distinguish them from the C_i coefficients used for aTGCs in Section 9.1.

The reconstructed transverse mass of the ZZ system, m_{T}^{ZZ}, seen in Figure 10, is identified as the most sensitive observable and is used to extract limits on these dimension-8 SMEFT operators. A binned likelihood fit is performed on the m_{T}^{ZZ} differential distribution to derive 95% CL intervals for the Wilson coefficients. Systematic uncertainties are included as nuisance parameters in the fit, and the resulting limits are summarised in Table 9, where limits are derived by setting all Wilson coefficients to zero but the one tested. To ensure the validity of the SMEFT expansion, unitarity-preserving cut-offs are applied to the BSM contributions by restricting $m_{ZZ} < E_c$, where E_c is the energy cut-off scale. All coefficients are found to be consistent with zero. The most stringent constraints are obtained for f_{T0} and f_{T1}. The present limits are better by more than a factor of two relative to previous ATLAS results obtained with $ZZ \to 4\ell$ events [13].

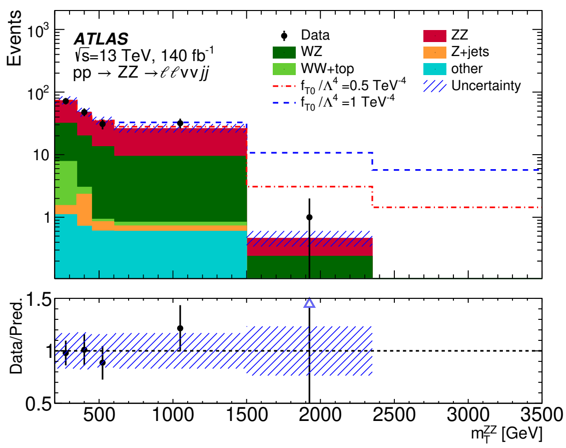

Figure 10: Distribution of the transverse mass of the ZZ system, m_{T}^{ZZ}, at detector level. The dashed band represents the total uncertainty in the pre-fit SM prediction, with no normalization factors applied from the signal extraction fit. The expected effects of aQGC induced by the SMEFT operator f_{T0}, for two different values of the Wilson coefficient, are also shown.

Figures 11 and 12 show the evolution of the limits on the Wilson coefficients $f_{\mathrm{T,i}}$, as a function of E_c. The unitarity bounds shown in Figures 11 and 12 indicate the parameter values above which the SMEFT description breaks down due to violation of perturbative unitarity. They are computed following the prescription in Ref. [90], based on the energy scale at which the partonic scattering amplitude exceeds the unitarity limit.

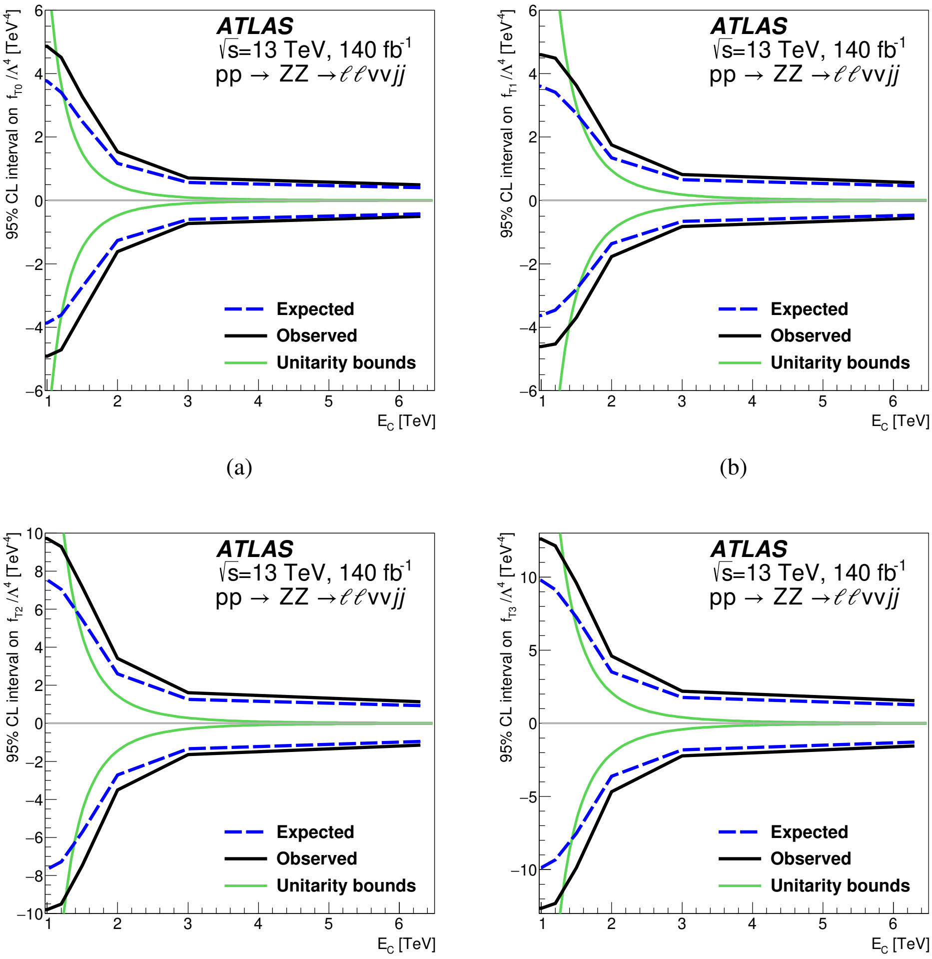

Figure 11: The expected and observed 95% CL intervals for the (a) f_{T0}, (b) f_{T1}, (c) f_{T2} and (d) f_{T3} Wilson coefficients are derived as a function of the cut-off scale, E_{c}, which imposes a restriction such that the BSM amplitudes of interference and pure dimension-eight are set to zero when $m_{ZZ} < E_{\mathrm{c}}$. These constraints are determined by performing a one-dimensional fit to the m_{T}^{ZZ} distribution in the $\ell\ell\nu\nu jj$ signal region. The dashed (solid) lines show the expected (observed) 95% CL limits, and the solid curve corresponds to the unitarity bounds [90].

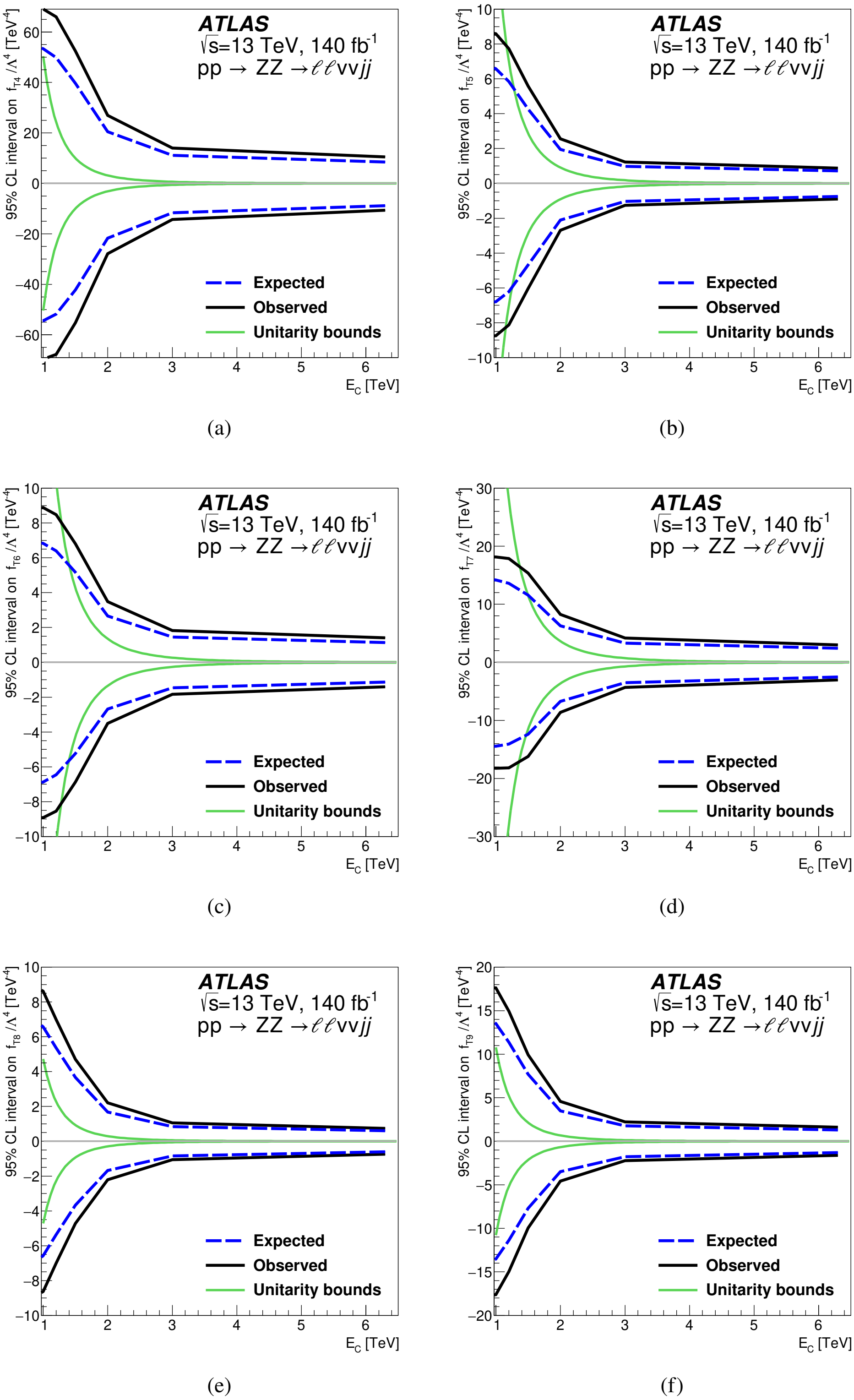

Figure 12: The expected and observed 95% CL intervals for the (a) f_{T4}, (b) f_{T5}, (c) f_{T6}, (d) f_{T7}, (e) f_{T8} and (f) f_{T9} Wilson coefficients are derived as a function of the cut-off scale, E_c, which imposes a restriction such that the BSM amplitudes of interference and pure dimension-eight are set to zero when $m_{ZZ} < E_c$. These constraints are determined by performing a one-dimensional fit to the m_T^{ZZ} distribution in the $\ell\ell\nu\nu jj$ signal region. The dashed (solid) lines show the expected (observed) 95% CL limits, and the solid curve corresponds to the unitarity bounds [90].

Table 9: Expected and observed 95% CL intervals on the dimension-8 Wilson coefficients, quoted in units of TeV^{-4}, for different cut-off scales.

Wilson Coefficient	**No cut-off**		E_c = 1 TeV		E_c = 1.5 TeV	
[TeV^{-4}]	Expected	Observed	Expected	Observed	Expected	Observed
f_{T0}/Λ^4	[−0.42, 0.40]	[−0.50, 0.49]	[−3.9, 3.8]	[−4.9, 4.9]	[−2.8, 2.6]	[−4.0, 3.4]
f_{T1}/Λ^4	[−0.46, 0.46]	[−0.56, 0.56]	[−3.7, 3.6]	[−4.6, 4.6]	[−2.9, 2.8]	[−3.8, 3.8]
f_{T2}/Λ^4	[−0.95, 0.93]	[−1.1, 1.1]	[−7.7, 7.6]	[−9.8, 9.7]	[−5.9, 5.6]	[−7.7, 7.4]
f_{T3}/Λ^4	[−1.3, 1.3]	[−1.6, 1.6]	[−9.9, 9.9]	[−13, 13]	[−7.7, 7.4]	[−10, 9.7]
f_{T4}/Λ^4	[−8.8, 8.5]	[−11, 11]	[−55, 54]	[−69, 69]	[−43, 41]	[−56, 53]
f_{T5}/Λ^4	[−0.75, 0.71]	[−0.89, 0.87]	[−6.9, 6.7]	[−8.7, 8.6]	[−4.8, 4.4]	[−6.2, 5.8]
f_{T6}/Λ^4	[−1.1, 1.1]	[−1.4, 1.4]	[−6.9, 6.9]	[−8.9, 8.9]	[−5.4, 5.3]	[−7.1, 7.0]
f_{T7}/Λ^4	[−2.5, 2.4]	[−3.0, 3.0]	[−14, 14]	[−18, 18]	[−12, 12]	[−17, 16]
f_{T8}/Λ^4	[−0.60, 0.60]	[−0.74, 0.74]	[−6.7, 6.7]	[−8.7, 8.7]	[−3.8, 3.8]	[−4.9, 4.9]
f_{T9}/Λ^4	[−1.3, 1.3]	[−1.6, 1.6]	[−14, 14]	[−18, 18]	[−7.9, 7.9]	[−10, 10]

10 Conclusion

Integrated and differential cross-sections for Z boson pair production in the $ZZ \to \ell\ell\nu\nu$ final state, where $\ell = e, \mu$, are measured in both inclusive ZZ and $ZZjj$ production modes at $\sqrt{s}$ = 13 TeV using 140 fb^{-1} of ATLAS data collected at the LHC. The $ZZjj$ measurement requires at least two jets. The inclusive $ZZ \to \ell\ell\nu\nu$ and $ZZjj \to \ell\ell\nu\nu jj$ fiducial cross-sections are measured as 21.0 ± 1.0 fb and $0.96^{+0.18}_{-0.16}$ fb, respectively. Compared with earlier results using a partial Run-2 dataset, the total uncertainty in the inclusive ZZ fiducial measurement improves from 7.0% to 4.6% and is limited by the statistical uncertainty. The measured values are in agreement with the corresponding SM predictions of 20.1 ± 1.1 fb and 0.94 ± 0.20 fb from Sherpa+MadGraph5. The Matrix prediction for the inclusive $ZZ \to \ell\ell\nu\nu$ fiducial cross-section is 21.03 ± 0.30 fb, demonstrating that the theory uncertainty in the prediction is reduced from 5.8% to 1.5% thanks to calculations incorporating NNLO QCD and NLO EW corrections. The inclusive $ZZ \to \ell\ell\nu\nu$ cross-section is extrapolated to the total phase space, yielding a value of 15.38 ± 0.81 pb, in agreement with the SM prediction of 15.40 ± 0.38 pb from Matrix. Differential cross-sections for both ZZ and $ZZjj$ productions are measured as functions of observables that provide high-precision tests of the SM and input for modelling studies. The transverse momentum of the dilepton system is used to constrain anomalous neutral triple gauge couplings via both the effective vertex approach and the SMEFT framework. In the vertex-function formalism, limits are set on f_4^Z, f_4^γ, f_5^γ and f_5^Z, improving previous results in this final state by a factor of 1.7. In the SMEFT interpretation, limits are derived on the Wilson coefficients C_{G+}/Λ^4, C_{G-}/Λ^4, C_{BW}/Λ^4, C_{BB}/Λ^4, $C_{\tilde{B}W}/\Lambda^4$ and C_{WW}/Λ^4. In the $ZZjj$ channel, the transverse mass of the ZZ system is used to constrain dimension-eight operators contributing to aQGCs, with limits improving sensitivity by a factor of 2 relative to the $4\ell jj$ channel due to the larger branching ratio of the $\ell\ell\nu\nu$ final state. Overall, the results show excellent agreement with SM predictions and provide significantly improved sensitivity to new physics in the electroweak sector.

Acknowledgements

We thank CERN for the very successful operation of the LHC and its injectors, as well as the support staff at CERN and at our institutions worldwide without whom ATLAS could not be operated efficiently.

The crucial computing support from all WLCG partners is acknowledged gratefully, in particular from CERN, the ATLAS Tier-1 facilities at TRIUMF/SFU (Canada), NDGF (Denmark, Norway, Sweden), CC-IN2P3 (France), KIT/GridKA (Germany), INFN-CNAF (Italy), NL-T1 (Netherlands), PIC (Spain), RAL (UK) and BNL (USA), the Tier-2 facilities worldwide and large non-WLCG resource providers. Major contributors of computing resources are listed in Ref. [91].

We gratefully acknowledge the support of ANPCyT, Argentina; YerPhI, Armenia; ARC, Australia; BMWFW and FWF, Austria; ANAS, Azerbaijan; CNPq and FAPESP, Brazil; NSERC, NRC and CFI, Canada; CERN; ANID, Chile; CAS, MOST and NSFC, China; Minciencias, Colombia; MEYS CR, Czech Republic; DNRF and DNSRC, Denmark; IN2P3-CNRS and CEA-DRF/IRFU, France; SRNSFG, Georgia; BMFTR, HGF and MPG, Germany; GSRI, Greece; RGC and Hong Kong SAR, China; ICHEP and Academy of Sciences and Humanities, Israel; INFN, Italy; MEXT and JSPS, Japan; CNRST, Morocco; NWO, Netherlands; RCN, Norway; MNiSW, Poland; FCT, Portugal; MNE/IFA, Romania; MSTDI, Serbia; MSSR, Slovakia; ARIS and MVZI, Slovenia; DSI/NRF, South Africa; MICIU/AEI, Spain; SRC and Wallenberg Foundation, Sweden; SERI, SNSF and Cantons of Bern and Geneva, Switzerland; NSTC, Taipei; TENMAK, Türkiye; STFC/UKRI, United Kingdom; DOE and NSF, United States of America.

Individual groups and members have received support from BCKDF, CANARIE, CRC and DRAC, Canada; CERN-CZ, FORTE and PRIMUS, Czech Republic; COST, ERC, ERDF, Horizon 2020, ICSC-NextGenerationEU and Marie Skłodowska-Curie Actions, European Union; Investissements d'Avenir Labex, Investissements d'Avenir Idex and ANR, France; DFG and AvH Foundation, Germany; Herakleitos, Thales and Aristeia programmes co-financed by EU-ESF and the Greek NSRF, Greece; BSF-NSF and MINERVA, Israel; NCN and NAWA, Poland; La Caixa Banking Foundation, CERCA Programme Generalitat de Catalunya and PROMETEO and GenT Programmes Generalitat Valenciana, Spain; Göran Gustafssons Stiftelse, Sweden; The Royal Society and Leverhulme Trust, United Kingdom.

In addition, individual members wish to acknowledge support from CERN: European Organization for Nuclear Research (CERN DOCT); Chile: Agencia Nacional de Investigación y Desarrollo (FONDECYT 1230812, FONDECYT 1240864, Fondecyt 3240661, Fondecyt Regular 1240721); China: Chinese Ministry of Science and Technology (MOST-2023YFA1605700, MOST-2023YFA1609300), National Natural Science Foundation of China (NSFC - 12175119, NSFC 12275265); Czech Republic: Czech Science Foundation (GACR - 24-11373S), Ministry of Education Youth and Sports (ERC-CZ-LL2327, FORTE CZ.02.01.01/00/22_008/0004632), PRIMUS Research Programme (PRIMUS/21/SCI/017); EU: H2020 European Research Council (ERC - 101002463); European Union: European Research Council (BARD No. 101116429, ERC - 948254, ERC 101089007), European Regional Development Fund (SMASH COFUND 101081355, SLO ERDF), European Union, Future Artificial Intelligence Research (FAIR-NextGenerationEU PE00000013), Italian Center for High Performance Computing, Big Data and Quantum Computing (ICSC, NextGenerationEU); France: Agence Nationale de la Recherche (ANR-21-CE31-0022, ANR-22-EDIR-0002, ANR-24-CE31-0504-01); Germany: Baden-Württemberg Stiftung (BW Stiftung-Postdoc Eliteprogramme), Deutsche Forschungsgemeinschaft (DFG - 469666862, DFG - CR 312/5-2); China: Research Grants Council (GRF); Italy: Istituto Nazionale di Fisica Nucleare (ICSC, NextGenerationEU), Ministero dell'Università e della Ricerca (NextGenEU 153D23001490006 M4C2.1.1, NextGenEU I53D23000820006 M4C2.1.1, NextGenEU I53D23001490006 M4C2.1.1, SOE2024_0000023); Japan:

Japan Society for the Promotion of Science (JSPS KAKENHI JP22H01227, JSPS KAKENHI JP22H04944, JSPS KAKENHI JP22KK0227, JSPS KAKENHI JP24K23939, JSPS KAKENHI JP24KK0251, JSPS KAKENHI JP25H00650, JSPS KAKENHI JP25H01291, JSPS KAKENHI JP25K01023); Norway: Research Council of Norway (RCN-314472); Poland: Ministry of Science and Higher Education (IDUB AGH, POB8, D4 no 9722), Polish National Science Centre (NCN 2021/42/E/ST2/00350, NCN OPUS 2023/51/B/ST2/02507, NCN UMO-2019/34/E/ST2/00393, UMO-2022/47/O/ST2/00148, UMO-2023/49/B/ST2/04085, UMO-2023/51/B/ST2/00920, UMO-2024/53/N/ST2/00869); Portugal: Foundation for Science and Technology (FCT); Spain: Generalitat Valenciana (ASFAE/2022/008), Ministry of Science and Innovation (MCIN & NextGenEU PCI2022-135018-2, MICIN & FEDER PID2021-125273NB, RYC2019-028510-I, RYC2020-030254-I, RYC2021-031273-I, RYC2022-038164-I), Ministerio de Ciencia, Innovación y Universidades/Agencia Estatal de Investigación (PID2022-142604OB-C22); Sweden: Carl Trygger Foundation (Carl Trygger Foundation CTS 22:2312), Swedish Research Council (Swedish Research Council 2023-04654, VR 2021-03651, VR 2022-03845, VR 2022-04683, VR 2023-03403, VR 2024-05451), Knut and Alice Wallenberg Foundation (KAW 2018.0458, KAW 2022.0358, KAW 2023.0366); Switzerland: Swiss National Science Foundation (SNSF - PCEFP2_194658); United Kingdom: Royal Society (NIF-R1-231091); United States of America: U.S. Department of Energy (ECA DE-AC02-76SF00515), Neubauer Family Foundation.

References

[1] L. Evans and P. Bryant, *LHC Machine*, JINST **3** (2008) S08001.

[2] G. J. Gounaris, J. Layssac and F. M. Renard, *New and standard physics contributions to anomalous Z and γ self-couplings*, Phys. Rev. D **62** (2000) 073013, arXiv: hep-ph/0003143 [hep-ph].

[3] ATLAS Collaboration, *Measurement of ZZ production in pp collisions at $\sqrt{s} = 7$ TeV and limits on anomalous ZZZ and ZZγ couplings with the ATLAS detector*, JHEP **03** (2013) 128, arXiv: 1211.6096 [hep-ex].

[4] ATLAS Collaboration, *Measurement of the ZZ production cross section in proton–proton collisions at $\sqrt{s} = 8$ TeV using the $ZZ \to \ell^-\ell^+\ell'^-\ell'^+$ and $ZZ \to \ell^-\ell^+\nu\bar{\nu}$ decay channels with the ATLAS detector*, JHEP **01** (2017) 099, arXiv: 1610.07585 [hep-ex].

[5] ATLAS Collaboration, *$ZZ \to \ell^+\ell^-\ell'^+\ell'^-$ cross-section measurements and search for anomalous triple gauge couplings in 13 TeV pp collisions with the ATLAS detector*, Phys. Rev. D **97** (2018) 032005, arXiv: 1709.07703 [hep-ex].

[6] ATLAS Collaboration, *Measurement of ZZ production in the $\ell\ell\nu\nu$ final state with the ATLAS detector in pp collisions at $\sqrt{s} = 13$ TeV*, JHEP **10** (2019) 127, arXiv: 1905.07163 [hep-ex].

[7] ATLAS Collaboration, *Measurement of ZZ production cross-sections in the four-lepton final state in pp collisions at $\sqrt{s} = 13.6$ TeV with the ATLAS experiment*, Phys. Lett. B **855** (2024) 138764, arXiv: 2311.09715 [hep-ex].

[8] CMS Collaboration, *Measurement of the ZZ production cross section and search for anomalous couplings in $2\ell2\ell'$ final states in pp collisions at $\sqrt{s} = 7$ TeV*, JHEP **01** (2013) 063, arXiv: 1211.4890 [hep-ex].

[9] CMS Collaboration, *Measurement of the $pp \to ZZ$ production cross section and constraints on anomalous triple gauge couplings in four-lepton final states at $\sqrt{s} = 8$ TeV*, Phys. Lett. B **740** (2015) 250, arXiv: 1406.0113 [hep-ex].

[10] CMS Collaboration, *Measurement of the ZZ production cross section and $Z \to \ell^+\ell^-\ell'^+\ell'^-$ branching fraction in pp collisions at $\sqrt{s} = 13$ TeV*, Phys. Lett. B **763** (2016) 280, arXiv: 1607.08834 [hep-ex].

[11] CMS Collaboration, *Measurements of $pp \to ZZ$ production cross sections and constraints on anomalous triple gauge couplings at $\sqrt{s} = 13$ TeV*, Eur. Phys. J. C **81** (2021) 200, arXiv: 2009.01186 [hep-ex].

[12] ATLAS Collaboration, *Observation of electroweak production of two jets and a Z-boson pair*, Nature Phys. **19** (2023) 237, arXiv: 2004.10612 [hep-ex].

[13] ATLAS Collaboration, *Differential cross-section measurements of the production of four charged leptons in association with two jets using the ATLAS detector*, JHEP **01** (2024) 004, arXiv: 2308.12324 [hep-ex].

[14] A. Falkowski and et al., *Anomalous triple gauge couplings in the effective field theory approach at the LHC*, JHEP **2017** (2017) 115, arXiv: 1609.06312.

[15] C. Degrande,
A basis of dimension-eight operators for anomalous neutral triple gauge boson interactions,
JHEP **02** (2014) 101, arXiv: 1308.6323 [hep-ph].

[16] J. Ellis, H.-J. He and R.-Q. Xiao,
Probing neutral triple gauge couplings at the LHC and future hadron colliders,
Phys. Rev. D **107** (2023) 035005, arXiv: 2206.11676.

[17] U. Baur and D. Rainwater,
Probing Neutral Gauge Boson Self-interactions in ZZ Production at Hadron Colliders,
Phys. Rev. D **62** (2000) 113011, arXiv: hep-ph/0008063 [hep-ph].

[18] ATLAS Collaboration, *The ATLAS Experiment at the CERN Large Hadron Collider*,
JINST **3** (2008) S08003.

[19] G. Avoni et al., *The new LUCID-2 detector for luminosity measurement and monitoring in ATLAS*,
JINST **13** (2018) P07017.

[20] ATLAS Collaboration, *Performance of the ATLAS trigger system in 2015*,
Eur. Phys. J. C **77** (2017) 317, arXiv: 1611.09661 [hep-ex].

[21] ATLAS Collaboration, *Software and computing for Run 3 of the ATLAS experiment at the LHC*,
Eur. Phys. J. C **85** (2025) 234, arXiv: 2404.06335 [hep-ex].

[22] ATLAS Collaboration,
Luminosity determination in pp collisions at $\sqrt{s}$ = 13 TeV using the ATLAS detector at the LHC,
Eur. Phys. J. C **83** (2023) 982, arXiv: 2212.09379 [hep-ex].

[23] ATLAS Collaboration, *ATLAS data quality operations and performance for 2015–2018 data-taking*,
JINST **15** (2020) P04003, arXiv: 1911.04632 [physics.ins-det].

[24] ATLAS Collaboration, *Performance of the ATLAS muon triggers in Run 2*,
JINST **15** (2020) P09015, arXiv: 2004.13447 [physics.ins-det].

[25] ATLAS Collaboration, *Performance of electron and photon triggers in ATLAS during LHC Run 2*,
Eur. Phys. J. C **80** (2020) 47, arXiv: 1909.00761 [hep-ex].

[26] ATLAS Collaboration, *The ATLAS Simulation Infrastructure*, Eur. Phys. J. C **70** (2010) 823,
arXiv: 1005.4568 [physics.ins-det].

[27] S. Agostinelli et al., *GEANT4 - A Simulation Toolkit*, Nucl. Instrum. Meth. A **506** (2003) 250.

[28] T. Sjöstrand, S. Mrenna and P. Skands, *A brief introduction to PYTHIA 8.1*,
Comput. Phys. Commun. **178** (2008) 852, arXiv: 0710.3820 [hep-ph].

[29] ATLAS Collaboration, *The Pythia 8 A3 tune description of ATLAS minimum bias and inelastic measurements incorporating the Donnachie–Landshoff diffractive model*,
ATL-PHYS-PUB-2016-017, 2016, URL: https://cds.cern.ch/record/2206965.

[30] E. Bothmann et al., *Event generation with Sherpa 2.2*, SciPost Phys. **7** (2019) 034,
arXiv: 1905.09127 [hep-ph].

[31] F. Caola, K. Melnikov, R. Röntsch and L. Tancredi,
QCD corrections to ZZ production in gluon fusion at the LHC, Phys. Rev. D **92** (2015) 094028,
arXiv: 1509.06734 [hep-ph].

[32] E. Accomando, A. Denner and A. Kaiser,
Logarithmic electroweak corrections to gauge-boson pair production at the LHC,
Nucl. Phys. B **706** (2005) 325, arXiv: hep-ph/0409247 [hep-ph].

[33] S. Kallweit, J. M. Lindert, S. Pozzorini and M. Schönherr, *NLO QCD+EW predictions for $2\ell 2\nu$ diboson signatures at the LHC*, JHEP **11** (2017) 120, arXiv: 1705.00598 [hep-ph].

[34] T. Gleisberg and S. Höche, *Comix, a new matrix element generator*, JHEP **12** (2008) 039, arXiv: 0808.3674 [hep-ph].

[35] S. Schumann and F. Krauss, *A parton shower algorithm based on Catani–Seymour dipole factorisation*, JHEP **03** (2008) 038, arXiv: 0709.1027 [hep-ph].

[36] S. Höche, F. Krauss, M. Schönherr and F. Siegert, *A critical appraisal of NLO+PS matching methods*, JHEP **09** (2012) 049, arXiv: 1111.1220 [hep-ph].

[37] S. Höche, F. Krauss, M. Schönherr and F. Siegert, *QCD matrix elements + parton showers. The NLO case*, JHEP **04** (2013) 027, arXiv: 1207.5030 [hep-ph].

[38] S. Catani, F. Krauss, B. R. Webber and R. Kuhn, *QCD Matrix Elements + Parton Showers*, JHEP **11** (2001) 063, arXiv: hep-ph/0109231.

[39] S. Höche, F. Krauss, S. Schumann and F. Siegert, *QCD matrix elements and truncated showers*, JHEP **05** (2009) 053, arXiv: 0903.1219 [hep-ph].

[40] F. Buccioni et al., *OpenLoops 2*, Eur. Phys. J. C **79** (2019) 866, arXiv: 1907.13071 [hep-ph].

[41] F. Cascioli, P. Maierhöfer and S. Pozzorini, *Scattering Amplitudes with Open Loops*, Phys. Rev. Lett. **108** (2012) 111601, arXiv: 1111.5206 [hep-ph].

[42] A. Denner, S. Dittmaier and L. Hofer, *Collier: A fortran-based complex one-loop library in extended regularizations*, Comput. Phys. Commun. **212** (2017) 220, arXiv: 1604.06792 [hep-ph].

[43] NNPDF Collaboration, R. D. Ball et al., *Parton distributions for the LHC run II*, JHEP **04** (2015) 040, arXiv: 1410.8849 [hep-ph].

[44] P. Nason, *A new method for combining NLO QCD with shower Monte Carlo algorithms*, JHEP **11** (2004) 040, arXiv: hep-ph/0409146.

[45] S. Frixione, P. Nason and C. Oleari, *Matching NLO QCD computations with parton shower simulations: the POWHEG method*, JHEP **11** (2007) 070, arXiv: 0709.2092 [hep-ph].

[46] S. Alioli, P. Nason, C. Oleari and E. Re, *A general framework for implementing NLO calculations in shower Monte Carlo programs: the POWHEG BOX*, JHEP **06** (2010) 043, arXiv: 1002.2581 [hep-ph].

[47] T. Sjöstrand et al., *An introduction to PYTHIA 8.2*, Comput. Phys. Commun. **191** (2015) 159, arXiv: 1410.3012 [hep-ph].

[48] ATLAS Collaboration, *Measurement of the Z/γ^* boson transverse momentum distribution in pp collisions at $\sqrt{s} = 7$ TeV with the ATLAS detector*, JHEP **09** (2014) 145, arXiv: 1406.3660 [hep-ex].

[49] H.-L. Lai et al., *New parton distributions for collider physics*, Phys. Rev. D **82** (2010) 074024, arXiv: 1007.2241 [hep-ph].

[50] J. Pumplin et al.,
New Generation of Parton Distributions with Uncertainties from Global QCD Analysis,
JHEP **07** (2002) 012, arXiv: hep-ph/0201195.

[51] J. Alwall, M. Herquet, F. Maltoni, O. Mattelaer and T. Stelzer, *MadGraph 5: going beyond*,
JHEP **06** (2011) 128, arXiv: 1106.0522 [hep-ph].

[52] J. Alwall et al., *The automated computation of tree-level and next-to-leading order differential cross sections, and their matching to parton shower simulations*, JHEP **07** (2014) 079,
arXiv: 1405.0301 [hep-ph].

[53] NNPDF Collaboration, R. D. Ball et al., *Parton distributions with LHC data*,
Nucl. Phys. B **867** (2013) 244, arXiv: 1207.1303 [hep-ph].

[54] ATLAS Collaboration, *ATLAS Pythia 8 tunes to* 7 *TeV data*, ATL-PHYS-PUB-2014-021, 2014,
URL: https://cds.cern.ch/record/1966419.

[55] ATLAS Collaboration, *Studies on top-quark Monte Carlo modelling for Top2016*,
ATL-PHYS-PUB-2016-020, 2016, URL: https://cds.cern.ch/record/2216168.

[56] S. Frixione, E. Laenen, P. Motylinski, C. White and B. R. Webber,
Single-top hadroproduction in association with a W boson, JHEP **07** (2008) 029,
arXiv: 0805.3067 [hep-ph].

[57] C. Anastasiou, L. Dixon, K. Melnikov and F. Petriello, *High-precision QCD at hadron colliders: Electroweak gauge boson rapidity distributions at next-to-next-to leading order*,
Phys. Rev. D **69** (2004) 094008, arXiv: hep-ph/0312266.

[58] D. J. Lange, *The EvtGen particle decay simulation package*,
Nucl. Instrum. Meth. A **462** (2001) 152.

[59] ATLAS Collaboration,
Electron and photon energy calibration with the ATLAS detector using LHC Run 2 data,
JINST **19** (2024) P02009, arXiv: 2309.05471 [hep-ex].

[60] ATLAS Collaboration, *Muon reconstruction and identification efficiency in ATLAS using the full Run 2 pp collision data set at $\sqrt{s} = 13$ TeV*, Eur. Phys. J. C **81** (2021) 578,
arXiv: 2012.00578 [hep-ex].

[61] ATLAS Collaboration, *Electron and photon efficiencies in LHC Run 2 with the ATLAS experiment*,
JHEP **05** (2024) 162, arXiv: 2308.13362 [hep-ex].

[62] M. Cacciari, G. P. Salam and G. Soyez, *The anti-k_t jet clustering algorithm*, JHEP **04** (2008) 063,
arXiv: 0802.1189 [hep-ph].

[63] M. Cacciari, G. P. Salam and G. Soyez, *FastJet user manual*, Eur. Phys. J. C **72** (2012) 1896,
arXiv: 1111.6097 [hep-ph].

[64] ATLAS Collaboration, *Jet energy scale and resolution measured in proton–proton collisions at $\sqrt{s} = 13$ TeV with the ATLAS detector*, Eur. Phys. J. C **81** (2021) 689,
arXiv: 2007.02645 [hep-ex].

[65] ATLAS Collaboration, *Performance of pile-up mitigation techniques for jets in pp collisions at $\sqrt{s} = 8$ TeV using the ATLAS detector*, Eur. Phys. J. C **76** (2016) 581,
arXiv: 1510.03823 [hep-ex].

[66] ATLAS Collaboration, *Measurement of the c-jet mistagging efficiency in $t\bar{t}$ events using pp collision data at $\sqrt{s} = 13$ TeV collected with the ATLAS detector*, Eur. Phys. J. C **82** (2022) 95, arXiv: 2109.10627 [hep-ex].

[67] ATLAS Collaboration, *Calibration of the light-flavour jet mistagging efficiency of the b-tagging algorithms with Z+jets events using 139 fb^{-1} of ATLAS proton–proton collision data at $\sqrt{s} = 13$ TeV*, Eur. Phys. J. C **83** (2023) 728, arXiv: 2301.06319 [hep-ex].

[68] ATLAS Collaboration, *Search for pair production of gluinos decaying via stop and sbottom in events with b-jets and large missing transverse momentum in pp collisions at $\sqrt{s} = 13$ TeV with the ATLAS detector*, Phys. Rev. D **94** (2016) 032003, arXiv: 1605.09318 [hep-ex].

[69] ATLAS Collaboration, *The performance of missing transverse momentum reconstruction and its significance with the ATLAS detector using 140 fb^{-1} of $\sqrt{s} = 13$ TeV pp collisions*, Eur. Phys. J. C **85** (2025) 606, arXiv: 2402.05858 [hep-ex].

[70] ATLAS Collaboration, *Measurement of the Inelastic Proton–Proton Cross Section at $\sqrt{s} = 13$ TeV with the ATLAS Detector at the LHC*, Phys. Rev. Lett. **117** (2016) 182002, arXiv: 1606.02625 [hep-ex].

[71] ATLAS Collaboration, *Electron and photon performance measurements with the ATLAS detector using the 2015–2017 LHC proton–proton collision data*, JINST **14** (2019) P12006, arXiv: 1908.00005 [hep-ex].

[72] ATLAS Collaboration, *Studies of the muon momentum calibration and performance of the ATLAS detector with pp collisions at $\sqrt{s} = 13$ TeV*, Eur. Phys. J. C **83** (2023) 686, arXiv: 2212.07338 [hep-ex].

[73] ATLAS Collaboration, *ATLAS b-jet identification performance and efficiency measurement with $t\bar{t}$ events in pp collisions at $\sqrt{s} = 13$ TeV*, Eur. Phys. J. C **79** (2019) 970, arXiv: 1907.05120 [hep-ex].

[74] E. Bothmann, M. Schönherr and S. Schumann, *Reweighting QCD matrix-element and parton-shower calculations*, Eur. Phys. J. C **76** (2016) 590, arXiv: 1606.08753 [hep-ph].

[75] J. Butterworth et al., *PDF4LHC recommendations for LHC Run II*, J. Phys. G **43** (2016) 023001, arXiv: 1510.03865 [hep-ph].

[76] M. Grazzini, S. Kallweit and M. Wiesemann, *Fully differential NNLO computations with MATRIX*, Eur.Phys.J.C **78** (2018), URL: http://dx.doi.org/10.1140/epjc/s10052-018-5771-7.

[77] ROOT Collaboration, *HistFactory: A tool for creating statistical models for use with RooFit and RooStats*, tech. rep. CERN-OPEN-2012-016, New York U., 2012, URL: https://cds.cern.ch/record/1456844.

[78] L. Moneta et al., *The RooStats Project*, PoS **ACAT2010** (2011) 057, arXiv: 1009.1003 [physics.data-an].

[79] Particle Data Group, P. Zyla et al., *Review of Particle Physics*, Prog. Theor. Exp. Phys. **2020** (2020) 083C01.

[80] G. D'Agostini, *A multidimensional unfolding method based on Bayes' theorem*, Nucl. Instrum. Meth. A **362** (1995) 487, ISSN: 0168-9002.

[81] D. Chang, W.-Y. Keung and P. B. Pal, *CP violation in the cubic coupling of neutral gauge bosons*, Phys. Rev. D **51** (1995) 1326, arXiv: hep-ph/9407294.

[82] ATLAS Collaboration, *Evidence of pair production of longitudinally polarised vector bosons and study of CP properties in $ZZ \to 4\ell$ events with the ATLAS detector at $\sqrt{s} = 13$ TeV*, JHEP **12** (2023) 107, arXiv: 2310.04350 [hep-ex].

[83] A. E. Semushin, E. Y. Soldatov and A. S. Kurova, *CP-violating effects of the neutral triple gauge couplings in $Z(\ell\ell)\gamma$ production at the LHC*, Phys. Rev. D **111** (2025) 115028, arXiv: 2503.20945 [hep-ph].

[84] G. J. Gounaris, J. Layssac and F. M. Renard, *Signatures of the anomalous $Z\gamma$ and ZZ production at lepton and hadron colliders*, Phys. Rev. D **61** (2000) 073013, arXiv: 9910395 [hep-ph], URL: http://dx.doi.org/10.1103/PhysRevD.61.073013.

[85] O. J. P. Éboli, M. C. Gonzalez-Garcia and J. K. Mizukoshi, *$pp \to jje^{\pm}\mu^{\pm}\nu\nu$ and $jje^{\pm}\mu^{\mp}\nu\nu$ at $O(\alpha_{em}^{6})$ and $O(\alpha_{em}^{4}\alpha_{s}^{2})$ for the study of the quartic electroweak gauge boson vertex at CERN LHC*, Phys. Rev. D **74** (2006) 073005, arXiv: 0606118 [hep-ph].

[86] C. Degrande et al., *UFO - The Universal FeynRules Output*, Comput. Phys. Commun. **183** (2012) 1201, arXiv: 1108.2040 [hep-ph].

[87] A. Biekötter, P. Gregg, F. Krauss and M. Schönherr, *Constraining CP violating operators in charged and neutral triple gauge couplings*, Phys. Lett. B **817** (2021) 136311, arXiv: 2102.01115 [hep-ph].

[88] K. Hagiwara, R. D. Peccei, D. Zeppenfeld and K. Hikasa, *Probing the Weak Boson Sector in e+ e- —> W+ W-*, Nucl. Phys. B **282** (1987) 253.

[89] O. Éboli and M. Gonzalez-Garcia, *Classifying the bosonic quartic couplings*, Phys. Rev. D **93** (2016) 093013, arXiv: 1604.03555 [hep-ph].

[90] E. d. S. Almeida, O. J. P. Éboli and M. C. Gonzalez–Garcia, *Unitarity constraints on anomalous quartic couplings*, Phys. Rev. D **101** (2020) 113003, arXiv: 2004.05174 [hep-ph].

[91] ATLAS Collaboration, *ATLAS Computing Acknowledgements*, ATL-SOFT-PUB-2025-001, 2025, URL: https://cds.cern.ch/record/2922210.

The ATLAS Collaboration

G. Aad[104], E. Aakvaag[17], B. Abbott[123], S. Abdelhameed[119a], K. Abeling[55], N.J. Abicht[49], S.H. Abidi[30], M. Aboelela[45], A. Aboulhorma[36e], H. Abramowicz[157], Y. Abulaiti[120], B.S. Acharya[69a,69b,m], A. Ackermann[63a], C. Adam Bourdarios[4], L. Adamczyk[87a], S.V. Addepalli[149], M.J. Addison[103], J. Adelman[118], A. Adiguzel[22c], T. Adye[137], A.A. Affolder[139], Y. Afik[40], M.N. Agaras[13], A. Aggarwal[102], C. Agheorghiesei[28c], F. Ahmadov[39,ad], S. Ahuja[97], S. Ahuja[169], X. Ai[143b], G. Aielli[76a,76b], A. Aikot[169], M. Ait Tamlihat[36e], B. Aitbenchikh[36a], M. Akbiyik[102], T.P.A. Åkesson[100], A.V. Akimov[151], D. Akiyama[174], N.N. Akolkar[25], S. Aktas[172], G.L. Alberghi[24b], J. Albert[171], U. Alberti[20], P. Albicocco[53], G.L. Albouy[60], S. Alderweireldt[52], Z.L. Alegria[124], M. Aleksa[37], I.N. Aleksandrov[39], C. Alexa[28b], T. Alexopoulos[10], F. Alfonsi[24b], M. Algren[56], M. Alhroob[173], B. Ali[135], H.M.J. Ali[93,w], S. Ali[32], S.W. Alibocus[94], M. Aliev[34c], G. Alimonti[71a], W. Alkakhi[55], C. Allaire[66], B.M.M. Allbrooke[152], D.R. Allen[124], J.S. Allen[103], J.F. Allen[52], P.P. Allport[21], A. Aloisio[72a,72b], F. Alonso[92], C. Alpigiani[142], Z.M.K. Alsolami[93], A. Alvarez Fernandez[102], M. Alves Cardoso[56], M.G. Alviggi[72a,72b], M. Aly[103], Y. Amaral Coutinho[83b], A. Ambler[106], C. Amelung[37], M. Amerl[103], C.G. Ames[111], T. Amezza[130], D. Amidei[108], B. Amini[54], K. Amirie[161], A. Amirkhanov[39], S.P. Amor Dos Santos[133a], K.R. Amos[169], D. Amperiadou[158], S. An[84], C. Anastopoulos[145], T. Andeen[11], J.K. Anders[94], A.C. Anderson[59], A. Andreazza[71a,71b], S. Angelidakis[9], A. Angerami[42], A.V. Anisenkov[39], A. Annovi[74a], C. Antel[37], E. Antipov[151], M. Antonelli[53], F. Anulli[75a], M. Aoki[84], T. Aoki[159], M.A. Aparo[152], L. Aperio Bella[48], M. Apicella[31], C. Appelt[157], A. Apyan[27], M. Arampatzi[10], S.J. Arbiol Val[88], C. Arcangeletti[53], A.T.H. Arce[51], J-F. Arguin[110], S. Argyropoulos[158], J.-H. Arling[48], O. Arnaez[4], H. Arnold[151], G. Artoni[75a,75b], H. Asada[113], K. Asai[121], S. Asatryan[179], N.A. Asbah[37], R.A. Ashby Pickering[173], A.M. Aslam[97], K. Assamagan[30], R. Astalos[29a], K.S.V. Astrand[100], S. Atashi[165], R.J. Atkin[34a], H. Atmani[36f], P.A. Atmasiddha[131], K. Augsten[135], A.D. Auriol[41], V.A. Austrup[103], A.S. Avad[96], G. Avolio[37], K. Axiotis[56], A. Azzam[13], D. Babal[29b], H. Bachacou[138], K. Bachas[158,q], A. Bachiu[35], E. Bachmann[50], M.J. Backes[63a], A. Badea[40], T.M. Baer[108], P. Bagnaia[75a,75b], M. Bahmani[19], D. Bahner[54], K. Bai[126], J.T. Baines[137], L. Baines[96], O.K. Baker[178], E. Bakos[16], D. Bakshi Gupta[8], L.E. Balabram Filho[83b], V. Balakrishnan[123], R. Balasubramanian[4], E.M. Baldin[38], P. Balek[87a], E. Ballabene[24b,24a], F. Balli[138], L.M. Baltes[63a], W.K. Balunas[33], J. Balz[102], I. Bamwidhi[119b], E. Banas[88], M. Bandieramonte[132], A. Bandyopadhyay[25], S. Bansal[25], L. Barak[157], M. Barakat[48], E.L. Barberio[107], D. Barberis[18b], M. Barbero[104], M.Z. Barel[117], T. Barillari[112], M-S. Barisits[37], T. Barklow[149], P. Baron[136], D.A. Baron Moreno[103], A. Baroncelli[62], A.J. Barr[129], J.D. Barr[98], F. Barreiro[101], J. Barreiro Guimarães da Costa[14], M.G. Barros Teixeira[133a], S. Barsov[38], F. Bartels[63a], R. Bartoldus[149], A.E. Barton[93], P. Bartos[29a], M. Baselga[49], S. Bashiri[88], A. Bassalat[66,b], M.J. Basso[162a], S. Bataju[45], R. Bate[170], R.L. Bates[59], S. Batlamous[101], M. Battaglia[139], D. Battulga[19], M. Bauce[75a,75b], M. Bauer[79], P. Bauer[25], L.T. Bayer[48], L.T. Bazzano Hurrell[31], J.B. Beacham[112], T. Beau[130], J.Y. Beaucamp[92], P.H. Beauchemin[164], P. Bechtle[25], H.P. Beck[20,p], K. Becker[173], A.J. Beddall[82], V.A. Bednyakov[39], C.P. Bee[151], L.J. Beemster[16], M. Begalli[83d], M. Begel[30], J.K. Behr[48], J.F. Beirer[37], F. Beisiegel[25], M. Belfkir[119b], G. Bella[157], L. Bellagamba[24b], A. Bellerive[35], C.D. Bellgraph[68], P. Bellos[21], K. Beloborodov[38], I. Benaoumeur[21], D. Benchekroun[36a], F. Bendebba[36a], Y. Benhammou[157], K.C. Benkendorfer[61], L. Beresford[48],

M. Beretta [53], E. Bergeaas Kuutmann [167], N. Berger [4], B. Bergmann [135], J. Beringer [18a], G. Bernardi [5], C. Bernius [149], F.U. Bernlochner [25], A. Berrocal Guardia [13], T. Berry [97], P. Berta [136], A. Berthold [50], A. Berti [133a], R. Bertrand [104], S. Bethke [112], A. Betti [75a,75b], A.J. Bevan [96], L. Bezio [56], N.K. Bhalla [54], S. Bharthuar [112], S. Bhatta [151], P. Bhattarai [149], Z.M. Bhatti [120], K.D. Bhide [54], V.S. Bhopatkar [124], R.M. Bianchi [132], G. Bianco [24b,24a], O. Biebel [111], M. Biglietti [77a], C.S. Billingsley [45], Y. Bimgdi [36f], M. Bindi [55], A. Bingham [177], A. Bingul [22b], C. Bini [75a,75b], G.A. Bird [33], M. Birman [175], M. Biros [136], S. Biryukov [152], T. Bisanz [49], E. Bisceglie [24b,24a], J.P. Biswal [137], D. Biswas [147], I. Bloch [48], A. Blue [59], U. Blumenschein [96], V.S. Bobrovnikov [39], L. Boccardo [57b,57a], M. Boehler [54], B. Boehm [172], D. Bogavac [13], A.G. Bogdanchikov [38], L.S. Boggia [130], V. Boisvert [97], P. Bokan [37], T. Bold [87a], M. Bomben [5], M. Bona [96], M. Boonekamp [138], A.G. Borbély [59], I.S. Bordulev [38], G. Borissov [93], D. Bortoletto [129], D. Boscherini [24b], M. Bosman [13], K. Bouaouda [36a], N. Bouchhar [169], L. Boudet [4], J. Boudreau [132], E.V. Bouhova-Thacker [93], D. Boumediene [41], R. Bouquet [57b,57a], A. Boveia [122], J. Boyd [37], D. Boye [30], I.R. Boyko [39], L. Bozianu [56], J. Bracinik [21], N. Brahimi [4], G. Brandt [177], O. Brandt [33], B. Brau [105], J.E. Brau [126], R. Brener [175], L. Brenner [117], R. Brenner [167], S. Bressler [175], G. Brianti [78a,78b], D. Britton [59], D. Britzger [112], I. Brock [25], R. Brock [109], G. Brooijmans [42], A.J. Brooks [68], E.M. Brooks [162b], E. Brost [30], L.M. Brown [171,162a], L.E. Bruce [61], T.L. Bruckler [129], P.A. Bruckman de Renstrom [88], B. Brüers [48], A. Bruni [24b], G. Bruni [24b], D. Brunner [47a,47b], M. Bruschi [24b], N. Bruscino [75a,75b], T. Buanes [17], Q. Buat [142], D. Buchin [112], A.G. Buckley [59], O. Bulekov [82], B.A. Bullard [149], S. Burdin [94], C.D. Burgard [49], A.M. Burger [91], B. Burghgrave [8], O. Burlayenko [54], J. Burleson [168], J.C. Burzynski [148], E.L. Busch [42], V. Büscher [102], P.J. Bussey [59], O. But [25], J.M. Butler [26], C.M. Buttar [59], J.M. Butterworth [98], W. Buttinger [137], C.J. Buxo Vazquez [109], A.R. Buzykaev [39], S. Cabrera Urbán [169], L. Cadamuro [66], H. Cai [37], Y. Cai [24b,114c,24a], Y. Cai [114a], V.M.M. Cairo [37], O. Cakir [3a], N. Calace [37], P. Calafiura [18a], G. Calderini [130], P. Calfayan [35], L. Calic [100], G. Callea [59], L.P. Caloba [83b], D. Calvet [41], S. Calvet [41], R. Camacho Toro [130], S. Camarda [37], D. Camarero Munoz [27], P. Camarri [76a,76b], C. Camincher [171], M. Campanelli [98], A. Camplani [43], V. Canale [72a,72b], A.C. Canbay [3a], E. Canonero [97], J. Cantero [169], Y. Cao [168], F. Capocasa [27], M. Capua [44b,44a], A. Carbone [71a,71b], R. Cardarelli [76a], J.C.J. Cardenas [8], M.P. Cardiff [27], G. Carducci [44b,44a], T. Carli [37], G. Carlino [72a], J.I. Carlotto [13], B.T. Carlson [132,r], E.M. Carlson [171], J. Carmignani [94], L. Carminati [71a,71b], A. Carnelli [4], M. Carnesale [37], S. Caron [116], E. Carquin [140g], I.B. Carr [107], S. Carrá [73a,73b], G. Carratta [24b,24a], C. Carrion Martinez [169], A.M. Carroll [126], M.P. Casado [13,h], P. Casolaro [72a,72b], M. Caspar [48], W.R. Castiglioni [40], F.L. Castillo [4], L. Castillo Garcia [13], V. Castillo Gimenez [169], N.F. Castro [133a,133e], A. Catinaccio [37], J.R. Catmore [128], T. Cavaliere [4], V. Cavaliere [30], L.J. Caviedes Betancourt [23b], E. Celebi [82], S. Cella [37], V. Cepaitis [56], K. Cerny [125], A.S. Cerqueira [83a], A. Cerri [74a,am], L. Cerrito [76a,76b], F. Cerutti [18a], B. Cervato [71a,71b], A. Cervelli [24b], G. Cesarini [53], S.A. Cetin [82], P.M. Chabrillat [130], R. Chakkappai [66], S. Chakraborty [173], A. Chambers [61], J. Chan [18a], W.Y. Chan [159], J.D. Chapman [33], E. Chapon [138], B. Chargeishvili [155b], D.G. Charlton [21], C. Chauhan [136], Y. Che [114a], S. Chekanov [6], G.A. Chelkov [39,a], B. Chen [157], B. Chen [171], H. Chen [114a], H. Chen [30], J. Chen [144a], J. Chen [148], M. Chen [129], S. Chen [89], S.J. Chen [114a], X. Chen [144a], X. Chen [15,ah], Z. Chen [62], C.L. Cheng [176], H.C. Cheng [64a], S. Cheong [149], A. Cheplakov [39], E. Cherepanova [117], R. Cherkaoui El Moursli [36e], E. Cheu [7], K. Cheung [65], L. Chevalier [138], V. Chiarella [53], G. Chiarelli [74a], G. Chiodini [70a], A.S. Chisholm [21], A. Chitan [28b], M. Chitishvili [169], M.V. Chizhov [39,s], K. Choi [11], Y. Chou [142], E.Y.S. Chow [116], K.L. Chu [175], M.C. Chu [64a], X. Chu [14,114c], Z. Chubinidze [53], J. Chudoba [134], J.J. Chwastowski [88],

D. Cieri[112], K.M. Ciesla[87a], V. Cindro[95], A. Ciocio[18a], F. Cirotto[72a,72b], Z.H. Citron[175], M. Citterio[71a], D.A. Ciubotaru[28b], A. Clark[56], P.J. Clark[52], N. Clarke Hall[98], C. Clarry[161], S.E. Clawson[48], C. Clement[47a,47b], L. Clissa[24b,24a], Y. Coadou[104], M. Cobal[69a,69c], A. Coccaro[57b], R.F. Coelho Barrue[133a], R. Coelho Lopes De Sa[105], S. Coelli[71a], L.S. Colangeli[161], B. Cole[42], P. Collado Soto[101], J. Collot[60], R. Coluccia[70a,70b], P. Conde Muiño[133a,133g], M.P. Connell[34c], S.H. Connell[34c], E.I. Conroy[129], M. Contreras Cossio[11], F. Conventi[72a,aj], A.M. Cooper-Sarkar[129], L. Corazzina[75a,75b], F.A. Corchia[24b,24a], A. Cordeiro Oudot Choi[142], L.D. Corpe[41], M. Corradi[75a,75b], F. Corriveau[106,ab], A. Cortes-Gonzalez[159], M.J. Costa[169], F. Costanza[4], D. Costanzo[145], J. Couthures[4], G. Cowan[97], K. Cranmer[176], L. Cremer[49], D. Cremonini[24b,24a], S. Crépé-Renaudin[60], F. Crescioli[130], T. Cresta[73a,73b], M. Cristinziani[147], M. Cristoforetti[78a,78b], E. Critelli[98], V. Croft[117], G. Crosetti[44b,44a], A. Cueto[101], H. Cui[98], Z. Cui[7], B.M. Cunnett[152], W.R. Cunningham[59], F. Curcio[169], J.R. Curran[52], M.J. Da Cunha Sargedas De Sousa[57b,57a], J.V. Da Fonseca Pinto[83b], C. Da Via[103], W. Dabrowski[87a], T. Dado[37], S. Dahbi[154], T. Dai[108], D. Dal Santo[20], C. Dallapiccola[105], M. Dam[43], G. D'amen[30], V. D'Amico[111], J.R. Dandoy[35], M. D'Andrea[57b,57a], D. Dannheim[37], G. D'anniballe[74a,74b], M. Danninger[148], V. Dao[151], G. Darbo[57b], S.J. Das[30], F. Dattola[48], S. D'Auria[71a,71b], A. D'Avanzo[72a,72b], T. Davidek[136], J. Davidson[173], I. Dawson[96], K. De[8], C. De Almeida Rossi[161], R. De Asmundis[72a], N. De Biase[48], S. De Castro[24b,24a], N. De Groot[116], P. de Jong[117], H. De la Torre[118], A. De Maria[114a], A. De Salvo[75a], U. De Sanctis[76a,76b], F. De Santis[70a,70b], A. De Santo[152], J.B. De Vivie De Regie[60], J. Debevc[95], D.V. Dedovich[39], J. Degens[94], A.M. Deiana[45], J. Del Peso[101], L. Delagrange[130], F. Deliot[138], C.M. Delitzsch[49], M. Della Pietra[72a,72b], D. Della Volpe[56], A. Dell'Acqua[37], L. Dell'Asta[71a,71b], M. Delmastro[4], C.C. Delogu[102], P.A. Delsart[60], S. Demers[178], M. Demichev[39], S.P. Denisov[38], H. Denizli[22a,l], L. D'Eramo[41], D. Derendarz[88], F. Derue[130], P. Dervan[94,*], A.M. Desai[1], K. Desch[25], F.A. Di Bello[57b,57a], A. Di Ciaccio[76a,76b], L. Di Ciaccio[4], A. Di Domenico[75a,75b], C. Di Donato[72a,72b], A. Di Girolamo[37], G. Di Gregorio[62], A. Di Luca[78a,78b], B. Di Micco[77a,77b], R. Di Nardo[77a,77b], K.F. Di Petrillo[40], M. Diamantopoulou[35], F.A. Dias[117], M.A. Diaz[140a,140b], A.R. Didenko[39], M. Didenko[169], S.D. Diefenbacher[18a], E.B. Diehl[108], S. Díez Cornell[48], C. Diez Pardos[147], C. Dimitriadi[150], A. Dimitrievska[21], A. Dimri[151], Y. Ding[62], J. Dingfelder[25], T. Dingley[129], I-M. Dinu[28b], S.J. Dittmeier[63b], F. Dittus[37], M. Divisek[136], B. Dixit[94], F. Djama[104], T. Djobava[155b], C. Doglioni[103,100], A. Dohnalova[29a], Z. Dolezal[136], K. Domijan[87a], K.M. Dona[40], M. Donadelli[83d], B. Dong[109], J. Donini[41], A. D'Onofrio[72a,72b], M. D'Onofrio[94], J. Dopke[137], A. Doria[72a], N. Dos Santos Fernandes[133a], I.A. Dos Santos Luz[83e], P. Dougan[103], M.T. Dova[92], A.T. Doyle[59], M.P. Drescher[55], E. Dreyer[175], I. Drivas-koulouris[10], M. Drnevich[120], D. Du[62], T.A. du Pree[117], Z. Duan[114a], M. Dubau[4], F. Dubinin[39], M. Dubovsky[29a], E. Duchovni[175], G. Duckeck[111], P.K. Duckett[98], O.A. Ducu[28b], D. Duda[52], A. Dudarev[37], M.M. Dudek[88], E.R. Duden[27], M. D'uffizi[103], L. Duflot[66], M. Dührssen[37], I. Duminica[28g], A.E. Dumitriu[28b], M. Dunford[63a], K. Dunne[47a,47b], A. Duperrin[104], H. Duran Yildiz[3a], A. Durglishvili[155b], G.I. Dyckes[18a], M. Dyndal[87a], B.S. Dziedzic[37], Z.O. Earnshaw[152], G.H. Eberwein[129], B. Eckerova[29a], S. Eggebrecht[55], E. Egidio Purcino De Souza[83e], G. Eigen[17], K. Einsweiler[18a], T. Ekelof[167], P.A. Ekman[100], S. El Farkh[36b], Y. El Ghazali[62], H. El Jarrari[34j], A. El Moussaouy[36a], D. Elitez[37], M. Ellert[167], F. Ellinghaus[177], T.A. Elliot[97], N. Ellis[37], J. Elmsheuser[30], M. Elsawy[119a], M. Elsing[37], D. Emeliyanov[137], Y. Enari[84], S. Epari[110], D. Ernani Martins Neto[88], F. Ernst[37], M. Escalier[66], C. Escobar[169],

E. Etzion[157], G. Evans[133a,133b], H. Evans[68], L.S. Evans[48], A. Ezhilov[38], S. Ezzarqtouni[36a], F. Fabbri[24b,24a], L. Fabbri[24b,24a], G. Facini[98], V. Fadeyev[139], R.M. Fakhrutdinov[38], D. Fakoudis[102], S. Falciano[75a], L.F. Falda Ulhoa Coelho[133a], F. Fallavollita[112], G. Falsetti[44b,44a], J. Faltova[136], C. Fan[168], K.Y. Fan[64b], Y. Fan[14], Y. Fang[14,114c], M. Fanti[71a,71b], M. Faraj[69a,69b], Z. Farazpay[99], A. Farbin[8], A. Farilla[77a], K. Farman[154], T. Farooque[109], J.N. Farr[178], M.S. Farrington[61], S.M. Farrington[137,52], F. Fassi[36e], D. Fassouliotis[9], L. Fayard[66], P. Federic[136], P. Federicova[134], O.L. Fedin[38,a], M. Feickert[176], L. Feligioni[104], D.E. Fellers[18a], C. Feng[143a], Y. Feng[14], Z. Feng[117], M.J. Fenton[165], L. Ferencz[48], B. Fernandez Barbadillo[93], P. Fernandez Martinez[67], M.J.V. Fernoux[104], J. Ferrando[93], A. Ferrari[167], P. Ferrari[117,116], R. Ferrari[73a], D. Ferrere[56], C. Ferretti[108], M.P. Fewell[1], D. Fiacco[75a,75b], F. Fiedler[102], P. Fiedler[135], S. Filimonov[39], M.S. Filip[28b,t], A. Filipčič[95], E.K. Filmer[162a], F. Filthaut[116], M.C.N. Fiolhais[133a,133c,c], L. Fiorini[169], W.C. Fisher[109], T. Fitschen[103], P.M. Fitzhugh[138], I. Fleck[147], P. Fleischmann[108], T. Flick[177], M. Flores[34d,ag], L.R. Flores Castillo[64a], L. Flores Sanz De Acedo[37], F.M. Follega[78a,78b], N. Fomin[33], J.H. Foo[161], A. Formica[138], A.C. Forti[103], E. Fortin[37], A.W. Fortman[18a], L. Foster[18a], L. Fountas[9,i], D. Fournier[66], H. Fox[93], P. Francavilla[74a,74b], S. Francescato[61], S. Franchellucci[56], M. Franchini[24b,24a], S. Franchino[63a], D. Francis[37], L. Franco[116], L. Franconi[48], M. Franklin[61], G. Frattari[27], Y.Y. Frid[157], J. Friend[59], N. Fritzsche[37], A. Froch[56], D. Froidevaux[37], J.A. Frost[137], Y. Fu[109], S. Fuenzalida Garrido[140g], M. Fujimoto[151], K.Y. Fung[64a], E. Furtado De Simas Filho[83e], M. Furukawa[159], J. Fuster[169], A. Gaa[55], A. Gabrielli[24b,24a], A. Gabrielli[161], P. Gadow[37], G. Gagliardi[57b,57a], L.G. Gagnon[18a], S. Gaid[85b], S. Galantzan[157], J. Gallagher[1], E.J. Gallas[129], A.L. Gallen[167], B.J. Gallop[137], K.K. Gan[122], S. Ganguly[159], Y. Gao[52], A. Garabaglu[142], F.M. Garay Walls[140a,140b], C. García[169], A. Garcia Alonso[117], A.G. Garcia Caffaro[178], J.E. García Navarro[169], M.A. Garcia Ruiz[23b], M. Garcia-Sciveres[18a], G.L. Gardner[131], R.W. Gardner[40], N. Garelli[164], R.B. Garg[149], J.M. Gargan[33], C.A. Garner[161], C.M. Garvey[34a], V.K. Gassmann[164], G. Gaudio[73a], V. Gautam[13], P. Gauzzi[75a,75b], J. Gavranovic[95], I.L. Gavrilenko[133a], A. Gavrilyuk[38], C. Gay[170], G. Gaycken[126], E.N. Gazis[10], A. Gekow[122], C. Gemme[57b], M.H. Genest[60], A.D. Gentry[115], S. George[97], T. Geralis[46], A.A. Gerwin[123], P. Gessinger-Befurt[37], M.E. Geyik[177], M. Ghani[173], K. Ghorbanian[96], A. Ghosal[147], A. Ghosh[165], A. Ghosh[7], B. Giacobbe[24b], S. Giagu[75a,75b], T. Giani[117], A. Giannini[62], S.M. Gibson[97], M. Gignac[139], D.T. Gil[87b], A.K. Gilbert[87a], B.J. Gilbert[42], D. Gillberg[35], G. Gilles[117], D.M. Gingrich[2,ai], M.P. Giordani[69a,69c], P.F. Giraud[138], G. Giugliarelli[69a,69c], D. Giugni[71a], F. Giuli[76a,76b], I. Gkialas[9,i], L.K. Gladilin[38], C. Glasman[101], M. Glazewska[20], R.M. Gleason[165], G. Glemža[48], M. Glisic[126], I. Gnesi[44b], Y. Go[30], M. Goblirsch-Kolb[37], B. Gocke[49], D. Godin[110], B. Gokturk[22a], S. Goldfarb[107], T. Golling[56], M.G.D. Gololo[34c], D. Golubkov[38], J.P. Gombas[109], A. Gomes[133a,133b], G. Gomes Da Silva[147], A.J. Gomez Delegido[37], R. Gonçalo[133a], L. Gonella[21], A. Gongadze[155c], F. Gonnella[21], J.L. Gonski[149], R.Y. González Andana[52], S. González de la Hoz[169], M.V. Gonzalez Rodrigues[48], R. Gonzalez Suarez[167], S. Gonzalez-Sevilla[56], L. Goossens[37], B. Gorini[37], E. Gorini[70a,70b], A. Gorišek[95], T.C. Gosart[131], A.T. Goshaw[51], M.I. Gostkin[39], S. Goswami[124], C.A. Gottardo[37], S.A. Gotz[111], M. Gouighri[36b], A.G. Goussiou[142], N. Govender[34c], R.P. Grabarczyk[129], I. Grabowska-Bold[87a], K. Graham[35], E. Gramstad[128], S. Grancagnolo[70a,70b], C.M. Grant[1], P.M. Gravila[28f], F.G. Gravili[70a,70b], H.M. Gray[18a], M. Greco[112], M.J. Green[1], C. Grefe[25], A.S. Grefsrud[17], I.M. Gregor[48], K.T. Greif[165], P. Grenier[149], S.G. Grewe[112], A.A. Grillo[139], K. Grimm[32], S. Grinstein[13,x], J.-F. Grivaz[66], E. Gross[175], J. Grosse-Knetter[55], L. Guan[108], G. Guerrieri[37], R. Guevara[128], R. Gugel[102], J.A.M. Guhit [108], A. Guida [19], E. Guilloton [173], S. Guindon [37], F. Guo [14,114c], J. Guo [144a], L. Guo [48], L. Guo [114b,v], Y. Guo [108], Y. Guo [42], A. Gupta [49], R. Gupta [132], S. Gupta [27], S. Gurbuz [25], S.S. Gurdasani [48], G. Gustavino [75a,75b], P. Gutierrez [123], L.F. Gutierrez Zagazeta [131], M. Gutsche [50], C. Gutschow [98], C. Gwenlan [129], C.B. Gwilliam [94], E.S. Haaland [128], A. Haas [120], M. Habedank [59], C. Haber [18a], H.K. Hadavand [8], A. Haddad [41], A. Hadef [50], A.I. Hagan [93], J.J. Hahn [147], E.H. Haines [98], M. Haleem [172], J. Haley [124], G.D. Hallewell [104], J.A. Hallford [48], K. Hamano [171], H. Hamdaoui [167], M. Hamer [25], S.E.D. Hammoud [66], E.J. Hampshire [97], J. Han [143a], L. Han [114a], L. Han [62], S. Han [14], K. Hanagaki [84], M. Hance [139], D.A. Hangal [42], H. Hanif [148], M.D. Hank [131], J.B. Hansen [43], P.H. Hansen [43], T. Harenberg [177], S. Harkusha [179], M.L. Harris [105], Y.T. Harris [25], J. Harrison [13], N.M. Harrison [122], P.F. Harrison[173], M.L.E. Hart [98], N.M. Hartman [112], N.M. Hartmann [111], R.Z. Hasan [97,137], Y. Hasegawa [146], F. Haslbeck [129], S. Hassan [17], R. Hauser [109], M. Haviernik [136], C.M. Hawkes [21], R.J. Hawkings [37], Y. Hayashi [159], D. Hayden [109], C. Hayes [108], R.L. Hayes [117], C.P. Hays [129], J.M. Hays [96], H.S. Hayward [94], M. He [14,114c], Y. He [48], Y. He [98], N.B. Heatley [96], V. Hedberg [100], J. Heilman [35], S. Heim [48], T. Heim [18a], J.J. Heinrich [126], L. Heinrich [112], J. Hejbal [134], M. Helbig [50], A. Held [176], S. Hellesund [17], C.M. Helling [170], S. Hellman [47a,47b], A.M. Henriques Correia[37], H. Herde [100], Y. Hernández Jiménez [151], L.M. Herrmann [25], T. Herrmann [50], G. Herten [54], R. Hertenberger [111], L. Hervas [37], M.E. Hesping [102], N.P. Hessey [162a], J. Hessler [112], M. Hidaoui [36b], N. Hidic [136], E. Hill [161], T.S. Hillersoy [17], S.J. Hillier [21], J.R. Hinds [109], F. Hinterkeuser [25], M. Hirose [127], S. Hirose [163], D. Hirschbuehl [177], T.G. Hitchings [103], B. Hiti [95], J. Hobbs [151], R. Hobincu [28e], N. Hod [175], A.M. Hodges [168], M.C. Hodgkinson [145], B.H. Hodkinson [129], A. Hoecker [37], D.D. Hofer [108], J. Hofer [169], J. Hofner [102], M. Holzbock [37], L.B.A.H. Hommels [33], V. Homsak [129], B.P. Honan [103], J.J. Hong [68], T.M. Hong [132], B.H. Hooberman [168], W.H. Hopkins [6], M.C. Hoppesch [168], Y. Horii [113], M.E. Horstmann [112], S. Hou [154], M.R. Housenga [168], J. Howarth [59], J. Hoya [6], M. Hrabovsky [125], T. Hryn'ova [4], P.J. Hsu [65], S.-C. Hsu [142], T. Hsu [66], M. Hu [18a], Q. Hu [62], S. Huang [33], X. Huang [14,114c], Y. Huang [136], Y. Huang [114b], Y. Huang [14], Z. Huang [66], Z. Hubacek [135], F. Huegging [25], T.B. Huffman [129], M. Hufnagel Maranha De Faria [83a], C.A. Hugli [48], M. Huhtinen [37], S.K. Huiberts [128], R. Hulsken [106], C.E. Hultquist [18a], D.L. Humphreys [105], N. Huseynov [12], J. Huston [109], J. Huth [61], L. Huth [48], R. Hyneman [7], G. Iacobucci [56], G. Iakovidis [30], L. Iconomidou-Fayard [66], J.P. Iddon [37], P. Iengo [72a,72b], Y. Iiyama [159], T. Iizawa [159], Y. Ikegami [84], D. Iliadis [158], N. Ilic [161], H. Imam [36a], G. Inacio Goncalves [83d], S.A. Infante Cabanas [140c], T. Ingebretsen Carlson [47a,47b], J.M. Inglis [96], G. Introzzi [73a,73b], M. Iodice [77a], V. Ippolito [75a,75b], R.K. Irwin [94], M. Ishino [159], W. Islam [176], C. Issever [19], S. Istin [22a,ao], K. Itabashi [127], H. Ito [174], R. Iuppa [78a,78b], A. Ivina [175], V. Izzo [72a], P. Jacka [135], P. Jackson [1], P. Jain [48], K. Jakobs [54], T. Jakoubek [175], J. Jamieson [59], W. Jang [159], S. Jankovych [136], M. Javurkova [105], P. Jawahar [103], L. Jeanty [126], J. Jejelava [155a,ae], P. Jenni [54,f], C.E. Jessiman [35], C. Jia [143a], H. Jia [170], J. Jia [151], X. Jia [112,114c], Z. Jia [114a], C. Jiang [52], Q. Jiang [64b], S. Jiggins [48], M. Jimenez Ortega [169], J. Jimenez Pena [13], S. Jin [114a], A. Jinaru [28b], O. Jinnouchi [141], P. Johansson [145], K.A. Johns [7], J.W. Johnson [139], F.A. Jolly [48], D.M. Jones [152], E. Jones [48], K.S. Jones[8], P. Jones [33], R.W.L. Jones [93], T.J. Jones [94], H.L. Joos [55], R. Joshi [122], J. Jovicevic [16], X. Ju [18a], J.J. Junggeburth [37], T. Junkermann [63a], A. Juste Rozas [13,x], M.K. Juzek [88], S. Kabana [140f], A. Kaczmarska [88], S.A. Kadir[149], M. Kado [112], H. Kagan [122], M. Kagan [149], A. Kahn [131], C. Kahra [102], T. Kaji [159], E. Kajomovitz [156], N. Kakati [175], N. Kakoty [13], I. Kalaitzidou [54], S. Kandel [8], N. Kanellos [10], N.J. Kang [139], D. Kar [34j], E. Karentzos [25], K. Karki [8], O. Karkout [117], S.N. Karpov [39], Z.M. Karpova [39], V. Kartvelishvili [93,155b], A.N. Karyukhin [38], E. Kasimi [158], J. Katzy [48], S. Kaur [35], K. Kawade [146], M.P. Kawale [123], C. Kawamoto [89], T. Kawamoto [62], E.F. Kay [37], S. Kazakos [109], V.F. Kazanin [38], J.M. Keaveney [34a], R. Keeler [171], G.V. Kehris [61], J.S. Keller [35], J.M. Kelly [171], J.J. Kempster [152], O. Kepka [134], J. Kerr [162b], B.P. Kerridge [137], B.P. Kerševan [95], L. Keszeghova [29a], R.A. Khan [132], A. Khanov [124], A.G. Kharlamov [38], T. Kharlamova [38], E.E. Khoda [142], M. Kholodenko [133a], T.J. Khoo [19], G. Khoriauli [172], Y. Khoulaki [36a], Y.A.R. Khwaira [130], B. Kibirige[34j], D. Kim [6], D.W. Kim [18b], Y.K. Kim [40], N. Kimura [98], M.K. Kingston [55], A. Kirchhoff [55], C. Kirfel [25], F. Kirfel [25], J. Kirk [137], A.E. Kiryunin [112], S. Kita [163], O. Kivernyk [25], M. Klassen [164], C. Klein [35], L. Klein [172], M.H. Klein [45], S.B. Klein [56], U. Klein [94], A. Klimentov [30], T. Klioutchnikova [37], P. Kluit [117], S. Kluth [112], E. Kneringer [79], T.M. Knight [161], A. Knue [49], M. Kobel [50], D. Kobylianskii [175], S.F. Koch [129], M. Kocian [149], P. Kodyš [136], D.M. Koeck [126], T. Koffas [35], O. Kolay [50], I. Koletsou [4], T. Komarek [88], K. Köneke [55], A.X.Y. Kong [1], T. Kono [121], N. Konstantinidis [98], P. Kontaxakis [56], B. Konya [100], R. Kopeliansky [42], S. Koperny [87a], K. Korcyl [88], K. Kordas [158,d], A. Korn [98], S. Korn [55], I. Korolkov [13], N. Korotkova [38], B. Kortman [117], O. Kortner [112], S. Kortner [112], W.H. Kostecka [118], M. Kostov [29a], V.V. Kostyukhin [147], A. Kotsokechagia [37], A. Kotwal [51], A. Koulouris [37], A. Kourkoumeli-Charalampidi [73a,73b], C. Kourkoumelis [9], E. Kourlitis [112], O. Kovanda [126], R. Kowalewski [171], W. Kozanecki [126], A.S. Kozhin [38], V.A. Kramarenko [38], G. Kramberger [95], P. Kramer [25], M.W. Krasny [130], A. Krasznahorkay [105], A.C. Kraus [118], J.W. Kraus [177], J.A. Kremer [48], N.B. Krengel [147], T. Kresse [50], L. Kretschmann [177], J. Kretzschmar [94], P. Krieger [161], K. Krizka [21], K. Kroeninger [49], H. Kroha [112], J. Kroll [134], J. Kroll [131], K.S. Krowpman [109], U. Kruchonak [39], H. Krüger [25], N. Krumnack[81], M.C. Kruse [51], O. Kuchinskaia [39], S. Kuday [3a], S. Kuehn [37], R. Kuesters [54], T. Kuhl [48], V. Kukhtin [39], Y. Kulchitsky [39], S. Kuleshov [140d,140b], J. Kull [1], E.V. Kumar [111], M. Kumar [34j], N. Kumari [48], P. Kumari [162b], A. Kupco [134], A. Kupich [38], O. Kuprash [54], H. Kurashige [86], L.L. Kurchaninov [162a], O. Kurdysh [4], A. Kurova [38], M. Kuze [141], A.K. Kvam [105], J. Kvita [125], N.G. Kyriacou [142], M. Laassiri [30], C. Lacasta [169], F. Lacava [75a,75b], H. Lacker [19], D. Lacour [130], N.N. Lad [98], E. Ladygin [39], A. Lafarge [41], B. Laforge [130], T. Lagouri [178], F.Z. Lahbabi [36a], S. Lai [55,37], W.S. Lai [98], J.E. Lambert [171], S. Lammers [68], W. Lampl [7], C. Lampoudis [158,d], G. Lamprinoudis [172], A.N. Lancaster [118], E. Lançon [30], U. Landgraf [54], M.P.J. Landon [96], V.S. Lang [54], A.J. Lankford [165], F. Lanni [37], K. Lantzsch [25], A. Lanza [73a], M. Lanzac Berrocal [169], J.F. Laporte [138], T. Lari [71a], D. Larsen [17], L. Larson [11], F. Lasagni Manghi [24b], M. Lassnig [37], S.D. Lawlor [145], R. Lazaridou[165], M. Lazzaroni [71a,71b], E.T.T. Le [165], H.D.M. Le [109], E.M. Le Boulicaut [178], L.T. Le Pottier [18a], B. Leban [24b,24a], F. Ledroit-Guillon [60], T.F. Lee [162b], L.L. Leeuw [34c], M. Lefebvre [171], C. Leggett [18a], G. Lehmann Miotto [37], M. Leigh [56], W.A. Leight [105], W. Leinonen [116], A. Leisos [158,u], M.A.L. Leite [83c], C.E. Leitgeb [19], R. Leitner [136], K.J.C. Leney [45], T. Lenz [25], S. Leone [74a], C. Leonidopoulos [52], A. Leopold [150], J.H. Lepage Bourbonnais [35], R. Les [109], C.G. Lester [33], M. Levchenko [38], J. Levêque [4], L.J. Levinson [175], G. Levrini [24b,24a], M.P. Lewicki [88], C. Lewis [142], D.J. Lewis [4], L. Lewitt [145], A. Li [30], B. Li [143a], C. Li[108], C-Q. Li [112], H. Li [143a], H. Li [103], H. Li [15], H. Li[62], H. Li [143a], J. Li [144a], K. Li [14], L. Li [144a], R. Li [178], S. Li [14,114c], S. Li [144b,144a], T. Li [5], X. Li [106], Y. Li[14], Z. Li [159], Z. Li [14,114c], Z. Li [62], S. Liang [14,114c], Z. Liang [14], M. Liberatore [138], B. Liberti [76a], G.B. Libotte [83d], K. Lie [64c], J. Lieber Marin [83e], H. Lien [68], H. Lin [108], S.F. Lin [151], L. Linden [111], R.E. Lindley [7], J.H. Lindon [37], J. Ling [61], E. Lipeles [131], A. Lipniacka [17], A. Lister [170], J.D. Little [68], B. Liu [14], B.X. Liu [114b], D. Liu [144b], D. Liu [139], E.H.L. Liu [21], J.K.K. Liu [120], K. Liu [144b], K. Liu [144b,144a], M. Liu [62], M.Y. Liu [62], P. Liu [14],

Q. Liu [149], S. Liu [151], X. Liu [62], X. Liu [143a], Y. Liu [114b,114c], Y. Liu [168], Y.L. Liu [143a], Y.W. Liu [62], Z. Liu [66,k], S.L. Lloyd [96], E.M. Lobodzinska [48], P. Loch [7], E. Lodhi [161], K. Lohwasser [145], E. Loiacono [48], J.D. Lomas [21], J.D. Long [42], I. Longarini [165], R. Longo [168], A. Lopez Solis [13], N.A. Lopez-canelas [7], N. Lorenzo Martinez [4], A.M. Lory [111], M. Losada [119a], G. Löschcke Centeno [4], X. Lou [47a,47b], X. Lou [14,114c], A. Lounis [66], P.A. Love [93], M. Lu [66], S. Lu [131], Y.J. Lu [154], H.J. Lubatti [142], C. Luci [75a,75b], F.L. Lucio Alves [114a], F. Luehring [68], B.S. Lunday [131], O. Lundberg [150], J. Lunde [37], N.A. Luongo [6], M.S. Lutz [37], A.B. Lux [26], D. Lynn [30], R. Lysak [134], V. Lysenko [135], E. Lytken [100], V. Lyubushkin [39], T. Lyubushkina [39], M.M. Lyukova [151], H. Ma [30], K. Ma [62], L.L. Ma [143a], W. Ma [62], Y. Ma [124], J.C. MacDonald [102], P.C. Machado De Abreu Farias [83e], D. Macina [37], R. Madar [41], T. Madula [98], J. Maeda [86], T. Maeno [30], P.T. Mafa [34c,j], H. Maguire [145], M. Maheshwari [33], V. Maiboroda [66], A. Maio [133a,133b,133d], K. Maj [87a], O. Majersky [48], S. Majewski [126], R. Makhmanazarov [38], N. Makovec [66], V. Maksimovic [16], B. Malaescu [130], J. Malamant[128], Pa. Malecki [88], V.P. Maleev [38], F. Malek [60,o], M. Mali [95], D. Malito [97], U. Mallik [80,*], A. Maloizel [5], S. Maltezos[10], A. Malvezzi Lopes [83d], S. Malyukov[39], J. Mamuzic [95], G. Mancini [53], M.N. Mancini [27], G. Manco [73a,73b], J.P. Mandalia [96], S.S. Mandarry [152], I. Mandić [95], L. Manhaes de Andrade Filho [83a], I.M. Maniatis [175], J. Manjarres Ramos [91], D.C. Mankad [175], A. Mann [111], T. Manoussos [37], M.N. Mantinan [40], S. Manzoni [37], L. Mao [144a], X. Mapekula [34c], A. Marantis [158], R.R. Marcelo Gregorio [96], G. Marchiori [5], C. Marcon [71a], E. Maricic [16], M. Marinescu [48], S. Marium [48], M. Marjanovic [123], A. Markhoos [54], M. Markovitch [66], M.K. Maroun [105], M.C. Marr [148], G.T. Marsden[103], E.J. Marshall [93], Z. Marshall [18a], S. Marti-Garcia [169], J. Martin [98], T.A. Martin [137], V.J. Martin [52], B. Martin dit Latour [17], L. Martinelli [75a,75b], M. Martinez [13,x], P. Martinez Agullo [169], V.I. Martinez Outschoorn [105], P. Martinez Suarez [37], S. Martin-Haugh [137], G. Martinovicova [136], V.S. Martoiu [28b], A.C. Martyniuk [98], A. Marzin [37], D. Mascione [78a,78b], L. Masetti [102], J. Masik [103], A.L. Maslennikov [39], S.L. Mason [42], P. Massarotti [72a,72b], P. Mastrandrea [74a,74b], A. Mastroberardino [44b,44a], T. Masubuchi [127], T.T. Mathew [126], J. Matousek [136], D.M. Mattern [49], K. Mauer [48], J. Maurer [28b], T. Maurin [59], A.J. Maury [66], B. Maček [95], C. Mavungu Tsava [104], D.A. Maximov [38], A.E. May [103], E. Mayer [41], R. Mazini [34j], I. Maznas [118], S.M. Mazza [139], E. Mazzeo [37], J.P. Mc Gowan [171], S.P. Mc Kee [108], C.A. Mc Lean [6], C.C. McCracken [170], E.F. McDonald [107], A.E. McDougall [117], L.F. Mcelhinney [93], J.A. Mcfayden [152], R.P. McGovern [131], R.P. Mckenzie [34j], T.C. Mclachlan [48], D.J. Mclaughlin [98], S.J. McMahon [137], C.M. Mcpartland [94], R.A. McPherson [171,ab], S. Mehlhase [111], A. Mehta [94], D. Melini [169], B.R. Mellado Garcia [34j], A.H. Melo [55], F. Meloni [48], A.M. Mendes Jacques Da Costa [103], L. Meng [93], S. Menke [112], M. Mentink [37], E. Meoni [44b,44a], G. Mercado [118], S. Merianos [158], C. Merlassino [69a,69c], C. Meroni [71a,71b], J. Metcalfe [6], A.S. Mete [6], E. Meuser [102], C. Meyer [68], J-P. Meyer [138], Y. Miao[114a], R.P. Middleton [137], M. Mihovilovic [66], L. Mijović [52], G. Mikenberg [175], M. Mikestikova [134], M. Mikuž [95], H. Mildner [102], A. Milic [37], D.W. Miller [40], E.H. Miller [149], A. Milov [175], D.A. Milstead[47a,47b], T. Min[114a], A.A. Minaenko [38], I.A. Minashvili [155b], A.I. Mincer [120], B. Mindur [87a], M. Mineev [39], Y. Mino [89], L.M. Mir [13], M. Miralles Lopez [59], M. Mironova [18a], M. Missio [41], A. Mitra [173], V.A. Mitsou [169], Y. Mitsumori [113], O. Miu [161], P.S. Miyagawa [96], T. Mkrtchyan [37], M. Mlinarevic [98], T. Mlinarevic [98], M. Mlynarikova [136], L. Mlynarska [87a], C. Mo [144a], S. Mobius [20], M.H. Mohamed Farook [115], S. Mohapatra [42], M.F. Mohd Soberi [52], S. Mohiuddin [124], G. Mokgatitswane [34j], L. Moleri [175], U. Molinatti [129], L.G. Mollier [20], B. Mondal [134], S. Mondal [135], K. Mönig [48], E. Monnier [104], L. Monsonis Romero[169], J. Montejo Berlingen [13], A. Montella [47a,47b], M. Montella [122], F. Montereali [77a,77b], F. Monticelli [92], S. Monzani [69a,69c],

A. Morancho Tarda[43], N. Morange[66], A.L. Moreira De Carvalho[48], M. Moreno Llácer[169], C. Moreno Martinez[56], J.M. Moreno Perez[23b], P. Morettini[57b], S. Morgenstern[37], M. Morii[61], M. Morinaga[159], M. Moritsu[90], F. Morodei[75a,75b], P. Moschovakos[37], B. Moser[54], M. Mosidze[155b], T. Moskalets[45], P. Moskvitina[116], J. Moss[32], P. Moszkowicz[87a], T. Motta Quirino[83d], A. Moussa[36d], Y. Moyal[175], H. Moyano Gomez[13], E.J.W. Moyse[105], T.G. Mroz[88], S. Muanza[104], M. Mucha[25], J. Mueller[132], R. Müller[37], G.A. Mullier[167], A.J. Mullin[33], J.J. Mullin[51], A.C. Mullins[45], A.E. Mulski[61], D.P. Mungo[161], D. Munoz Perez[169], F.J. Munoz Sanchez[103], W.J. Murray[173,137], M. Muškinja[95], C. Mwewa[48], A.G. Myagkov[38,a], A.J. Myers[8], G. Myers[108], M. Myska[135], B.P. Nachman[149], K. Nagai[129], K. Nagano[84], R. Nagasaka[159], J.L. Nagle[30,al], E. Nagy[104], A.M. Nairz[37], Y. Nakahama[84], K. Nakamura[84], K. Nakkalil[5], A. Nandi[63b], H. Nanjo[127], E.A. Narayanan[45], Y. Narukawa[159], I. Naryshkin[38], L. Nasella[71a,71b], S. Nasri[119b], C. Nass[25], G. Navarro[23a], A. Nayaz[19], P.Y. Nechaeva[38], S. Nechaeva[24b,24a], F. Nechansky[134], L. Nedic[129], T.J. Neep[21], A. Negri[73a,73b], M. Negrini[24b], C. Nellist[117], C. Nelson[106], K. Nelson[108], S. Nemecek[134], M. Nessi[37,g], M.S. Neubauer[168], J. Newell[94], P.R. Newman[21], Y.W.Y. Ng[168], B. Ngair[119a], H.D.N. Nguyen[110], J.D. Nichols[123], R.B. Nickerson[129], R. Nicolaidou[138], J. Nielsen[139], M. Niemeyer[55], J. Niermann[37], N. Nikiforou[37], V. Nikolaenko[38,a], I. Nikolic-Audit[130], P. Nilsson[30], I. Ninca[48], G. Ninio[157], A. Nisati[75a], R. Nisius[112], N. Nitika[175], E.K. Nkadimeng[34b], T. Nobe[159], D. Noll[149], T. Nommensen[153], M.B. Norfolk[145], B.J. Norman[35], L.C. Nosler[18a], M. Noury[36a], J. Novak[95], T. Novak[95], R. Novotny[135], L. Nozka[125], K. Ntekas[165], D. Ntounis[149], N.M.J. Nunes De Moura Junior[83b], J. Ocariz[130], I. Ochoa[133a], S. Oerdek[48,y], J.T. Offermann[40], A. Ogrodnik[88], A. Oh[103], C.C. Ohm[150], H. Oide[84], M.L. Ojeda[37], Y. Okumura[159], L.F. Oleiro Seabra[133a], I. Oleksiyuk[56], G. Oliveira Correa[13], D. Oliveira Damazio[30], J.L. Oliver[1], R. Omar[68], Ö.O. Öncel[54], A.P. O'Neill[20], A. Onofre[133a,133e,e], P.U.E. Onyisi[11], M.J. Oreglia[40], D. Orestano[77a,77b], R. Orlandini[77a,77b], R.S. Orr[161], L.M. Osojnak[42], Y. Osumi[113], G. Otero y Garzon[31], H. Otono[90], M. Ouchrif[36d], F. Ould-Saada[128], T. Ovsiannikova[142], M. Owen[59], R.E. Owen[137], V.E. Ozcan[22a], F. Ozturk[88], N. Ozturk[8], S. Ozturk[82], H.A. Pacey[129], K. Pachal[162a], A. Pacheco Pages[13], C. Padilla Aranda[13], G. Padovano[75a,75b], S. Pagan Griso[18a], J. Pampel[25], J. Pan[178], D.K. Panchal[11], C.E. Pandini[60], J.G. Panduro Vazquez[137], H.D. Pandya[1], H. Pang[138], P. Pani[48], G. Panizzo[69a,69c], L. Panwar[130], L. Paolozzi[56], S. Parajuli[168], A. Paramonov[6], C. Paraskevopoulos[53], D. Paredes Hernandez[64b], S.R. Paredes Saenz[52], A. Pareti[73a,73b], K.R. Park[42], T.H. Park[112], F. Parodi[57b,57a], J.A. Parsons[42], U. Parzefall[54], B. Pascual Dias[41], L. Pascual Dominguez[101], E. Pasqualucci[75a], S. Passaggio[57b], F. Pastore[97], P. Patel[88], U.M. Patel[51], J.R. Pater[103], T. Pauly[37], F. Pauwels[136], C.I. Pazos[164], M. Pedersen[128], R. Pedro[133a], S.V. Peleganchuk[38], O. Penc[134], S. Peng[15], G.D. Penn[178], K.E. Penski[111], M. Penzin[38], B.S. Peralva[83d], A.P. Pereira Peixoto[142], L. Pereira Sanchez[149], D.V. Perepelitsa[30,al], G. Perera[105], E. Perez Codina[37], M. Perganti[10], H. Pernegger[37], S. Perrella[75a,75b], K. Peters[48], R.F.Y. Peters[103], B.A. Petersen[37], T.C. Petersen[43], E. Petit[104], V. Petousis[135], A.R. Petri[71a,71b], C. Petridou[158,d], T. Petru[136], M. Pettee[18a], A. Petukhov[82], K. Petukhova[37], R. Pezoa[140g], L. Pezzotti[24b,24a], G. Pezzullo[178], L. Pfaffenbichler[37], A.J. Pfleger[79], T.M. Pham[176], T. Pham[107], P.W. Phillips[137], G. Piacquadio[151], E. Pianori[18a], F. Piazza[126], R. Piegaia[31], D. Pietreanu[28b], A.D. Pilkington[103], M. Pinamonti[69a,69c], J.L. Pinfold[2], G. Pinheiro Matos[42], B.C. Pinheiro Pereira[133a], J. Pinol Bel[13], A.E. Pinto Pinoargote[130], L. Pintucci[69a,69c], K.M. Piper[152], A. Pirttikoski[56], D.A. Pizzi[35], L. Pizzimento[64b], A. Plebani[33], M.-A. Pleier[30], V. Pleskot[136], E. Plotnikova[39], G. Poddar[96], R. Poettgen[100],

L. Poggioli [130], S. Polacek [136], G. Polesello [73a], A. Poley [148], A. Polini [24b], C.S. Pollard [173], Z.B. Pollock [122], E. Pompa Pacchi [123], N.I. Pond [98], D. Ponomarenko [68], L. Pontecorvo [37], S. Popa [28a], G.A. Popeneciu [28d], A. Poreba [37], D.M. Portillo Quintero [162a], S. Pospisil [135], M.A. Postill [145], P. Postolache [28c], K. Potamianos [173], P.A. Potepa [87a], I.N. Potrap [39], C.J. Potter [33], H. Potti [153], J. Poveda [169], M.E. Pozo Astigarraga [37], R. Pozzi [37], A. Prades Ibanez [76a,76b], S.R. Pradhan [145], J. Pretel [171], D. Price [103], M. Primavera [70a], L. Primomo [69a,69c], M.A. Principe Martin [101], R. Privara [125], T. Procter [87b], M.L. Proffitt [142], N. Proklova [131], K. Prokofiev [64c], G. Proto [112], J. Proudfoot [6], M. Przybycien [87a], W.W. Przygoda [87b], A. Psallidas [46], J.E. Puddefoot [145], D. Pudzha [53], H.I. Purnell [1], D. Pyatiizbyantseva [116], J. Qian [108], R. Qian [109], D. Qichen [129], Y. Qin [13], T. Qiu [52], A. Quadt [55], M. Queitsch-Maitland [103], G. Quetant [56], R.P. Quinn [170], G. Rabanal Bolanos [61], D. Rafanoharana [112], F. Raffaeli [76a,76b], F. Ragusa [71a,71b], J.L. Rainbolt [40], S. Rajagopalan [30], E. Ramakoti [39], L. Rambelli [57b,57a], I.A. Ramirez-Berend [35], K. Ran [108,114c], D.S. Rankin [131], N.P. Rapheeha [34j], H. Rasheed [28b], A. Rastogi [18a], S. Rave [102], S. Ravera [57b,57a], B. Ravina [37], I. Ravinovich [175], M. Raymond [37], A.L. Read [128], N.P. Readioff [145], D.M. Rebuzzi [73a,73b], A.S. Reed [59], K. Reeves [27], D. Reikher [37], A. Rej [49], C. Rembser [37], H. Ren [62], M. Renda [28b], F. Renner [48], A.G. Rennie [59], M. Repik [56], A.L. Rescia [57b,57a], S. Resconi [71a], M. Ressegotti [57b,57a], S. Rettie [117], W.F. Rettie [35], M.M. Revering [33], E. Reynolds [18a], O.L. Rezanova [39], P. Reznicek [136], H. Riani [36d], N. Ribaric [51], B. Ricci [69a,69c], E. Ricci [78a,78b], R. Richter [112], S. Richter [47a,47b], E. Richter-Was [87b], M. Ridel [130], S. Ridouani [36d], P. Rieck [120], P. Riedler [37], E.M. Riefel [47a,47b], J.O. Rieger [117], M. Rijssenbeek [151], M. Rimoldi [37], L. Rinaldi [24b,24a], P. Rincke [167,55], G. Ripellino [167], I. Riu [13], J.C. Rivera Vergara [171], F. Rizatdinova [124], E. Rizvi [96], B.R. Roberts [18a], S.S. Roberts [139], D. Robinson [33], A. Robson [59], A. Rocchi [76a,76b], C. Roda [74a,74b], F.A. Rodriguez [118], S. Rodriguez Bosca [37], Y. Rodriguez Garcia [23a], A.M. Rodríguez Vera [118], S. Roe[37], J.T. Roemer [37], O. Røhne [128], R.A. Rojas [37], C.P.A. Roland [130], A. Romaniouk [79], E. Romano [73a,73b], M. Romano [24b], A.C. Romero Hernandez [168], N. Rompotis [94], L. Roos [130], S. Rosati [75a], B.J. Rosser [40], E. Rossi [129], E. Rossi [72a,72b], L.P. Rossi [61], L. Rossini [54], R. Rosten [122], M. Rotaru [28b], D. Rousseau [66], D. Rousso [48], S. Roy-Garand [161], A. Rozanov [104], Z.M.A. Rozario [59], Y. Rozen [156], A. Rubio Jimenez [169], V.H. Ruelas Rivera [19], T.A. Ruggeri [1], A. Ruggiero [129], A. Ruiz-Martinez [169], A. Rummler [37], G.B. Rupnik Boero [37], Z. Rurikova [54], N.A. Rusakovich [39], S. Ruscelli [49], H.L. Russell [171], G. Russo [75a,75b], J.P. Rutherfoord [7], S. Rutherford Colmenares [33], M. Rybar [136], P. Rybczynski [87a], A. Ryzhov [45], J.A. Sabater Iglesias [56], H.F-W. Sadrozinski [139], F. Safai Tehrani [75a], S. Saha [1], M. Sahinsoy [82], B. Sahoo [175], A. Saibel [169], B.T. Saifuddin [123], M. Saimpert [138], G.T. Saito [83c], M. Saito [159], T. Saito [159], A. Sala [71a,71b], A. Salnikov [149], J. Salt [169], A. Salvador Salas [157], F. Salvatore [152], A. Salzburger [37], D. Sammel [54], E. Sampson [93], D. Sampsonidis [158,d], D. Sampsonidou [126], M.A.A. Samy [59], J. Sánchez [169], V. Sanchez Sebastian [169], H. Sandaker [128], C.O. Sander [48], J.A. Sandesara [176], M. Sandhoff [177], C. Sandoval [23b], L. Sanfilippo [63a], D.P.C. Sankey [137], T. Sano [89], A. Sansoni [53], M. Santana Queiroz [18b], L. Santi [37], C. Santoni [41], H. Santos [133a,133b], A. Santra [175], E. Sanzani [24b,24a], K.A. Saoucha [85b], J.G. Saraiva [133a,133d], J. Sardain [7], O. Sasaki [84], K. Sato [163], C. Sauer[37], E. Sauvan [4], P. Savard [161,ai], R. Sawada [159], C. Sawyer [137], L. Sawyer [99], A.M. Sayed [27], C. Sbarra [24b], A. Sbrizzi [24b,24a], T. Scanlon [98], J. Schaarschmidt [142], U. Schäfer [102], A.C. Schaffer [66,45], D. Schaile [111], R.D. Schamberger [151], C. Scharf [19], M.M. Schefer [20], V.A. Schegelsky [38], D. Scheirich [136], M. Schernau [140f], C. Scheulen [56], C. Schiavi [57b,57a], M. Schioppa [44b,44a], B. Schlag [149], S. Schlenker [37], J. Schmeing [177], E. Schmidt [112], M.A. Schmidt [177], K. Schmieden [25], C. Schmitt [102],

N. Schmitt [102], S. Schmitt [48], N.A. Schneider [111], L. Schoeffel [138], A. Schoening [63b], P.G. Scholer [35], E. Schopf [147], M. Schott [25], S. Schramm [56], T. Schroer [56], H-C. Schultz-Coulon [63a], M. Schumacher [54], B.A. Schumm [139], Ph. Schune [138], H.R. Schwartz [7], A. Schwartzman [149], T.A. Schwarz [108], Ph. Schwemling [138], R. Schwienhorst [109], F.G. Sciacca [20], A. Sciandra [30], G. Sciolla [27], F. Scuri [74a], C.D. Sebastiani [37], K. Sedlaczek [118], S.C. Seidel [115], A. Seiden [139], B.D. Seidlitz [42], C. Seitz [48], J.M. Seixas [83b], G. Sekhniaidze [72a], L. Selem [60], N. Semprini-Cesari [24b,24a], A. Semushin [179], D. Sengupta [56], V. Senthilkumar [169], L. Serin [66], M. Sessa [72a,72b], H. Severini [123], F. Sforza [57b,57a], A. Sfyrla [56], Q. Sha [14], H. Shaddix [118], A.H. Shah [33], R. Shaheen [150], J.D. Shahinian [131], M. Shamim [37], L.Y. Shan [14], M. Shapiro [18a], A. Sharma [37], A.S. Sharma [170], P. Sharma [30], P.B. Shatalov [38], K. Shaw [152], S.M. Shaw [103], Q. Shen [14], D.J. Sheppard [148], P. Sherwood [98], L. Shi [98], X. Shi [14], S. Shimizu [84], I.P.J. Shipsey [129,*], S. Shirabe [90], M. Shiyakova [39,z], M.J. Shochet [40], D.R. Shope [128], B. Shrestha [123], S. Shrestha [122,an], I. Shreyber [39], M.J. Shroff [171], P. Sicho [134], A.M. Sickles [168], E. Sideras Haddad [34j,166], A.C. Sidley [117], A. Sidoti [24b], F. Siegert [50], Dj. Sijacki [16], F. Sili [62], J.M. Silva [52], I. Silva Ferreira [83b], M.V. Silva Oliveira [30], S.B. Silverstein [47a], S. Simion[66], R. Simoniello [37], E.L. Simpson [103], H. Simpson [152], L.R. Simpson [6], S. Simsek [82], S. Sindhu [55], P. Sinervo [161], S.N. Singh [27], S. Singh [30], S. Sinha [48], S. Sinha [103], M. Sioli [24b,24a], K. Sioulas [9], I. Siral [37], E. Sitnikova [48], J. Sjölin [47a,47b], A. Skaf [55], E. Skorda [21], P. Skubic [123], M. Slawinska [88], I. Slazyk [17], I. Sliusar [128], V. Smakhtin[175], B.H. Smart [137], S.Yu. Smirnov [140b], Y. Smirnov [82], L.N. Smirnova [38,a], O. Smirnova [100], A.C. Smith [42], D.R. Smith[165], J.L. Smith [103], M.B. Smith [35], R. Smith[149], H. Smitmanns [102], M. Smizanska [93], K. Smolek [135], P. Smolyanskiy [135], A.A. Snesarev [39], H.L. Snoek [117], S. Snyder [30], R. Sobie [171,ab], A. Soffer [157], C.A. Solans Sanchez [37], E.Yu. Soldatov [39], U. Soldevila [169], A.A. Solodkov [34j], S. Solomon [27], A. Soloshenko [39], K. Solovieva [54], O.V. Solovyanov [41], P. Sommer [50], A. Sonay [13], A. Sopczak [135], A.L. Sopio [52], F. Sopkova [29b], J.D. Sorenson [115], I.R. Sotarriva Alvarez [141], V. Sothilingam[63a], O.J. Soto Sandoval [140c,140b], S. Sottocornola [68], R. Soualah [85a], Z. Soumaimi [36e], D. South [48], N. Soybelman [175], S. Spagnolo [70a,70b], M. Spalla [112], D. Sperlich [54], B. Spisso [72a,72b], D.P. Spiteri [59], L. Splendori [104], M. Spousta [136], E.J. Staats [35], R. Stamen [63a], E. Stanecka [88], W. Stanek-Maslouska [48], M.V. Stange [50], B. Stanislaus [18a], M.M. Stanitzki [48], E.A. Starchenko [38], G.H. Stark [139], J. Stark [91], P. Staroba [134], P. Starovoitov [85b], R. Staszewski [88], C. Stauch [111], G. Stavropoulos [46], A. Stefl [37], A. Stein [102], P. Steinberg [30], B. Stelzer [148,162a], H.J. Stelzer [132], O. Stelzer [162a], H. Stenzel [58], T.J. Stevenson [152], G.A. Stewart [37], J.R. Stewart [124], G. Stoicea [28b], M. Stolarski [133a], S. Stonjek [112], A. Straessner [50], J. Strandberg [150], S. Strandberg [47a,47b], M. Stratmann [177], M. Strauss [123], T. Strebler [104], P. Strizenec [29b], R. Ströhmer [172], D.M. Strom [126], R. Stroynowski [45], A. Strubig [47a,47b], S.A. Stucci [30], B. Stugu [17], J. Stupak [123], N.A. Styles [48], D. Su [149], S. Su [62], X. Su [62], D. Suchy [29a], A.D. Sudhakar Ponnu [55], K. Sugizaki [131], V.V. Sulin [38], D.M.S. Sultan [129], L. Sultanaliyeva [25], S. Sultansoy [3b], S. Sun [176], W. Sun [14], N. Sur [100], M.R. Sutton [152], M. Svatos [134], P.N. Swallow [33], M. Swiatlowski [162a], A. Swoboda [37], I. Sykora [29a], M. Sykora [136], T. Sykora [136], D. Ta [102], K. Tackmann [48,y], A. Taffard [165], R. Tafirout [162a], Y. Takubo [84], M. Talby [104], A.A. Talyshev [38], K.C. Tam [64b], N.M. Tamir [157], A. Tanaka [159], J. Tanaka [159], R. Tanaka [66], M. Tanasini [151], Z. Tao [170], S. Tapia Araya [140g], S. Tapprogge [102], A. Tarek Abouelfadl Mohamed [37], S. Tarem [156], K. Tariq [14], G. Tarna [37], G.F. Tartarelli [71a], M.J. Tartarin [91], P. Tas [136], M. Tasevsky [134], E. Tassi [44b,44a], A.C. Tate [168], Y. Tayalati [36e,aa], G.N. Taylor [107], W. Taylor [162b], R.J. Taylor Vara [169], A.S. Tegetmeier [91], P. Teixeira-Dias [97], J.J. Teoh [161], K. Terashi [159], J. Terron [101], S. Terzo [13], M. Testa [53], R.J. Teuscher [161,ab], A. Thaler [79], O. Theiner [56], T. Theveneaux-Pelzer [104], D.W. Thomas[97], J.P. Thomas [21], E.A. Thompson [18a], P.D. Thompson [21], E. Thomson [131], R.E. Thornberry [45], C. Tian [62], Y. Tian [56], V. Tikhomirov [82], Yu.A. Tikhonov [39], S. Timoshenko[38], D. Timoshyn [136], E.X.L. Ting [1], P. Tipton [178], A. Tishelman-Charny [30], K. Todome [141], S. Todorova-Nova [136], L. Toffolin [69a,69c], M. Togawa [84], J. Tojo [90], S. Tokár [29a], O. Toldaiev [68], G. Tolkachev [104], M. Tomoto [84], L. Tompkins [149,n], E. Torrence [126], H. Torres [91], D.I. Torres Arza [140g], E. Torró Pastor [169], M. Toscani [31], C. Tosciri [40], M. Tost [11], D.R. Tovey [145], T. Trefzger [172], P.M. Tricarico [13], A. Tricoli [30], I.M. Trigger [162a], S. Trincaz-Duvoid [130], D.A. Trischuk [171], A. Tropina[39], D. Truncali [76a,76b], L. Truong [34c], M. Trzebinski [88], A. Trzupek [88], F. Tsai [151], M. Tsai [108], A. Tsiamis [158], P.V. Tsiareshka[39], S. Tsigaridas [162a], A. Tsirigotis [158,u], V. Tsiskaridze [155a], E.G. Tskhadadze [155a], Y. Tsujikawa [89], I.I. Tsukerman [38], V. Tsulaia [18a], S. Tsuno [84], K. Tsuri [121], D. Tsybychev [151], Y. Tu [64b], A. Tudorache [28b], V. Tudorache [28b], S.B. Tuncay [129], S. Turchikhin [57b,57a], I. Turk Cakir [3a], R. Turra [71a], T. Turtuvshin [39,ac], P.M. Tuts [42], S. Tzamarias [158,d], Y. Uematsu [84], F. Ukegawa [163], P.A. Ulloa Poblete [140c,140b], E.N. Umaka [30], G. Unal [37], A. Undrus [30], G. Unel [165], J. Urban [29b], P. Urrejola [140e], G. Usai [8], R. Ushioda [160], M. Usman [110], F. Ustuner [52], Z. Uysal [82], V. Vacek [135], B. Vachon [106], T. Vafeiadis [37], A. Vaitkus [98], C. Valderanis [111], E. Valdes Santurio [47a,47b], M. Valente [37], S. Valentinetti [24b,24a], A. Valero [169], E. Valiente Moreno [169], A. Vallier [91], J.A. Valls Ferrer [169], D.R. Van Arneman [117], A. Van Der Graaf [49], H.Z. Van Der Schyf [34j], P. Van Gemmeren [6], M. Van Rijnbach [37], S. Van Stroud [98], I. Van Vulpen [117], P. Vana [136], M. Vanadia [76a,76b], U.M. Vande Voorde [150], W. Vandelli [37], E.R. Vandewall [149], D. Vannicola [157], L. Vannoli [53], R. Vari [75a], M. Varma [178], E.W. Varnes [7], C. Varni [118], D. Varouchas [66], L. Varriale [169], K.E. Varvell [153], M.E. Vasile [28b], L. Vaslin[84], M.D. Vassilev [149], A. Vasyukov [39], L.M. Vaughan [124], R. Vavricka[136], T. Vazquez Schroeder [13], J. Veatch [32], V. Vecchio [103], M.J. Veen [105], I. Veliscek [30], I. Velkovska [95], L.M. Veloce [161], F. Veloso [133a,133c], A.G. Veltman [52], S. Veneziano [75a], A. Ventura [70a,70b], A. Verbytskyi [112], M. Verducci [74a,74b], C. Vergis [96], M. Verissimo De Araujo [83b], W. Verkerke [117], J.C. Vermeulen [117], C. Vernieri [149], M. Vessella [165], M.C. Vetterli [148,ai], A. Vgenopoulos [102], N. Viaux Maira [140g,af], T. Vickey [145], O.E. Vickey Boeriu [145], G.H.A. Viehhauser [129], L. Vigani [63b], M. Vigl [112], M. Villa [24b,24a], M. Villaplana Perez [169], E.M. Villhauer[40], E. Vilucchi [53], M. Vincent [169], M.G. Vincter [35], A. Visibile [117], A. Visive [117], C. Vittori [37], I. Vivarelli [24b,24a], M.I. Vivas Albornoz [48], E. Voevodina [112], F. Vogel [111], J.C. Voigt [50], P. Vokac [135], Yu. Volkotrub [87b], L. Vomberg [25], E. Von Toerne [25], B. Vormwald [37], K. Vorobev [51], M. Vos [169], K. Voss [147], M. Vozak [37], L. Vozdecky [123], N. Vranjes [16], M. Vranjes Milosavljevic [16], M. Vreeswijk [117], N.K. Vu [144b,144a], R. Vuillermet [37], O. Vujinovic [102], I. Vukotic [40], I.K. Vyas [35], J.F. Wack [33], S. Wada [163], C. Wagner[149], J.M. Wagner [18a], W. Wagner [177], S. Wahdan [177], H. Wahlberg [92], C.H. Waits [123], J. Walder [137], R. Walker [111], K. Walkingshaw Pass [59], W. Walkowiak [147], A. Wall [131], E.J. Wallin [100], T. Wamorkar [18a], K. Wandall-Christensen [169], A. Wang [62], A.Z. Wang [139], C. Wang [102], C. Wang [11], H. Wang [18a], J. Wang [64c], P. Wang [103], P. Wang [98], R. Wang [61], R. Wang [6], S.M. Wang [154], S. Wang [14], T. Wang [116], T. Wang [62], W.T. Wang [129], W. Wang [14], X. Wang [168], X. Wang [144a], X. Wang [48], Y. Wang [151], Y. Wang [62], Z. Wang [108], Z. Wang [144b], Z. Wang [108], C. Wanotayaroj [84], A. Warburton [106], A.L. Warnerbring [147], S. Waterhouse [97], A.T. Watson [21], H. Watson [52], M.F. Watson [21], E. Watton [37], G. Watts [142], B.M. Waugh [98], J.M. Webb [54], C. Weber [30], H.A. Weber [19], M.S. Weber [20], S.M. Weber [63a], C. Wei [62], Y. Wei [54], A.R. Weidberg [129], E.J. Weik [120], J. Weingarten [49], C. Weiser [54], C.J. Wells [48], T. Wenaus [30], T. Wengler [37], N.S. Wenke[112], N. Wermes [25], M. Wessels [63a], A.M. Wharton [93], A.S. White [61], A. White [8], M.J. White [1], D. Whiteson [165], L. Wickremasinghe [127],

W. Wiedenmann[176], M. Wielers[137], R. Wierda[150], C. Wiglesworth[43], H.G. Wilkens[37], J.J.H. Wilkinson[33], D.M. Williams[42], H.H. Williams[131], S. Williams[33], S. Willocq[105], B.J. Wilson[103], D.J. Wilson[103], P.J. Windischhofer[40], F.I. Winkel[31], F. Winklmeier[126], B.T. Winter[54], M. Wittgen[149], M. Wobisch[99], T. Wojtkowski[60], Z. Wolffs[117], J. Wollrath[37], M.W. Wolter[88], H. Wolters[133a,133c], M.C. Wong[139], E.L. Woodward[42], S.D. Worm[48], B.K. Wosiek[88], K.W. Woźniak[88], S. Wozniewski[55], K. Wraight[59], C. Wu[161], C. Wu[21], J. Wu[159], M. Wu[114b], M. Wu[116], S.L. Wu[176], S. Wu[14,ak], X. Wu[62], Y.Q. Wu[161], Y. Wu[62], Z. Wu[4], Z. Wu[114a], J. Wuerzinger[112], T.R. Wyatt[103], B.M. Wynne[52], S. Xella[43], L. Xia[114a], M. Xie[62], A. Xiong[126], D. Xu[14], H. Xu[62], L. Xu[62], R. Xu[131], T. Xu[108], Y. Xu[142], Z. Xu[52], R. Xue[132], B. Yabsley[153], S. Yacoob[34a], Y. Yamaguchi[84], E. Yamashita[159], H. Yamauchi[163], T. Yamazaki[18a], Y. Yamazaki[86], S. Yan[59], Z. Yan[105], H.J. Yang[144a,144b], H.T. Yang[62], S. Yang[62], T. Yang[64c], X. Yang[37], X. Yang[14], Y. Yang[159], Y. Yang[62], W-M. Yao[18a], C.L. Yardley[152], J. Ye[14], S. Ye[30], X. Ye[62], Y. Yeh[98], I. Yeletskikh[39], B. Yeo[18b], M.R. Yexley[98], T.P. Yildirim[129], K. Yorita[174], C.J.S. Young[37], C. Young[149], N.D. Young[126], Y. Yu[62], J. Yuan[14,114c], M. Yuan[108], R. Yuan[144b], L. Yue[98], M. Zaazoua[62], B. Zabinski[88], I. Zahir[36a], A. Zaio[57b,57a], Z.K. Zak[88], T. Zakareishvili[169], S. Zambito[56], J.A. Zamora Saa[140d], J. Zang[159], R. Zanzottera[71a,71b], O. Zaplatilek[135], C. Zeitnitz[177], H. Zeng[14], D.T. Zenger Jr[27], O. Zenin[38], T. Ženiš[29a], S. Zenz[96], D. Zerwas[66], M. Zhai[14,114c], D.F. Zhang[145], G. Zhang[14,ak], J. Zhang[143a], J. Zhang[6], L. Zhang[62], L. Zhang[114a], P. Zhang[14,114c], R. Zhang[114a], S. Zhang[91], T. Zhang[159], Y. Zhang[142], Y. Zhang[98], Y. Zhang[62], Y. Zhang[114a], Z. Zhang[18a], Z. Zhang[143a], Z. Zhang[66], H. Zhao[142], T. Zhao[143a], Y. Zhao[35], Z. Zhao[62], Z. Zhao[62], A. Zhemchugov[39], J. Zheng[114a], K. Zheng[168], X. Zheng[62], Z. Zheng[149], D. Zhong[168], B. Zhou[108], H. Zhou[7], N. Zhou[144a], Y. Zhou[15], Y. Zhou[114a], Y. Zhou[7], J. Zhu[108], X. Zhu[144b], Y. Zhu[144a], Y. Zhu[62], X. Zhuang[14], K. Zhukov[68], N.I. Zimine[39], J. Zinsser[63b], M. Ziolkowski[147], L. Živković[16], A. Zoccoli[24b,24a], K. Zoch[61], A. Zografos[37], T.G. Zorbas[145], O. Zormpa[46], D. Zubov[158], L. Zwalinski[37].

[1]Department of Physics, University of Adelaide, Adelaide; Australia.
[2]Department of Physics, University of Alberta, Edmonton AB; Canada.
[3(a)]Department of Physics, Ankara University, Ankara;[(b)]Division of Physics, TOBB University of Economics and Technology, Ankara; Türkiye.
[4]LAPP, Université Savoie Mont Blanc, CNRS/IN2P3, Annecy; France.
[5]APC, Université Paris Cité, CNRS/IN2P3, Paris; France.
[6]High Energy Physics Division, Argonne National Laboratory, Argonne IL; United States of America.
[7]Department of Physics, University of Arizona, Tucson AZ; United States of America.
[8]Department of Physics, University of Texas at Arlington, Arlington TX; United States of America.
[9]Physics Department, National and Kapodistrian University of Athens, Athens; Greece.
[10]Physics Department, National Technical University of Athens, Zografou; Greece.
[11]Department of Physics, University of Texas at Austin, Austin TX; United States of America.
[12]Institute of Physics, Azerbaijan Academy of Sciences, Baku; Azerbaijan.
[13]Institut de Física d'Altes Energies (IFAE), Barcelona Institute of Science and Technology, Barcelona; Spain.
[14]Institute of High Energy Physics, Chinese Academy of Sciences, Beijing; China.
[15]Physics Department, Tsinghua University, Beijing; China.
[16]Institute of Physics, University of Belgrade, Belgrade; Serbia.
[17]Department for Physics and Technology, University of Bergen, Bergen; Norway.

[18(a)]Physics Division, Lawrence Berkeley National Laboratory, Berkeley CA;[(b)]University of California, Berkeley CA; United States of America.
[19]Institut für Physik, Humboldt Universität zu Berlin, Berlin; Germany.
[20]Albert Einstein Center for Fundamental Physics and Laboratory for High Energy Physics, University of Bern, Bern; Switzerland.
[21]School of Physics and Astronomy, University of Birmingham, Birmingham; United Kingdom.
[22(a)]Department of Physics, Bogazici University, Istanbul;[(b)]Department of Physics Engineering, Gaziantep University, Gaziantep;[(c)]Department of Physics, Istanbul University, Istanbul; Türkiye.
[23(a)]Facultad de Ciencias y Centro de Investigaciónes, Universidad Antonio Nariño, Bogotá;[(b)]Departamento de Física, Universidad Nacional de Colombia, Bogotá; Colombia.
[24(a)]Dipartimento di Fisica e Astronomia A. Righi, Università di Bologna, Bologna;[(b)]INFN Sezione di Bologna; Italy.
[25]Physikalisches Institut, Universität Bonn, Bonn; Germany.
[26]Department of Physics, Boston University, Boston MA; United States of America.
[27]Department of Physics, Brandeis University, Waltham MA; United States of America.
[28(a)]Transilvania University of Brasov, Brasov;[(b)]Horia Hulubei National Institute of Physics and Nuclear Engineering, Bucharest;[(c)]Department of Physics, Alexandru Ioan Cuza University of Iasi, Iasi;[(d)]National Institute for Research and Development of Isotopic and Molecular Technologies, Physics Department, Cluj-Napoca;[(e)]National University of Science and Technology Politechnica, Bucharest;[(f)]West University in Timisoara, Timisoara;[(g)]Faculty of Physics, University of Bucharest, Bucharest; Romania.
[29(a)]Faculty of Mathematics, Physics and Informatics, Comenius University, Bratislava;[(b)]Department of Subnuclear Physics, Institute of Experimental Physics of the Slovak Academy of Sciences, Kosice; Slovak Republic.
[30]Physics Department, Brookhaven National Laboratory, Upton NY; United States of America.
[31]Universidad de Buenos Aires, Facultad de Ciencias Exactas y Naturales, Departamento de Física, y CONICET, Instituto de Física de Buenos Aires (IFIBA), Buenos Aires; Argentina.
[32]California State University, CA; United States of America.
[33]Cavendish Laboratory, University of Cambridge, Cambridge; United Kingdom.
[34(a)]Department of Physics, University of Cape Town, Cape Town;[(b)]iThemba Labs, Western Cape;[(c)]Department of Mechanical Engineering Science, University of Johannesburg, Johannesburg;[(d)]National Institute of Physics, University of the Philippines Diliman (Philippines);[(e)]Department of Physics, Stellenbosch University, Matieland;[(f)]University of KwaZulu-Natal, School of Agriculture and Science, Mathematics, Westville;[(g)]University of South Africa, Department of Physics, Pretoria;[(h)]University of Pretoria, Department of Mechanical and Aeronautical Engineering, Pretoria;[(i)]University of Zululand, KwaDlangezwa;[(j)]School of Physics, University of the Witwatersrand, Johannesburg; South Africa.
[35]Department of Physics, Carleton University, Ottawa ON; Canada.
[36(a)]Faculté des Sciences Ain Chock, Université Hassan II de Casablanca;[(b)]Faculté des Sciences, Université Ibn-Tofail, Kénitra;[(c)]Faculté des Sciences Semlalia, Université Cadi Ayyad, LPHEA-Marrakech;[(d)]LPMR, Faculté des Sciences, Université Mohamed Premier, Oujda;[(e)]Faculté des sciences, Université Mohammed V, Rabat;[(f)]Institute of Applied Physics, Mohammed VI Polytechnic University, Ben Guerir; Morocco.
[37]CERN, Geneva; Switzerland.
[38]Affiliated with an institute formerly covered by a cooperation agreement with CERN.
[39]Affiliated with an international laboratory covered by a cooperation agreement with CERN.
[40]Enrico Fermi Institute, University of Chicago, Chicago IL; United States of America.
[41]LPC, Université Clermont Auvergne, CNRS/IN2P3, Clermont-Ferrand; France.

[42]Nevis Laboratory, Columbia University, Irvington NY; United States of America.
[43]Niels Bohr Institute, University of Copenhagen, Copenhagen; Denmark.
[44(a)]Dipartimento di Fisica, Università della Calabria, Rende;[(b)]INFN Gruppo Collegato di Cosenza, Laboratori Nazionali di Frascati; Italy.
[45]Physics Department, Southern Methodist University, Dallas TX; United States of America.
[46]National Centre for Scientific Research "Demokritos", Agia Paraskevi; Greece.
[47(a)]Department of Physics, Stockholm University;[(b)]Oskar Klein Centre, Stockholm; Sweden.
[48]Deutsches Elektronen-Synchrotron DESY, Hamburg and Zeuthen; Germany.
[49]Fakultät Physik, Technische Universität Dortmund, Dortmund; Germany.
[50]Institut für Kern- und Teilchenphysik, Technische Universität Dresden, Dresden; Germany.
[51]Department of Physics, Duke University, Durham NC; United States of America.
[52]SUPA - School of Physics and Astronomy, University of Edinburgh, Edinburgh; United Kingdom.
[53]INFN e Laboratori Nazionali di Frascati, Frascati; Italy.
[54]Physikalisches Institut, Albert-Ludwigs-Universität Freiburg, Freiburg; Germany.
[55]II. Physikalisches Institut, Georg-August-Universität Göttingen, Göttingen; Germany.
[56]Département de Physique Nucléaire et Corpusculaire, Université de Genève, Genève; Switzerland.
[57(a)]Dipartimento di Fisica, Università di Genova, Genova;[(b)]INFN Sezione di Genova; Italy.
[58]II. Physikalisches Institut, Justus-Liebig-Universität Giessen, Giessen; Germany.
[59]SUPA - School of Physics and Astronomy, University of Glasgow, Glasgow; United Kingdom.
[60]LPSC, Université Grenoble Alpes, CNRS/IN2P3, Grenoble INP, Grenoble; France.
[61]Laboratory for Particle Physics and Cosmology, Harvard University, Cambridge MA; United States of America.
[62]Department of Modern Physics and State Key Laboratory of Particle Detection and Electronics, University of Science and Technology of China, Hefei; China.
[63(a)]Kirchhoff-Institut für Physik, Ruprecht-Karls-Universität Heidelberg, Heidelberg;[(b)]Physikalisches Institut, Ruprecht-Karls-Universität Heidelberg, Heidelberg; Germany.
[64(a)]Department of Physics, Chinese University of Hong Kong, Shatin, N.T., Hong Kong;[(b)]Department of Physics, University of Hong Kong, Hong Kong;[(c)]Department of Physics and Institute for Advanced Study, Hong Kong University of Science and Technology, Clear Water Bay, Kowloon, Hong Kong; China.
[65]Department of Physics, National Tsing Hua University, Hsinchu; Taiwan.
[66]IJCLab, Université Paris-Saclay, CNRS/IN2P3, 91405, Orsay; France.
[67]Centro Nacional de Microelectrónica (IMB-CNM-CSIC), Barcelona; Spain.
[68]Department of Physics, Indiana University, Bloomington IN; United States of America.
[69(a)]INFN Gruppo Collegato di Udine, Sezione di Trieste, Udine;[(b)]ICTP, Trieste;[(c)]Dipartimento Politecnico di Ingegneria e Architettura, Università di Udine, Udine; Italy.
[70(a)]INFN Sezione di Lecce;[(b)]Dipartimento di Matematica e Fisica, Università del Salento, Lecce; Italy.
[71(a)]INFN Sezione di Milano;[(b)]Dipartimento di Fisica, Università di Milano, Milano; Italy.
[72(a)]INFN Sezione di Napoli;[(b)]Dipartimento di Fisica, Università di Napoli, Napoli; Italy.
[73(a)]INFN Sezione di Pavia;[(b)]Dipartimento di Fisica, Università di Pavia, Pavia; Italy.
[74(a)]INFN Sezione di Pisa;[(b)]Dipartimento di Fisica E. Fermi, Università di Pisa, Pisa; Italy.
[75(a)]INFN Sezione di Roma;[(b)]Dipartimento di Fisica, Sapienza Università di Roma, Roma; Italy.
[76(a)]INFN Sezione di Roma Tor Vergata;[(b)]Dipartimento di Fisica, Università di Roma Tor Vergata, Roma; Italy.
[77(a)]INFN Sezione di Roma Tre;[(b)]Dipartimento di Matematica e Fisica, Università Roma Tre, Roma; Italy.
[78(a)]INFN-TIFPA;[(b)]Università degli Studi di Trento, Trento; Italy.
[79]Universität Innsbruck, Department of Astro and Particle Physics, Innsbruck; Austria.

[80]University of Iowa, Iowa City IA; United States of America.
[81]Department of Physics and Astronomy, Iowa State University, Ames IA; United States of America.
[82]Istinye University, Sariyer, Istanbul; Türkiye.
[83(a)]Departamento de Engenharia Elétrica, Universidade Federal de Juiz de Fora (UFJF), Juiz de Fora;[(b)]Universidade Federal do Rio De Janeiro COPPE/EE/IF, Rio de Janeiro;[(c)]Instituto de Física, Universidade de São Paulo, São Paulo;[(d)]Rio de Janeiro State University, Rio de Janeiro;[(e)]Federal University of Bahia, Bahia; Brazil.
[84]KEK, High Energy Accelerator Research Organization, Tsukuba; Japan.
[85(a)]Khalifa University of Science and Technology, Abu Dhabi;[(b)]University of Sharjah, Sharjah; United Arab Emirates.
[86]Graduate School of Science, Kobe University, Kobe; Japan.
[87(a)]AGH University of Krakow, Faculty of Physics and Applied Computer Science, Krakow;[(b)]Marian Smoluchowski Institute of Physics, Jagiellonian University, Krakow; Poland.
[88]Institute of Nuclear Physics Polish Academy of Sciences, Krakow; Poland.
[89]Faculty of Science, Kyoto University, Kyoto; Japan.
[90]Research Center for Advanced Particle Physics and Department of Physics, Kyushu University, Fukuoka ; Japan.
[91]L2IT, Université de Toulouse, CNRS/IN2P3, UPS, Toulouse; France.
[92]Instituto de Física La Plata, Universidad Nacional de La Plata and CONICET, La Plata; Argentina.
[93]Physics Department, Lancaster University, Lancaster; United Kingdom.
[94]Oliver Lodge Laboratory, University of Liverpool, Liverpool; United Kingdom.
[95]Department of Experimental Particle Physics, Jožef Stefan Institute and Department of Physics, University of Ljubljana, Ljubljana; Slovenia.
[96]Department of Physics and Astronomy, Queen Mary University of London, London; United Kingdom.
[97]Department of Physics, Royal Holloway University of London, Egham; United Kingdom.
[98]Department of Physics and Astronomy, University College London, London; United Kingdom.
[99]Louisiana Tech University, Ruston LA; United States of America.
[100]Fysiska institutionen, Lunds universitet, Lund; Sweden.
[101]Departamento de Física Teorica C-15 and CIAFF, Universidad Autónoma de Madrid, Madrid; Spain.
[102]Institut für Physik, Universität Mainz, Mainz; Germany.
[103]School of Physics and Astronomy, University of Manchester, Manchester; United Kingdom.
[104]CPPM, Aix-Marseille Université, CNRS/IN2P3, Marseille; France.
[105]Department of Physics, University of Massachusetts, Amherst MA; United States of America.
[106]Department of Physics, McGill University, Montreal QC; Canada.
[107]School of Physics, University of Melbourne, Victoria; Australia.
[108]Department of Physics, University of Michigan, Ann Arbor MI; United States of America.
[109]Department of Physics and Astronomy, Michigan State University, East Lansing MI; United States of America.
[110]Group of Particle Physics, University of Montreal, Montreal QC; Canada.
[111]Fakultät für Physik, Ludwig-Maximilians-Universität München, München; Germany.
[112]Max-Planck-Institut für Physik (Werner-Heisenberg-Institut), München; Germany.
[113]Graduate School of Science and Kobayashi-Maskawa Institute, Nagoya University, Nagoya; Japan.
[114(a)]Department of Physics, Nanjing University, Nanjing;[(b)]School of Science, Shenzhen Campus of Sun Yat-sen University;[(c)]University of Chinese Academy of Science (UCAS), Beijing; China.
[115]Department of Physics and Astronomy, University of New Mexico, Albuquerque NM; United States of America.
[116]Institute for Mathematics, Astrophysics and Particle Physics, Radboud University/Nikhef, Nijmegen;

Netherlands.
[117]Nikhef National Institute for Subatomic Physics and University of Amsterdam, Amsterdam; Netherlands.
[118]Department of Physics, Northern Illinois University, DeKalb IL; United States of America.
[119(a)]New York University Abu Dhabi, Abu Dhabi;[(b)]United Arab Emirates University, Al Ain; United Arab Emirates.
[120]Department of Physics, New York University, New York NY; United States of America.
[121]Ochanomizu University, Otsuka, Bunkyo-ku, Tokyo; Japan.
[122]Ohio State University, Columbus OH; United States of America.
[123]Homer L. Dodge Department of Physics and Astronomy, University of Oklahoma, Norman OK; United States of America.
[124]Department of Physics, Oklahoma State University, Stillwater OK; United States of America.
[125]Palacký University, Joint Laboratory of Optics, Olomouc; Czech Republic.
[126]Institute for Fundamental Science, University of Oregon, Eugene, OR; United States of America.
[127]Graduate School of Science, University of Osaka, Osaka; Japan.
[128]Department of Physics, University of Oslo, Oslo; Norway.
[129]Department of Physics, Oxford University, Oxford; United Kingdom.
[130]LPNHE, Sorbonne Université, Université Paris Cité, CNRS/IN2P3, Paris; France.
[131]Department of Physics, University of Pennsylvania, Philadelphia PA; United States of America.
[132]Department of Physics and Astronomy, University of Pittsburgh, Pittsburgh PA; United States of America.
[133(a)]Laboratório de Instrumentação e Física Experimental de Partículas - LIP, Lisboa;[(b)]Departamento de Física, Faculdade de Ciências, Universidade de Lisboa, Lisboa;[(c)]Departamento de Física, Universidade de Coimbra, Coimbra;[(d)]Centro de Física Nuclear da Universidade de Lisboa, Lisboa;[(e)]Departamento de Física, Escola de Ciências, Universidade do Minho, Braga;[(f)]Departamento de Física Teórica y del Cosmos, Universidad de Granada, Granada (Spain);[(g)]Departamento de Física, Instituto Superior Técnico, Universidade de Lisboa, Lisboa; Portugal.
[134]Institute of Physics of the Czech Academy of Sciences, Prague; Czech Republic.
[135]Czech Technical University in Prague, Prague; Czech Republic.
[136]Charles University, Faculty of Mathematics and Physics, Prague; Czech Republic.
[137]Particle Physics Department, Rutherford Appleton Laboratory, Didcot; United Kingdom.
[138]IRFU, CEA, Université Paris-Saclay, Gif-sur-Yvette; France.
[139]Santa Cruz Institute for Particle Physics, University of California Santa Cruz, Santa Cruz CA; United States of America.
[140(a)]Departamento de Física, Pontificia Universidad Católica de Chile, Santiago;[(b)]Millennium Institute for Subatomic physics at high energy frontier (SAPHIR), Santiago;[(c)]Instituto de Investigación Multidisciplinario en Ciencia y Tecnología, y Departamento de Física, Universidad de La Serena;[(d)]Universidad Andres Bello, Department of Physics, Santiago;[(e)]Universidad San Sebastian, Recoleta;[(f)]Instituto de Alta Investigación, Universidad de Tarapacá, Arica;[(g)]Departamento de Física, Universidad Técnica Federico Santa María, Valparaíso; Chile.
[141]Department of Physics, Institute of Science, Tokyo; Japan.
[142]Department of Physics, University of Washington, Seattle WA; United States of America.
[143(a)]Institute of Frontier and Interdisciplinary Science and Key Laboratory of Particle Physics and Particle Irradiation (MOE), Shandong University, Qingdao;[(b)]School of Physics, Zhengzhou University; China.
[144(a)]State Key Laboratory of Dark Matter Physics, School of Physics and Astronomy, Shanghai Jiao Tong University, Key Laboratory for Particle Astrophysics and Cosmology (MOE), SKLPPC, Shanghai;[(b)]State Key Laboratory of Dark Matter Physics, Tsung-Dao Lee Institute, Shanghai Jiao Tong University,

Shanghai; China.
[145]Department of Physics and Astronomy, University of Sheffield, Sheffield; United Kingdom.
[146]Department of Physics, Shinshu University, Nagano; Japan.
[147]Department Physik, Universität Siegen, Siegen; Germany.
[148]Department of Physics, Simon Fraser University, Burnaby BC; Canada.
[149]SLAC National Accelerator Laboratory, Stanford CA; United States of America.
[150]Department of Physics, Royal Institute of Technology, Stockholm; Sweden.
[151]Departments of Physics and Astronomy, Stony Brook University, Stony Brook NY; United States of America.
[152]Department of Physics and Astronomy, University of Sussex, Brighton; United Kingdom.
[153]School of Physics, University of Sydney, Sydney; Australia.
[154]Institute of Physics, Academia Sinica, Taipei; Taiwan.
[155](a)E. Andronikashvili Institute of Physics, Iv. Javakhishvili Tbilisi State University, Tbilisi;(b)High Energy Physics Institute, Tbilisi State University, Tbilisi;(c)University of Georgia, Tbilisi; Georgia.
[156]Department of Physics, Technion, Israel Institute of Technology, Haifa; Israel.
[157]Raymond and Beverly Sackler School of Physics and Astronomy, Tel Aviv University, Tel Aviv; Israel.
[158]Department of Physics, Aristotle University of Thessaloniki, Thessaloniki; Greece.
[159]International Center for Elementary Particle Physics and Department of Physics, University of Tokyo, Tokyo; Japan.
[160]Graduate School of Science and Technology, Tokyo Metropolitan University, Tokyo; Japan.
[161]Department of Physics, University of Toronto, Toronto ON; Canada.
[162](a)TRIUMF, Vancouver BC;(b)Department of Physics and Astronomy, York University, Toronto ON; Canada.
[163]Division of Physics and Tomonaga Center for the History of the Universe, Faculty of Pure and Applied Sciences, University of Tsukuba, Tsukuba; Japan.
[164]Department of Physics and Astronomy, Tufts University, Medford MA; United States of America.
[165]Department of Physics and Astronomy, University of California Irvine, Irvine CA; United States of America.
[166]University of West Attica, Athens; Greece.
[167]Department of Physics and Astronomy, University of Uppsala, Uppsala; Sweden.
[168]Department of Physics, University of Illinois, Urbana IL; United States of America.
[169]Instituto de Física Corpuscular (IFIC), Centro Mixto Universidad de Valencia - CSIC, Valencia; Spain.
[170]Department of Physics, University of British Columbia, Vancouver BC; Canada.
[171]Department of Physics and Astronomy, University of Victoria, Victoria BC; Canada.
[172]Fakultät für Physik und Astronomie, Julius-Maximilians-Universität Würzburg, Würzburg; Germany.
[173]Department of Physics, University of Warwick, Coventry; United Kingdom.
[174]Waseda University, Tokyo; Japan.
[175]Department of Particle Physics and Astrophysics, Weizmann Institute of Science, Rehovot; Israel.
[176]Department of Physics, University of Wisconsin, Madison WI; United States of America.
[177]Fakultät für Mathematik und Naturwissenschaften, Fachgruppe Physik, Bergische Universität Wuppertal, Wuppertal; Germany.
[178]Department of Physics, Yale University, New Haven CT; United States of America.
[179]Yerevan Physics Institute, Yerevan; Armenia.
[a] Also at Affiliated with an institute formerly covered by a cooperation agreement with CERN.
[b] Also at An-Najah National University, Nablus; Palestine.
[c] Also at Borough of Manhattan Community College, City University of New York, New York NY; United States of America.

[d] Also at Center for Interdisciplinary Research and Innovation (CIRI-AUTH), Thessaloniki; Greece.
[e] Also at Centre of Physics of the Universities of Minho and Porto (CF-UM-UP); Portugal.
[f] Also at CERN, Geneva; Switzerland.
[g] Also at Département de Physique Nucléaire et Corpusculaire, Université de Genève, Genève; Switzerland.
[h] Also at Departament de Fisica de la Universitat Autonoma de Barcelona, Barcelona; Spain.
[i] Also at Department of Financial and Management Engineering, University of the Aegean, Chios; Greece.
[j] Also at Department of Mathematical Sciences, University of South Africa, Johannesburg; South Africa.
[k] Also at Department of Modern Physics and State Key Laboratory of Particle Detection and Electronics, University of Science and Technology of China, Hefei; China.
[l] Also at Department of Physics, Bolu Abant Izzet Baysal University, Bolu; Türkiye.
[m] Also at Department of Physics, King's College London, London; United Kingdom.
[n] Also at Department of Physics, Stanford University, Stanford CA; United States of America.
[o] Also at Department of Physics, Stellenbosch University; South Africa.
[p] Also at Department of Physics, University of Fribourg, Fribourg; Switzerland.
[q] Also at Department of Physics, University of Thessaly; Greece.
[r] Also at Department of Physics, Westmont College, Santa Barbara; United States of America.
[s] Also at Faculty of Physics, Sofia University, 'St. Kliment Ohridski', Sofia; Bulgaria.
[t] Also at Faculty of Physics, University of Bucharest; Romania.
[u] Also at Hellenic Open University, Patras; Greece.
[v] Also at Henan University; China.
[w] Also at Imam Mohammad Ibn Saud Islamic University; Saudi Arabia.
[x] Also at Institucio Catalana de Recerca i Estudis Avancats, ICREA, Barcelona; Spain.
[y] Also at Institut für Experimentalphysik, Universität Hamburg, Hamburg; Germany.
[z] Also at Institute for Nuclear Research and Nuclear Energy (INRNE) of the Bulgarian Academy of Sciences, Sofia; Bulgaria.
[aa] Also at Institute of Applied Physics, Mohammed VI Polytechnic University, Ben Guerir; Morocco.
[ab] Also at Institute of Particle Physics (IPP); Canada.
[ac] Also at Institute of Physics and Technology, Mongolian Academy of Sciences, Ulaanbaatar; Mongolia.
[ad] Also at Institute of Physics, Azerbaijan Academy of Sciences, Baku; Azerbaijan.
[ae] Also at Institute of Theoretical Physics, Ilia State University, Tbilisi; Georgia.
[af] Also at Millennium Institute for Subatomic physics at high energy frontier (SAPHIR), Santiago; Chile.
[ag] Also at National Institute of Physics, University of the Philippines Diliman (Philippines); Philippines.
[ah] Also at The Collaborative Innovation Center of Quantum Matter (CICQM), Beijing; China.
[ai] Also at TRIUMF, Vancouver BC; Canada.
[aj] Also at Università di Napoli Parthenope, Napoli; Italy.
[ak] Also at University of Chinese Academy of Sciences (UCAS), Beijing; China.
[al] Also at University of Colorado Boulder, Department of Physics, Colorado; United States of America.
[am] Also at University of Siena; Italy.
[an] Also at Washington College, Chestertown, MD; United States of America.
[ao] Also at Yeditepe University, Physics Department, Istanbul; Türkiye.
[*] Deceased